Pázmány Péter Catholic University

Faculty of Information Technology and Bionics

Roska Tamás Doctoral School of Sciences and Technology

Balázs Széky

Analysis of Stromal Stem Cells in Healthy and Diseased Skin

PhD Dissertation

Scientific Advisors:

Dr. Krisztián Németh PhD

Dr. Miklós Gyöngy PhD

Budapest

2024

Table of Contents

List of Abbreviations

7-AAD – 7-aminoactinomycin D

AFP - α-fetoprotein

ALB – albumin

ALP – alkaline phosphatase

APC – allophycocyanin

ARS – alizarin red S

BDNF – brain-derived neurotrophic factor

BMP4 – bone morphogenic protein 4

BSA – bovine serum albumin

CAF – cancer-associated fibroblast

CEBPα - CCAAT enhancer-binding protein α

CFP – common fibroblast progenitor

CK7/18 – Cytokeratin 7/18

CSC – cancer stem cell

DAPI - 4',6-diamidino-2-phenylindole

DCT – dopachrome tautomerase

DE - definitive endoderm

DF – dermal fibroblast

DMEM - Dulbecco's Modified Eagle Medium

DPC – dermal papilla (stem) cell

EGF – epidermal growth factor

EMT – epithelial-to-mesenchymal transition

ENO2 – enolase-2/ neuron-specific enolase

ET-3 – Endothelin-3

(h)ESC - (human) Embryonic Stem Cell

ET-3 – endothelin-3

FACS – fluorescence-activated cell sorting

FAP – fibroblast activation protein

FBS – fetal bovine serum

FC – flow cytometry

FcR – constant fragment-binding receptor

FGF2/bfGF - fibroblast growth factor 2/ basic fibroblast growth factor

FITC – fluorescein-5-isothiocyanate

GAPDH – glyceraldehyde 3-phosphate-dehydrogenase

GFAP – glial fibrillary acidic protein

GPC – glial progenitor cell

GP100 – glycoprotein 100 (encoded by the *PMEL* gene)

HF – Hair follicle

HGF – hepatocyte growth factor

ICC – immunocytochemistry

IDO – indoleamine-2,3-dioxygenase

IBMX – 3-isobuthyl-2-methylxanthine

iPSC – induced pluripotent stem cell

MAF – melanoma-associated fibroblast

MAP2 – microtubule-associated protein-2

M-CSF1 – macrophage-colony stimulating factor 1

MITF – microphthalmia-associated transcription factor

MLNA – melan-A

(BM)-MSC – (bone marrow) mesenchymal stem/stromal cell

MUSE – multi-lineage differentiation stress enduring (cell)

NDF – normal dermal fibroblast

NES – Nestin

NSC – neural stem cell

OCN – osteocalcin

OCT3/4 - octamer-binding transcription factor ¾ (encoded by the gene *POU5F1*)

oRG – outer radial glia

ORO – oil red O

PE – phycoerythrin

Pen/Strep – Penicillin/Streptomycin

PFA – Paraformaldehyde

PMA - Phorbol-myristyl-acetate

PMEL – pre-melanosome protein

POU5F1 - POU domain, class 5, transcription factor 1

PODXL – Podocalyxin like

PPARy – peroxisome proliferator-activated receptor-y

qRT-PCR – quantitative real time-polymerase chain reaction

RGP – radial growth phase (melanoma)

SCF – stem cell factor

SKP - skin-derived precursor

SOX2 – SRY (sex determining region Y)-box 2

SSEA3 – stage-specific embryonic antigene-3

TG2 – transglutaminase 2

TGF-β - transforming growth factor β

TRA-1-60 – T-cell receptor alpha locus (encoded by the *PODXL* gene)

TYRP1 – tyrosinase-related protein 1

VEGF – vascular endothelial growth factor

vRG – ventricular radial glia

VGP – vertical growth phase

1. Introduction

1.1. Stem cells and their subtypes

Stem cells are indispensable functional units of embryogenesis, organ development and tissue homeostasis [1]. Every type of stem cell is an undifferentiated cell having two basic functions.

(1) They are capable of self-renewal, thus maintaining their undifferentiated state by continuous proliferation.
(2) Stem cells generate differentiated tissue cells with specific morphology and functions.

The delicate balance between stem cell self-renewal and differentiation is regulated by the intricate interplay of cell-cycle proteins, pluripotency and lineage-specific transcription factors and histone-modifying enzymes [2]-[4]. On the other hand, stem cell self-renewal and differentiation relies not exclusively on cell-autonomous programs, but also on the matrix proteins [5] and soluble messengers [6] of the surrounding cellular niche. Stem cells can generate differentiated daughter cells by both symmetrical and asymmetrical cell division [7]. Asymmetric stem cell division generates a daughter stem cell, and a daughter cell, which is committed towards differentiation. For example, radial glia stem cells in the developing nervous system undergo asymmetric proliferation, which generates radial glia cells and differentiated daughter cells, such as neuronal and intermediate progenitor cells [8]. Symmetrical stem cell division results in two daughter cells, which are either stem cells or differentiated cells. For example, mammary gland and intestinal epithelial stem cells differentiate by symmetric cell division, which is regulated by microenvironmental signals [9]-[10]. Both symmetric and asymmetric stem cell division generate cells, which are committed towards certain lineages. These lineage-specified cells, called progenitor cells are endowed with the potential of giving rise to functional tissue cells throughout further rounds of proliferation, (Fig.1).

According to their source of origin, stem cells can be categorized broadly into three mayor subtypes: embryonic stem cells (ESC), adult stem cells and induced pluripotent stem cells. ESCs are pluripotent as they differentiate into cell lines from all three germ layers: ectodermal, mesodermal, and endodermal lineages. Hence, ESCs are the cellular source of organ specific, adult stem cells, such as bone-marrow stem cells, cardiac stem cells,

neural stem cells, intestinal stem cells and skin stem cells. These adult, multipotent stem cells generate at least two cell types, which are specific to a given tissue and regulate tissue homeostasis in concert with mature differentiated cells of their microenvironment. On the other hand, less is known about their capacity to undergo trans-differentiation, thus, producing other cell types beyond their lineage under certain circumstances, such as wound healing and tissue damage.

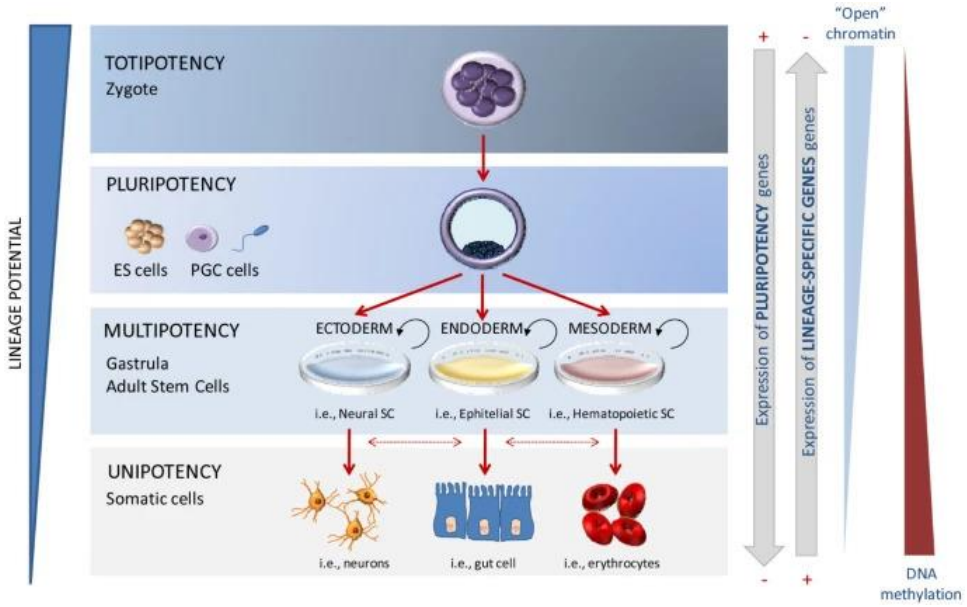

Figure 1. Stem cell differentiation potential and lineage commitment. *Totipotent stem cells of the zygote generate embryonic cells and extraembryonic placental tissue. In contrast, embryonic pluripotent stem cells have tri-lineage differentiation potential, thus, they give rise to ectodermal, endodermal, and mesodermal lineage cells. Formation of these three germ layers is accompanied by changes in the stem cells epigenome, including DNA-methylation, chromatin accessibility and histone modifications. Tight regulation of the epigenetic modifications leads to the repression of pluripotency genes, and to the upregulation of lineage-specific genes in multipotent ectodermal, endodermal, and mesodermal lineage cells. Lineage restriction becomes more pronounced in the somatic stem cells, which differentiate into one specified cell type in a tissue. Source: [4]*

In contrast to multipotent stem cells, unipotent stem cells, (such as epidermal keratinocyte stem cells [11]) give rise to only on cell type besides their self-renewal.

1.2 Ectodermal, Endodermal and Mesodermal Differentiation of Stem Cells:

1.2.1. Ectodermal Differentiation

Neural Lineage Differentiation

During the embryonic development, stem cells of the blastocyst are specialized into three germ layers: ectodermal, mesodermal, and endodermal layers [12]. The ectodermal layer is further specified into non-neural ectoderm and neuroectoderm, which are divided by the neural plate border [13]. Signaling molecules and morphogens from the underlying mesoderm layer induce the elevation and folding of the neural plate borders and subsequent closure of the neural tube [14]. The cells delaminating from the neural fold form the neural crest cells, while the non-neural ectoderm elevates above the neural tube. While the neural tube generates the cells of the central nervous system, neural crest cells differentiate into the cells of the peripheral nervous system, melanocytes, smooth muscle, and glial cells. On the other hand, non-neural ectodermal cells differentiate into the cells of the epidermis, such as epidermal keratinocytes. Neural stem cells (NSCs) emerge from primitive neuroepithelial progenitor cells, which constitute the neural plate during embryonic development, [15]. NSCs are multipotent stem cells, which self-renew and proliferate in the presence of sonic hedgehog, epidermal growth factor (EGF) and fibroblast growth factor-2 (FGF2). During brain development a specialized form of NSC, the radial glia cell emerges (Fig.2), which play crucial roles in neurogenesis, neuronal migration, cortical development, and glial cell differentiation. Although neuronal subtype specification is highly dependent on region-specific morphogen gradients, the neurogenic hormone brain-derived neurotrophic factor (BDNF) is inevitable for neuronal differentiation, as well as for the maintenance of neuronal survival and functions, [16]. Given the current models of *in vivo* neurogenesis, neural lineage differentiation can be recapitulated *in vitro i*n pluripotent stem cells PSCs by inducing the formation of embryoid bodies in non-adherent conditions [17]. PSCs in embryoid bodies differentiate into NSC-like cells, which form neurospheres in culture medium supplemented with EGF, FGF-2, N2 and the neurogenic vitamin B-27. Neurospheres can be attached into poly-D-lysine coated dishes for further culturing, where they form adherent clusters of neural rosettes. Neural rosettes can be maintained in culture by continuous passaging and supplementation with

EGF and FGF-2. Furthermore, NSCs in neural rosettes undergo neuronal differentiation upon withdrawal of EGF and FGF-2 and addition of BDNF.

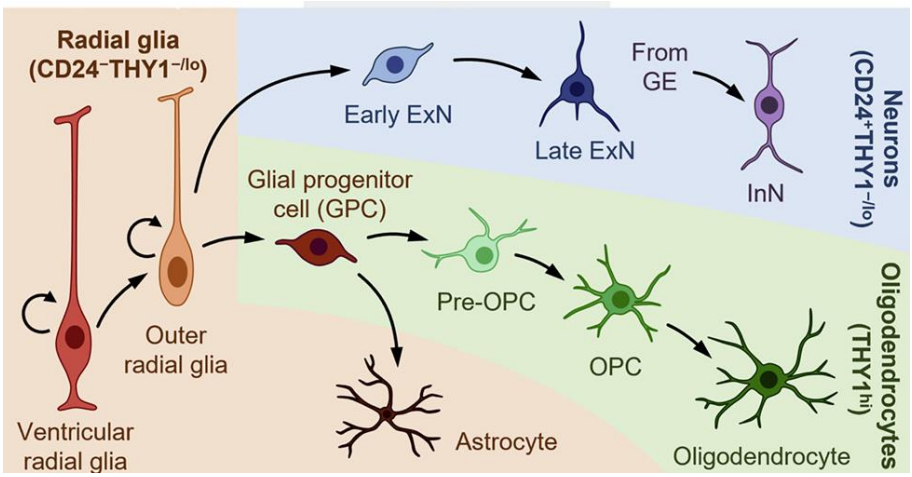

Figure 2. Neuronal and glial lineage specification is driven by asymmetric proliferation of the outer radial glia stem cells*. Outer radial glia (oRG) is a multipotent neural stem cell, which is generated from ventricular radial glia cells (vRG). ORGs can generate neuronal and glial progenitor cells (GPCs) by asymmetric proliferation. Glial progenitor cells can give rise to astrocytes, or pre-oligodendrocyte progenitor cells (pre-OPCs), which are committed towards differentiating into myelinating oligodendrocytes. Early and late excitatory neuronal progenitor cells (ExNs) are derived from oRG, whereas inhibitory neuronal progenitor cells (InNs) migrate from the ganglionic eminence (GE) to their niches. The expression of cellular markers CD24 and THY1 discriminates radial glia (CD24-THY-/low) from OPCs (THY+), neuronal cells (CD24+THY-/low) and astrocytes. Source: [18]*

***In vitro* Melanocyte Differentiation:**

While the epidermal keratinocytes and skin fibroblasts originate from non-neural ectoderm and mesodermal layers, melanocytes are of neural crest origin, [19], [20]. Melanocytes emerge from neural crest cells emerging at the neural plate border, which are migrating through the dermis to their epidermal niches, (Fig.3). Migrating NSCs give rise to Sox10-expressing, bipotent neural crest stem cells with both glial and melanocyte differentiation potential. These bipotent NSCS, termed melanoblasts express not only stem cell specific molecules (such as the stem cell factor (SCF)-receptor cKIT), but also MITF, a key transcription factor involved in melanogenesis. Melanoblasts acquire two different cell fates depending on their final niches. One subset of melanoblasts migrate into the hair follicle bulge to form melanocyte stem cells for hair pigmentation. The other half of the melanoblasts integrate into the epidermis giving rise to epidermal melanocytes. Epidermal melanocytes for extensive dendritic contacts with epidermal keratinocytes providing photoreception and skin pigmentation. Melanogenesis is a complex, multistep process involving UV-mediated transcriptional induction of melanin-synthesis enzymes, melanosome formation and intercellular melanosome transportation from melanocytes to keratinocytes [21]. UV-induced DNA damage in keratinocytes activates p53-mediated transcription of POMC gene, which is translated and cleaved into active form of pigmentation hormone, α-MSH. α-MSH binding to melanocortin receptor-1 (MCR1) on epidermal melanocytes stimulates the expression of MITF, the master regulator of melanin-biosynthetic enzymes; dopachrome-tautomerase 1 (DCT1), tyrosinase-related protein 1 (TYRP1), tyrosine-hydroxylase (TH), glycoprotein-100 (GP100) and pre-melanosome protein (PMEL). While DCT1, TH and TYRP1 play role in melanin biosynthesis, PMEL and GP100 are essential for melanosome structure and biogenesis.

Methods for the *in vitro* generation of melanocytes were published for both pluripotent stem cells and fibroblasts [22]. Key step in this procedure is the *in vitro* induction of melanoblast-like progenitors by the induction of cKIT and melanoblast-specific genes with SCF, endothelin-3 and Wnt3a. Wnt3a not only stimulates melanoblast commitment, but also facilitates functional and morphological maturation of melanocytes. Melanoblast cells adhere and survive with high efficiency on fibronectin coated surfaces in medium containing, insulin, transferrin, hydrocortisone, ascorbic-acid and high concentration of glucose.

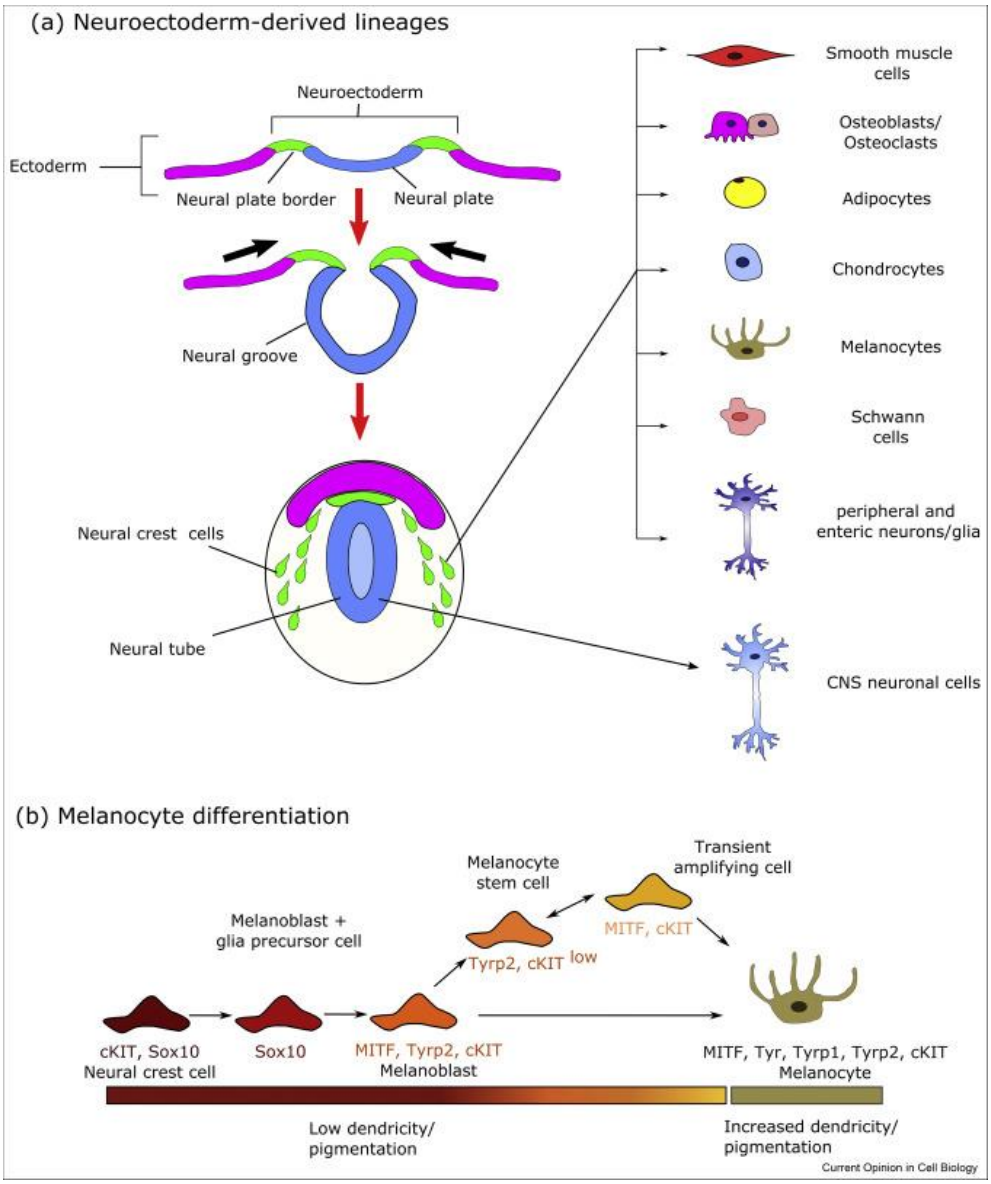

Figure 3. Developmental origin of melanocytes. *(a) During the closure of the neural tube, the neural crest emerges from the delamination of the neural plate border. The neural crest stem cells give rise to several cell types, including Schwann cells, peripheral nerves, and melanocytes. (b) cKIT+Sox10+ neural crest subset generates bipotent Sox10+ progenitor cells, which become melanoblasts committed towards melanocytes differentiation. These melanoblasts already express the transcription factor MITF, the master regulator of melanogenic genes. Melanoblasts mature into arborising, melanin-producing melanocytes through the enrichment of transient amplifying MITF+cKIT+ cells. Source: [19]*

Further maturation of melanocyte lineage cells towards pigment producing melanocytes can be achieved by stimulating melanogenesis with αMSH or cholera-toxin, which mimics

the effects of αMSH by activating G-protein effectors required for the initiation of melanogenesis.

1.2.2. Mesodermal Lineage Differentiation

Mesodermal cells generate skeletal, muscular, and connective tissue cells during development. Tissues of mesodermal origin contain stem cell subsets, such as mesenchymal stem/stromal cells, which can replace and repair the damaged tissues by differentiation and regulation of local inflammatory immune responses.

MSCs from the bone marrow, skin and adipose tissue produce osteocytes and adipocytes besides other mesodermal lineage cells (chondrocytes, smooth muscle cells, etc.) *in vitro* and *in vivo*. Osteogenesis or adipogenesis are regulated by the intricate balance in the activation lineage-specific transcription factors in MSCs, [23] (Fig.4). While Runt-related transcription factor 2 (Runx2) is a master regulator of osteogenesis promoting osteoblast specification, osteogenic ECM production and matrix mineralization [24], Peroxisome proliferator activated receptor γ (PPAR-γ) upregulates genes, which are responsible for lipid metabolism, triglyceride synthesis, glucose uptake and insulin-signaling [25]. Osteogenic and adipogenic differentiation are activated by diverse signaling pathways, which are antagonizing each other. Wnt-signaling and β-catenin-mediated transcription activates osteogenesis, as well as FGFR- and BMP-signaling pathways [26]. Furthermore, the transcription factor YAP/TAZ is activated during osteogenesis, which promotes Runx2 expression, but represses PPAR-γ-dependent gene transcription [27]. On the other hand, activation of the insulin-receptor signaling pathway and metabolic signals, such as increased uptake of glucose and free fatty acids promote adipogenesis through the activation of PPAR-γ and inhibition of β-catenin.

Osteogenesis and adipogenesis are intricately regulated not only by soluble factors of stromal microenvironments, but also by composition and biophysical properties of the local extracellular matrices [28], [29]. Stiff and dense extracellular matrices induce osteogenesis, by increased contractility of actin-networks, followed by the activation of contraction-sensitive YAP/TAZ transcription factors. On the other hand, soft extracellular matrices inhibit YAP/TAZ but stimulate adipogenesis.

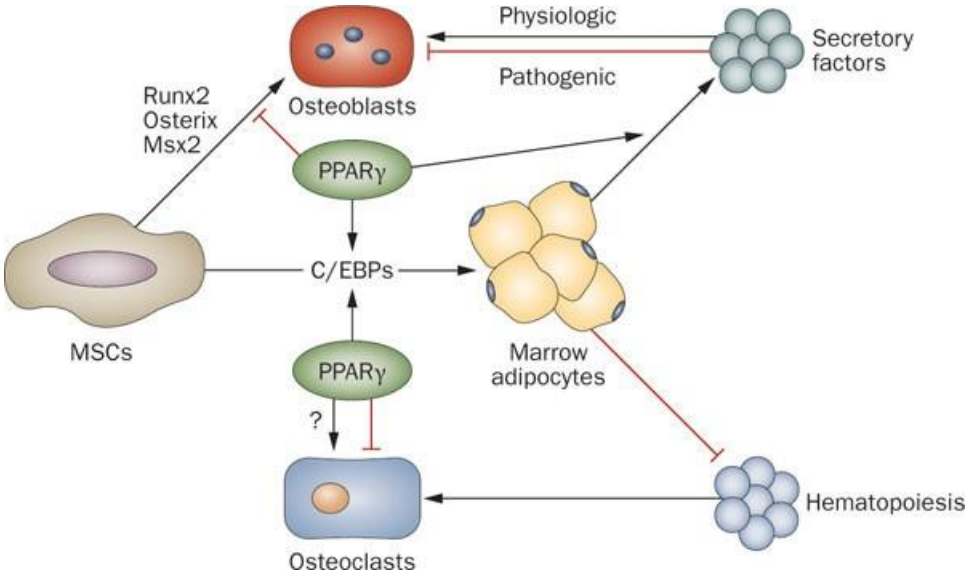

Figure 4. Transcriptional regulation of osteogenic and adipogenic differentiation. *Activation of Runx2, Osterix and Msx2 in MSCs produces osteoblasts. In contrast, PPARγ represses osteogenic transcription factors, and facilitates the activation of the adipogenic transcription factors, C/EBPs. Although PPARγ inhibits the generation of osteoblasts, its impact on osteoclast differentiation is still controversial. Marrow adipocytes exert a dual role on the regulation of osteoblast differentiation and osteoclast differentiation. Marrow adipocytes promote osteoblast differentiation through secreted factors, and by the suppression of osteoclast differentiation from hematopoietic stem cells. On the other hand, bone marrow adipocytes suppress the generation of osteocytes through soluble messengers in diseases, such as osteoporosis. Source: [30]*

Stromal cells of the bone marrow and skin undergo osteogenesis *in vitro* by stimulation with factors promoting Runx2 activation and matrix mineralization. Dexamethasone is a corticosteroid molecule with multiple effects on osteogenic differentiation, including the induction of YAP/TAZ expression and Runx2 activation [31], [32]. Synthesis and secretion of collagen-1 are stimulated by ascorbic-acid-2-phosphate [34], while β-glycerophosphate activates matrix mineralization and expression of BMP2 [33]. Adipogenesis can be triggered in vitro by activating insulin-receptors and PPAR-γ with insulin and diverse PPAR-γ agonists, respectively. For example, the antidiabetic agent troglitazone is a potent agonist of PPAR-γ, which upregulates adipocyte-specific genes and increases fatty acid biosynthesis, [35]. Protein-kinase A is another important signaling

effector in adipogenesis due to its ability to activate the transcription PPAR-γ. 3-Isobuthyl-1-methylxanthyne (IBMX) is a non-specific phosphodiesterase-inhibitor, which elevates cAMP-levels in the cells, thus facilitates PKA-mediated adipocyte-specific gene transcription, [36].

1.2.3. Endodermal Lineage differentiation

Pancreatic, intestinal, lung and hepatic cells arise from endodermal layer. Endodermal layer cells of the anterior primitive streak generate a specific progeny, the definitive endoderm (DE), which is the source of all mature endodermal lineages, including hepatocytes, cholangiocytes, thymus and thyroid gland cells. Multipotent stem cells of the DE is characterized as cells expressing stem cell factor receptor c-KIT and endodermal progenitor specific transcription factor SOX17 [37]. Further development of the DE diverges along the anterior-posterior axis of the embryonic gut tube due to diverse morphogenic gradients of WNT, BMP-4, TGF-β and SHH, [38]. The anterior DE cells have more neural crest-like characteristics due to the expression of neural cell adhesion molecule-1 (NCAM1, CD56) and NSC marker CD271, and they acquire the differentiation potential to generate cells of the lung, thymus, and thyroid gland. On the other hand, posterior DE cells express the pancreatic progenitor cell marker FOXA2, and give rise to the intestinal, pancreatic, and hepatic progenitor cells, [39].

While the activation of TGF-β/SMAD-signaling axis by Activin A and BMP4 is essential for DE formation, subsequent hepatic differentiation is initiated from the cells of the posterior, or foregut DE cells. Posterior DE cell clusters differentiate into hepatoblasts in the presence of hepatocyte growth factor (HGF) [40]. Hepatoblasts express hepatocyte specific transcription factor HNF4 and secrete high alfa-fetoprotein, but they are still devoid of mature hepatocyte markers albumin and cytochrome P450. Hepatoblasts are bipotent stem cells, which can mature into both cholangiocytes and hepatocytes. Hepatocyte maturation is promoted by hematopoetic cell derived cytokine Oncostatin M (OSM), which suppresses fetal liver hematopoiesis, and stimulates the expression of hepatocyte-specific genes, (Fig.5). Fetal hepatocytes are cubic shaped cells, which store glycogen, incorporate fatty acids into lipid droplets and metabolize drugs by CYP enzymes besides the secretion of albumin (ALB). In contrast to hepatocytes, cholangiocyte

maturation is promoted by stromal cells in a TGF-β-dependent manner. Cholangiocytes are epithelial-like cells regulating bile-acid synthesis and secretion**.**

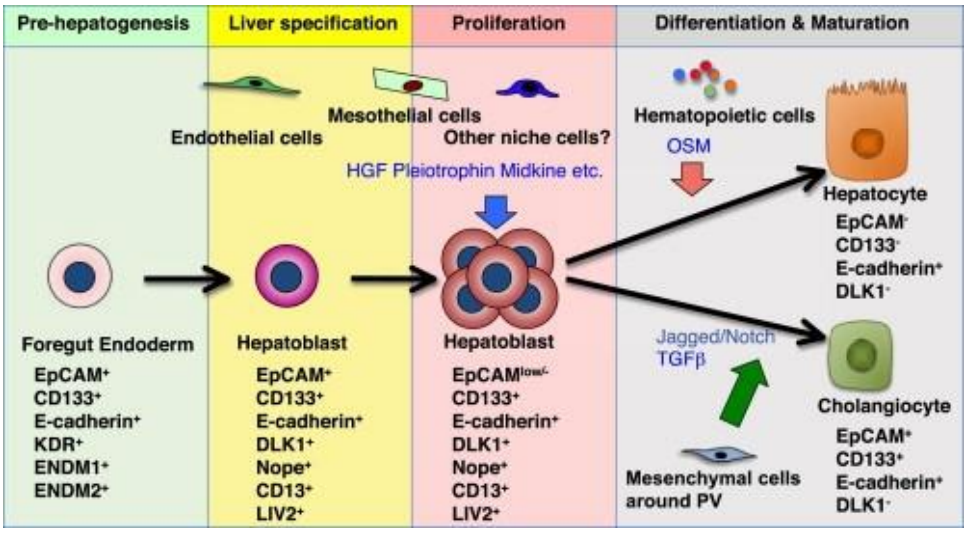

Figure 5. Differentiation of hepatocytes from foregut endoderm cells. *Hepatoblast cells are EpCAM+CD133+E-cadherin+ progenitor cells derived from the foregut endoderm. Their differentiation is driven by niche-dependent signals, such as HGF from mesothelial cells. Hepatoblasts give rise to mature hepatocytes in the presence of oncostatin-M (OSM), which is secreted by hematopoietic cells. On the other hand, mesenchymal cells stimulate cholangiocytes differentiation via TGF-β and Notch signaling. Source: [41]*

1.3. The human dermis as a stromal stem cell niche

Every organ needs tissue repair mechanisms to counterbalance injuries and cell aging. Maintenance of organ homeostasis is based on intricate regulation of the resident stem cell's activity by immune cells and differentiated tissue cells [42]. The balance between stem cell self-renewal and differentiation is tightly regulated by soluble messengers, morphogenic gradients [43], extracellular matrix components [44] and cell adhesion molecules of the surrounding microenvironment [45]. Furthermore, the distribution of oxygen in different tissues dictate stem cell fates through hypoxia-associated signaling and regulation of oxidative metabolism [46].

The biological milieu maintaining organ structure and function with cellular agents, soluble factors and extracellular matrices is called stroma. Stromal compartments are structurally heterogeneous microenvironments containing connective tissue producing cells, immune cells, glands, nerve endings, lymphatic vessels, and blood vessels [47], [48]. Likewise, the stroma provides micro-niches for multipotent stem cell subsets, such as hematopoietic stem cells and MSCs.

Skin is a complex, highly regenerative tissue encompassing diverse stromal compartments with distinct cellular compositions. Each layer provides a niche for heterogeneous stem cell populations of different origin. The interfollicular epidermis (IFE) consists of a stratified network of keratinocytes and keratin family proteins, which form a protective barrier against physical insults, chemical agents, allergens, and UV radiation [49]. The basal layer of epidermis contains keratinocyte stem cells, which proliferate towards the uppermost layer of skin upon activation. On the contrary, renewal of the hair follicles (HF) is periodic with cycles of cell proliferation, growth arrest and apoptosis [50], [51]. While progenitor cell dynamics of the IFE and the HF were subjects of several studies, the dermal stem cell populations and their interactions with their niches remain elusive.

The dermis is the stromal milieu of skin in mammals and humans, which is separated from the epidermis by a dense mesh of extracellular proteins, called the basal lamina. Though most of the dermis is made up by extracellular matrix proteins (collagens, fibronectin, laminin) produced by dermal fibroblasts, several micro-niches with diverse cellular compositions can be distinguished [52]-[53]. The main dermal niches are the papillary dermis, reticular dermis, and hypodermal adipose tissue, (Fig.6). The papillary

dermis contains blood vessels, hair follicle dermal papilla and nerve terminals embedded in loose extracellular matrix, while the reticular dermis has a dense network of connective tissue and enriched in glands, and capillaries. The subcutaneous layer is the main fat storage site in the skin due to its enrichment in adipocytes. Despite the remarkable cellular heterogeneity of the dermis, all dermal layers contain fibroblasts, which play central roles in the maintenance of the dermal connective tissue [54], adipocyte pool [55], wound healing [56], [57] hair follicle- and epidermal cell homeostasis [58]. In addition, stromal fibroblasts regulate immunity and inflammation at the epithelial/mesenchymal and hypodermal barriers of the dermis [59], [60].

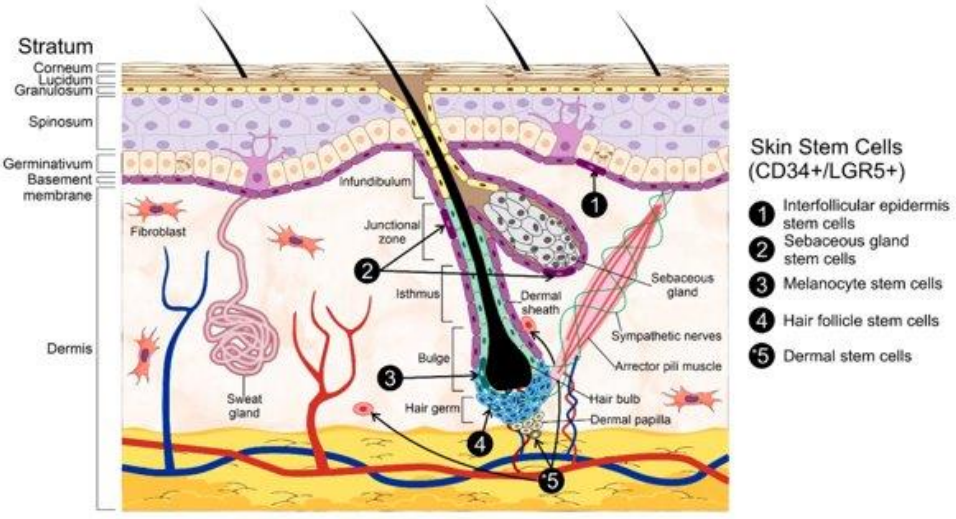

Figure 6. The structural and cellular heterogeneity of the human dermis. *The dermis lies between the epidermis and the subcutaneous adipose tissue. The dermis is connected to the epidermis by the basal lamina, which forms the appendages of the dermal papillae and sebaceous glands. While the dermal papilla is enriched in dermal papilla/ hair germ stem cells, different stem cell subsets (including melanocyte stem cells) are contained in the hair follicle bulge. Furthermore, the sebaceous glands harbor their own stem cell subsets. Source: [57]*

1.4. Fibroblasts in the human dermis: origin and heterogeneity

Fibroblasts are spindle-shaped, highly adherent stromal cells providing structural framework and nutritional support to various organs. Fibroblasts express extracellular matrix proteins (collagen, fibronectin), adhesion receptors and characteristic stromal cell markers, such as C44, CD90 and CD105, although, they lack hematopoietic lineage markers (CD45, CD11) [61]. Despite their similarity on the morphological and molecular level, fibroblasts constitute highly heterogeneous subsets across different organs or cellular micro-niches. Functional, phenotypic, and developmental heterogeneity of fibroblasts were explored by lineage tracing, chromatin structure analysis techniques and single-cell RNA sequencing. Cell fate mapping by reporter vector systems allowed the investigation of specific fibroblast subsets *in vivo* [61]-[63]. These studies suggest a common fibroblastic progenitor cell (CFP), which gives rise to all dermal fibroblast lineages, (Fig. 7). CFPs express PDGFα receptor, Lrig1 and Dlk1. CFPs give rise to both papillary and reticular dermal fibroblast progenitor cells, which are the cellular source of papillary (papillary fibroblasts, arrector pili muscle cells) and reticular lineages (reticular fibroblasts, hypodermal adipocytes). In addition to cell-specific lineage differentiation, fibroblast composition of dermal niches is regulated by soluble cell signaling molecules, cell-cell signaling and extracellular matrices. Moreover, the positional identity of fibroblasts is also dictated by cell-autonomous genetic programs, such as the spatio-temporal regulation of the HOX-genes [64].

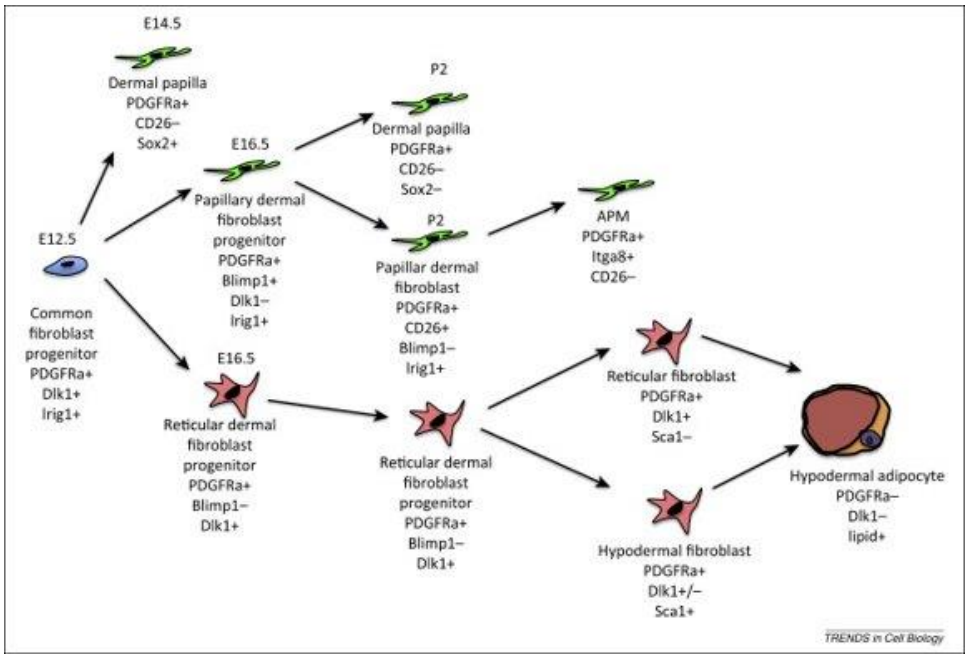

Figure 7: developmental origin of fibroblast heterogeneity in skin. *Fibroblast subsets of the dermis derive from a common fibroblast progenitor cell (blue), which is of neuroectodermal (facial skin) or mesodermal origin (non-facial skin). Based on local morphogenic gradients and cell-autonomous gene expression, common fibroblast progenitor cells give rise to papillary and reticular fibroblast lineages. While the papillary dermal fibroblast progenitors constitute the source of papillary fibroblasts, dermal papilla cells and arrector pili muscles (green), reticular fibroblast progenitors differentiate into hypodermal adipocytes and reticular fibroblasts (brown). Source:[61]*

Most of the fibroblasts in adult skin are supplied by the local fibroblast subsets and MSCs, although, non-fibroblastic cell types can be transformed into fibroblast cells by diverse mechanisms, (Fig. 8), [65],[66]. For example, epithelial cells can undergo epithelial-to-mesenchymal trans-differentiation to acquire fibroblastic cells. Similarly, monocytes, hematopoietic cells and pericytes can transdifferentiate into fibroblasts during wound healing, fibrosis and metastatic cancer spreading.

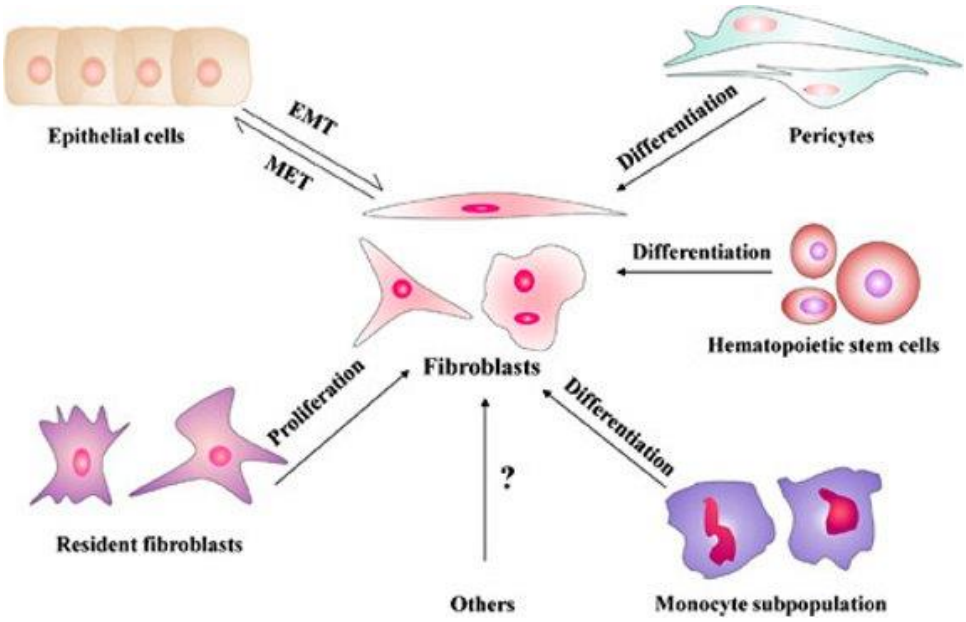

Figure 8: multiple cell sources of fibroblasts in adult skin. *Although the local MSCs generate fibroblasts, several other cells can undergo trans-differentiation to acquire fibroblastic phenotype. Epithelial-mesenchymal transformation allows epithelial cells to rewire their gene-expression to upregulate genes associated with cell motility, contractility, and fibroblast morphology. Besides epithelial cells, monocytes, pericytes and hematopoietic lineage cells also undergo fibroblastic transformation to ameliorate tissue damage and facilitate wound healing. Source: [66]*

1.5. Fibroblast functions

Fibroblasts maintain tissue structure and function throughout the synthesis and maintenance of extracellular matrix, metabolic supply, regulation of tissue regeneration and local immune homeostasis, (Figure 9).

Fibroblasts regulate synthesis, assembly and degradation of the major extracellular matrix proteins, collagen, and fibronectin [67], (Fig.5A-C). Fibronectin and collagen chains are synthetized and secreted by fibroblasts throughout the endoplasmic reticulum (ER) /secretory pathway, although, they assemble by distinct mechanisms. Self-assembly of collagen triple alfa-helices requires hydroxylation and glycosylation of proline and lysine residues of nascent alfa helices in the ER [68].

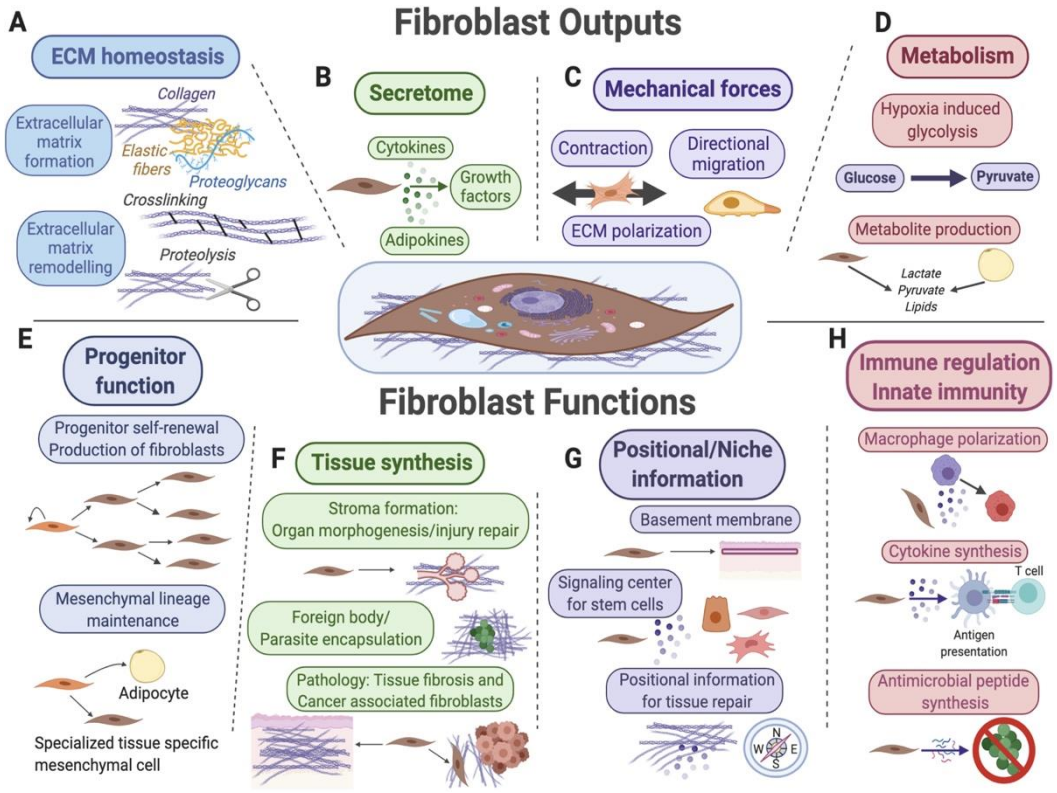

Figure 9: the functional diversity of fibroblasts. *(A) Fibroblasts produce assemble and remodel extracellular matrices (ECMs). (B) Fibroblasts secrete cytokines, adipokines, growth factors to regulate tissue development, regeneration, and inflammatory immune responses. (C) The biochemical and biophysical properties (stiffness'/rigidity) of ECMs regulates cell motility, contractility, gene expression and differentiation of fibroblasts. to supply the growth and differentiation of the resident tissue cells. (D) Fibroblasts regulate tissue metabolism, and they provide metabolic support to the tissue cells by the secretion of metabolites, such as pyruvate, lactate, and lipids. (E) Fibroblasts encompass stem cell subsets, which produce tissue specific stromal cells during tissue repair and development. (F) Fibroblasts regulate tissue synthesis, organ morphogenesis and fibrosis through the regulation of ECM-protein composition (G) Fibroblast-derived ECM and ECM-associated signaling molecules serve as positional cues by recruiting stromal and tissue cells to their niches. (H) Fibroblasts also recruit immune cells through the secretion of chemokines. Furthermore, they release soluble factors, which polarize macrophages, or facilitate antigen-presentation. Source: [65]*

Fibroblasts also produce and secrete enzymes, which mediate collagen crosslinking or degradation. The cleavage of procollagen triple helices and mature collagen is mediated

by collagenases [69] and matrix-metalloproteinases [70], whereas the assembly of procollagens into mature fibrils is regulated by lysyl-oxidases [71] and transglutaminase enzymes [72]. Fibronectin fibrillogenesis is initiated by the binding of fibronectin monomers to integrin receptors expressed by fibroblasts [73]. Fibronectin-integrin binding triggers actin-mediated contraction, which drives conformational changes of integrin-bound fibronectins by exposing their fibronectin-binding domains to other monomeric fibronectins. Collagens and fibronectin networks interact and bind other extracellular matrix proteins, such as proteoglycans and laminins. Structural and compositional modification of extracellular matrices by fibroblasts profoundly affects cell adhesion, migration, differentiation and receptor-mediated signaling [74],[75].

Fibroblasts maintain the immunological barriers of solid organs by intricate interplay with immune cells, (Fig.5H). Inflammatory cytokines, tissue damage signals, hypoxia rewires gene-expression in fibroblasts, which acquire a highly contractile, secretory, and myofibroblast phenotype [76]. Activated fibroblasts release cytokines, which increase vascular permeability, activate macrophages and chemokines to recruit lymphocytes [77]. In addition, inflammatory fibroblasts remodel the extracellular matrix by the upregulation of extracellular matrix production, contractile proteins, and cell-adhesion molecules [78]. On the other hand, fibroblasts also reshape their immunological microenvironment due to the polarization of pro-inflammatory (M1) and anti-inflammatory (M2) macrophage phenotypes [60].

Fibroblasts have critical importance in wound healing and tissue regeneration, (Fig. 5E-G). [79] Fibroblasts respond to UV-damage, pro-inflammatory cytokines, and damage-associated molecular signals by acquiring a highly secretory, contractile phenotype. Activated fibroblasts release pro-inflammatory cytokines and chemokines to recruit immune cells to the wounding site for the clearance of pathogens [80], [81]. Wound-associated fibroblasts release matrix-metalloproteinases to promote ECM-breakdown, which increases immune-cell infiltration and cell migration. [82] Furthermore, fibroblasts release TGF-β, VEGF and Angiotensin-1 to stimulate angiogenesis and granulation tissue formation [83]. In the late phase of wound healing fibroblasts contractility driven by α-SMA increases, which provides wound closure, ECM stiffness and cell differentiation [84].

Besides the crucial role of fibroblasts in tissue remodeling, immuno-modulation and angiogenesis, stromal fibroblast subsets with stem-cell characteristics were identified [85]. These cells have outstanding tissue regenerative potential due to their multipotent nature, which allow them to they can generate cells from multiple lineages. These dermal resident stem cell populations enhance cutaneous wound healing [86],[87], remyelination [88], angiogenesis [89], or facilitate the regeneration of diabetic wounds [90] and hepatic injuries [91]. Given their beneficial effects on tissue-repair observed in vitro and in vivo, the comprehensive analysis of dermal stem cells regarding their specific markers and differentiation potential could facilitate the development of dermal stem cell based regenerative therapies. Multipotent stem cell subsets of the skin connective tissue with high regenerative potential include dermal MSCs, multilineage differentiating, stress enduring cells and dermal papilla stem cells.

1.6. Fibroblast Stem Cells of the Dermis

1.6.1. Mesenchymal Stem Cells:

Bone marrow stromal stem cells were discovered by Alexander Friedenstein (1924-1998) [92] and Alexander Maksimov (1874-1928) [93]. While Maximov proposed that stromal cells in the bone-marrow compose a hematopoietic microenvironment (HME) required for physiological hematopoiesis, Friedenstein identified the HME-resident cells bearing stem cell properties. These stem cell populations, called mesenchymal stem cells (MSCs) have the potential to generate a broad range of cell types within the mesodermal lineage. Over the past decades MSCs were successfully isolated and expanded in culture not only from bone marrow, but from a variety of other tissues including dental pulp [94], umbilical cord blood [95], stromal vascular fraction [96] and dermis [85]. At the same time, largely heterogeneous MSC subpopulations found below the same niches and with high donor-to-donor variations.

Given the astounding heterogeneity of plastic adherent MSCs, the stem cell research community proposed uniform criteria for the identification of MSCs. To make a consensus, the International Society for Cellular Therapy (ISCT) established the minimal criteria for defining MSCs [97]. Firstly, MSCs regarded as plastic adherent cells with the ability of self-renewal and generation of osteogenic, chondrogenic and adipogenic progeny. Secondly,

all MSCs express CD73, CD90, and CD105, but they are negative for HLA-DR, hematopoietic markers, (such as CD34, CD44, CD54) and common leukocyte marker CD45.

Despite having these shared phenotypic signatures, MSCs represent a highly heterogeneous stem cell population in terms of their differentiation potential, cellular markers, and secreted molecules. For example, differentially expressed genes and different lineage generation potentials identified between bone marrow (BMMSC) and adipose tissue derived MSCs (ATMSC) [98]. BM-MSCs and AT-MSCs are positive for standard MSC markers, but differentially express other stem cell associated molecules, such as CD146 or CD271. Gene-expression patterns of BM-MSCs and AT-MSCs suggest lineage restriction; while BMMSCs are more biased to generate osteocytes, AT-MSCs preferentially differentiate into adipocytes [99]. The restriction of different MSCs to a set of lineages presumes distinct patterns of epigenetic modifications inherited from MSC progenitors. According to the latest literature, commitment of MSCs toward osteogenic and adipogenic lineages relies on distinct, but mutually exclusive mechanisms of transcriptional activation [100]. The tight interplay of micro-RNAs, transcription factors and histone modifying enzymes are involved in the maintenance of this epigenetic memory behind MSC lineage choices.

Over the past decades, adipose tissue has emerged as an abundant and easily accessible source of MSCs, [98]. MSCs are more enriched in the adipose tissue than in the bone marrow, as they represent 1% of adipose tissue cells in contrast with 0.001-0.002% of MSCs from the total number of bone marrow resident cells. Adipose tissue MSCs (AT-MSCs) migrate to the site of injured tissues, replace the damaged tissue by differentiation and secrete trophic, pro-angiogenic and anti-apoptotic factors [101]. Furthermore, AT-MSCs can be reprogrammed to induced-pluripotent stem cells (iPSCs) with high efficiency [102].

The human dermis also provides niches for diverse MSC subpopulations. Vaculik et al found CD271+ and SSEA4+ adherent dermal MSC subsets, which also expressed canonical MSC markers CD73, CD90 and CD105 [85]. Both CD271+ and SSEA4+ cells localized by cutaneous nerve fibers and generated adipocytes with high efficiency, but only the CD271+ fraction had osteogenic and chondrogenic potential. Dermal MSC subpopulations (DMSCs) have a crucial role in skin regeneration and cutaneous wound healing [103].

Dermal MSCs secrete trophic factors, cytokines, chemokines to facilitate angiogenesis, cell migration and cell proliferation. In addition, DMSCs suppress the homing and activation of inflammatory immune cells, which prevents chronic inflammation and subsequent fibrosis. Co-culture experiments demonstrated that keratinocytes promote the differentiation of DMSCs into myofibroblast and induce secretion of chemokines (SDF-1, CXCL-5) and cytokines (IL6, IL8) from DMSCs [104]. Intriguingly, DMSCs were proved to exert beneficial effects in liver repair in a mouse model of liver fibrosis [105].

MSCs regulate innate and adaptive immune responses due to their ability to modulate the inflammatory cell phenotypes in different tissues [106]. MSCs are activated by inflammatory mediators, such as TNF-α and IFN-γ, but their mode of activation depends on the quality and concentration of cytokines and other immune-mediator molecules present in their local environment. In the presence of pro-inflammatory mediators, activated MSCs exert anti-inflammatory effects by the release of inhibitory cytokines (PGE2, TGF-β) and by the polarization of T-cells and macrophages towards immunosuppressive T-reg and M2 phenotypes, respectively.

The fate of MSCs in their micro-niches are dictated by cell adhesion [107], oxygen levels [108], and soluble factors (cytokines, growth hormones, chemokine ligands) [109] [110], which are secreted by other niche resident cells. Conversely, MSCs exert regulatory functions on the neighboring cells of their niches beyond immune modulation. For instance, bone-marrow MSCs share perivascular and peri-endosteal microenvironments with hematopoietic progenitor cells (HSCs). Bernardi et al. found that murine HSCs and PDGFR+ MSCs share a hypoxic peri-endosteal microenvironment, where MSCs instruct the maturation of HSCs via the interplay of HIF factors and interferon-responsive genes [111]. Biomechanical cues, such as contractility and extracellular matrix stiffness also important regulators of MSC fate [112]. Integrin signaling mediated by stiff extracellular matrices activate transcription factors implicated in MSC fate determination. One of these transcriptional regulators, Yes-associated protein (YAP) is activated by the assembly of cortical actin fibers induced by stiff extracellular matrices. Nuclear translocation of YAP leads to the repression of adipogenic genes, and subsequent restriction of MSCs towards osteogenic differentiation [113].

Distinct microenvironments of the dermis were identified as potential MSC niches. Firstly, a subset of perivascular cells from different organs are identified as *bona fide* MSCs, cutaneous vasculature could serve also as a reservoir of such stem cells. Secondly, it has been shown that hair follicle dermal stem cells express MSC markers and create mesodermal cell types. The perivascular niche for dermal MSCs can be supported by the existence of dermal MSC populations expressing CD146, but negative for endothelial markers.

1.6.2. Multi-lineage Differentiating / Stress Enduring (MUSE) Cells:

Given the elevated risk of immunogenicity and teratogenicity of embryonic pluripotent stem cells, stem cell researchers sought to identify non-tumorigenic, pluripotent adult stem cells [114]. Diverse stem cell subsets were reported, which repair damaged tissues without tumorigenic transformation *in vivo,* (Table 1.1). These include multipotent adult progenitor cells (MAPCs) [96], marrow-isolated adult multilineage inducible (MIAMI) [115] cells and very small embryonic-like stem cells (VSEL) [116]. Despite showing pluripotent stem cell traits, not all the adult stem cell candidates expressed the basic pluripotency markers, and the poor reproducibility of experimental results urged further investigations. On the other hand, a few studies highlighted the existence of multipotent MSC subsets, which are responsible for the repair of ectodermal, endodermal, and mesodermal tissues [117]. These MSC subsets, termed „repair cells" can trans-differentiate beyond the mesodermal lineage, and some of them were reported to have triploblastic differentiation potential. It has been already observed that human MSCs (H-MSC) spontaneously form floating clusters reminiscent of those nodes of ESCs [118]. To analyze the pluripotency of these MSC clusters, Kuroda et al. dissociated cells from H-MSC spheres followed by the exposure to different stress conditions. Stress activated MSCs expressed pluripotency markers and generated ectodermal, endodermal, and mesodermal lineage cells on gelatin coated dishes [119]. Because these stress-resistant cells showed advanced differentiation potential, they bestowed with the name multilineage differentiating, stress enduring (MUSE) cells.

Table 1.1: multipotent adult stem cell subsets				
Stem cell subset	**Biological source**	**Pluripotency markers expressed**	**Differentiation Potential**	**Reference**
MIAMI	(human) bone marrow	Oct3/4, Rex-1, telomerase	mesodermal: osteocyte, adipocyte, endodermal: pancreatic islet cell, ectodermal: neural cells	[116]
VSEL	(murine) bone marrow, (human) ovarian surface epithelium, umbilical cord blood	SSEA4, Oct-4A, NANOG, Rex-1	ectodermal, endodermal, mesodermal cells (with germ-layer markers), endothelial cells and cardiomyocytes	[117]
MAPC	(human/mouse) bone marrow	Not assessed	visceral ectoderm, lung/gut/liver epithelium, hematopoietic lineages	[118]
MUSE	(human) bone marrow, adipose tissue	SSEA4, Oct3/4, TRA-1-60, Sox2, NANOG	neuronal differentiation, hepatocytes, melanocytes, osteocytes, adipocytes	[119]

In contrast to MSCs, MUSE cells have a round morphology, and they form hESC-like spheres, (the so-called M-clusters) in suspension, (Fig.10A-C). MUSE cells are ubiquitous; they can be isolated from dermal fibroblasts, stromal vascular fraction, and bone marrow. MUSE cells do not associate to any specified niches, like the dermal papillae, nerve terminals or blood vessels, but they are distributed sparsely in bone-marrow, adipose tissue, and dermis. Furthermore, MUSE cells switch to a migratory phenotype during tissue

damage, migrate the sites of injury, and they reconstitute the injured tissue with mature cell types. The migration of MUSE-cells is controlled by chemokine ligands, especially CXCL2 [119].

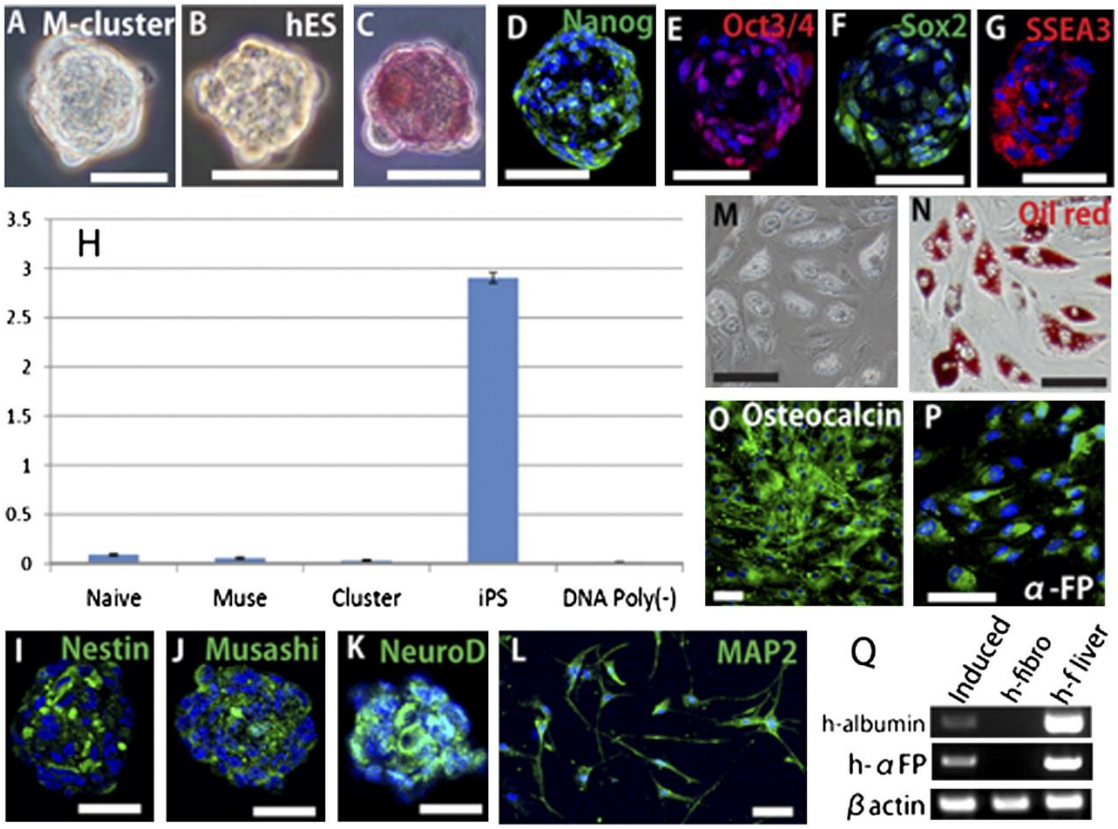

Figure 10. Pluripotency and tri-lineage differentiation of MUSE cells. *MUSE cells were enriched in 3-dimensional clusters of MSCs (M-cluster: A) after exposure to cellular stress (hypoxia, long-term trypsinization). These M-clusters show morphological similarity to those formed by human ESCs (B). Furthermore, M-clusters have high alkalic-phosphatase activity (C) and express pluripotent stem cell markers Nanog (D), Oct3/4 (E), Sox2 (F), SSEA3 (G). Despite their pluripotent stem cell traits, MUSE cells had significantly lower activity of telomerase activity (y axis of figure H, represented as fluorescence intensities in arbitrary units), compared to iPSCs, naive MSCs and non-MUSE clusters (H). MUSE cells undergo trilineage differentiation to form chondrocytes (M), osteocytes (N), adipocytes (O) and endodermal (AFP-positive) lineage cells (P, Q). MUSE cells also differentiate into ectodermal lineage cells expressing Nestin (I), Musashi (J), NeuroD (K) and MAP2 (L). Source:[120]*

The cell-autonomous and non-cell-autonomous mechanisms governing the mobilization of MUSE cells from their niches, and the molecular signals regulating MUSE cell migration remain to be elucidated.

MUSE cells are pluripotent stem cells bearing outstanding stress tolerance. They preserve their viability and self-renewal under harsh physicochemical conditions, such as

low temperature (4 °C), hypoxia (4% O_2), and long-term trypsinization. Under normal physiological conditions, MUSE cells preserve their quiescent, slow cycling state to maintain their ability to self-renew. After the exposure to stress *in vitro*, or tissue damage *in vivo* MUSE cells become activated, proliferate, and migrate to the damage sites. Several differentially expressed genes were discovered in MUSE cells compared to MSCs and dermal fibroblasts, including genes related to cell migration (CXCL2), survival (CDK6, MDH1, BRC1) and oxidative homeostasis (ALDH1A2, SOD2) [120], [121]. Furthermore, MUSE cells express pluripotency genes characterizing embryonic and induced pluripotent stem cells (OCT ¾, NANOG, Kfl, Myc), (Fig.10D-G). Another pluripotency marker specific for MUSE cells is the cell-surface glycosphingolipid, stage-specific embryonic antigen 3 (SSEA3), which enables separation of MUSE cells, as a CD105+SSEA3+ double positive fraction from dermal connective tissue, bone marrow aspirates and stromal vascular fractions [122].

Both *in vitro* and *in vivo* evidence suggest that MUSE cells have a triploblastic differentiation potential. Though they spontaneously generate ectodermal, mesodermal, and endodermal progeny on gelatin coated flask, their differentiation can be directed towards specific lineages in vitro by utilizing the appropriate differentiation medium [123], (Fig.10I-Q). For example, MUSE cells can give rise to osteoblasts and adipocytes with increased osteocalcin and oil red staining in osteogenic and adipogenic differentiation assays, respectively [124], (Fig.10M-N). MUSE cells express the endodermal marker α-fetoprotein and neural markers Nestin, MAP2 and neuroD when induced to differentiate into hepatocytes and neurons, respectively [125], [127], (Fig10.I-L). Moreover, melanocytes were generated from MUSE cells upon stimulation with melanocyte inducing factors (Wnt3a, stem-cell factor, endothelin-3). MUSE cell-derived melanocytes expressed melanocyte-specific genes (MITF, Tyrosinase) and migrating into the basal layer of epidermis in 3D cultures [128], [129]. The possibility that melanocytes were generated from MUSE cells suggests that MUSE cells could be a future therapeutic option for treatment of melanocyte dysfunctions.

The tissue-regenerative potential of MUSE cells was also demonstrated in several in vivo studies. In concert with their triploblastic differentiation, MUSE cells migrate into damaged skin, brain, muscle, and liver to reconstitute these tissues with functional differentiated cells. When transplanted into ischemic brain of mice, skin-derived MUSE

cells integrated into ischemic cortical areas, and differentiated into neural cells expressing NeuN, MAP2, GST-π and calbindin [130]. MUSE cells gave rise to functional neurons in these experiments, which was reflected in the improved motor functions and normalized hind-limb somatosensory evoked potentials. In another study, bone-marrow derived, GFP-labeled MUSE cells migrated into hepatic tissue and differentiated into hepatocytes, cholangiocytes, Kupffer cells and sinusoidal endothelial cells in partially dissected liver of immunocompromised mice [131]. In contrast, bone-marrow MSCs did not integrate into the liver upon partial hepatectomy, indicating that MUSE cells represent the predominant source among MSCs for hepatic regeneration. Given the observed beneficial effects of MUSE cell transplantation, it should be clarified whether MUSE cells exert their tissue-regenerative effects alone, or synergically with other cell types, such as bone marrow MSCs.

Unlike human ESCs and IPSCs, MUSE cells did not form teratomas when transplanted into murine testes despite having similar morphology and pluripotency markers to ESCs. The low teratogenicity of MUSE cells could be explained by the low expression levels of the Yamanaka factors (NANOG, Myc, Oct¾, Sox2) and their low telomerase activities, (Fig.10H). The expression of pluripotency-associated transcription factors raised the possibility that MUSE cells are reprogrammable to induced pluripotent stem cells, (iPSCs) [132]. Indeed, MUSE cells can be reprogrammed to IPSCs by the lentiviral delivery and overexpression of the Yamanaka factors. These MUSE iPSCs were able to differentiate towards all the three germ lines, and similarly to hESCs, they formed teratomas in mouse testis. The generation of IPSCs from MUSE cells points towards the elite model of IPSC theory that there is only a small subset of cells with the ability and appropriate set of transcription factors to generate IPSCs. In addition to their non-teratogenicity, MUSE cells suppress inflammatory responses, as well as cytotoxic CD8+ T-cell activation by a TGF-β-dependent manner [133]. These features make MUSE cells a promising source of pluripotent, non-tumorigenic stem cells and candidates for the generation of IPSCs from fibroblasts.

1.7. Cancer-associated Fibroblasts

Fibroblasts emerging within the tumor microenvironment affect cancer growth and spreading by several mechanisms. These stromal cells residing in solid tumor niches are termed "cancer-associated fibroblasts" (CAFs) due to their intricate interactions with cancer cells. In contrast to cancer cells and cancer stem cells, CAFs have a stable genotype, as they originate from tissue cells of their surrounding niches. Although this makes CAFs attractive targets for anti-cancer therapies, the heterogeneity of their origin and cellular phenotypes hampers their effective molecular targeting. CAFs are generated within the tumor niche from multiple cellular sources, such as pericytes, local stromal cells, epithelial cells, and adipocytes [134]. Local fibroblasts, MSCs and fibroblastic cells are activated by contact signaling (Notch, Ephrin) [135], inflammatory cytokines (IL-6, IL-1, TNFα) [136], stiff extracellular matrices [137], ROS and DNA damage [138]. CAFs are also generated from epithelial, non-fibroblastic cells by a phenotypic switch called epithelial-mesenchymal transition (EMT) [139]. EMT is induced by the activation of transcription factors SNAIL, TWIST and ZEB, which activate genes associated to cell motility, and down-regulate genes involved in cell adhesion. Cancer cells induce EMT in the local epithelial cells by secreting TGF-β, FGF and EGF. Activated CAFs undergo a profound shift in their gene-expression, which involves upregulation of genes related to cytokine/ growth factor signaling, extracellular matrix, EMT and angiogenesis. CAFs promote cancer growth by several mechanisms, which include immunosuppression, maintenance of chronic inflammation, promotion of cancer-drug resistance, angiogenesis, and ECM-remodeling, (Fig. 11).

Stromal cell immuno-regulation is a double-edged sword, which not only ameliorates autoimmunity and chronic inflammation, but also suppresses anti-tumor immune responses in the tumor microenvironment. CAFs recruit tumor-infiltrating macrophages to the tumor microenvironment by secreting chemokines, such as MCP-1, [140]. Furthermore, CAF-secreted cytokines, like IL-6, M-CSF and TGF-β drive macrophage polarization towards the immunosuppressive M2 phenotype, which inhibits anti-tumor immune responses, [141], [142]. In addition, fibroblast derived CSF1, CCL2 and ECM provides adhesion and survival of tumor-associated macrophages, which further activate fibroblasts by releasing IL-6, PDGFs and TGF-β, [143]. Besides macrophage polarization, tumor promoting CAFs secrete cytokines, such as PGE2 and TGF-β, all of which promote

differentiation of monocytes into immature dendritic cells and myeloid derived suppressors, inhibitory cells of effector T-cell function [143].

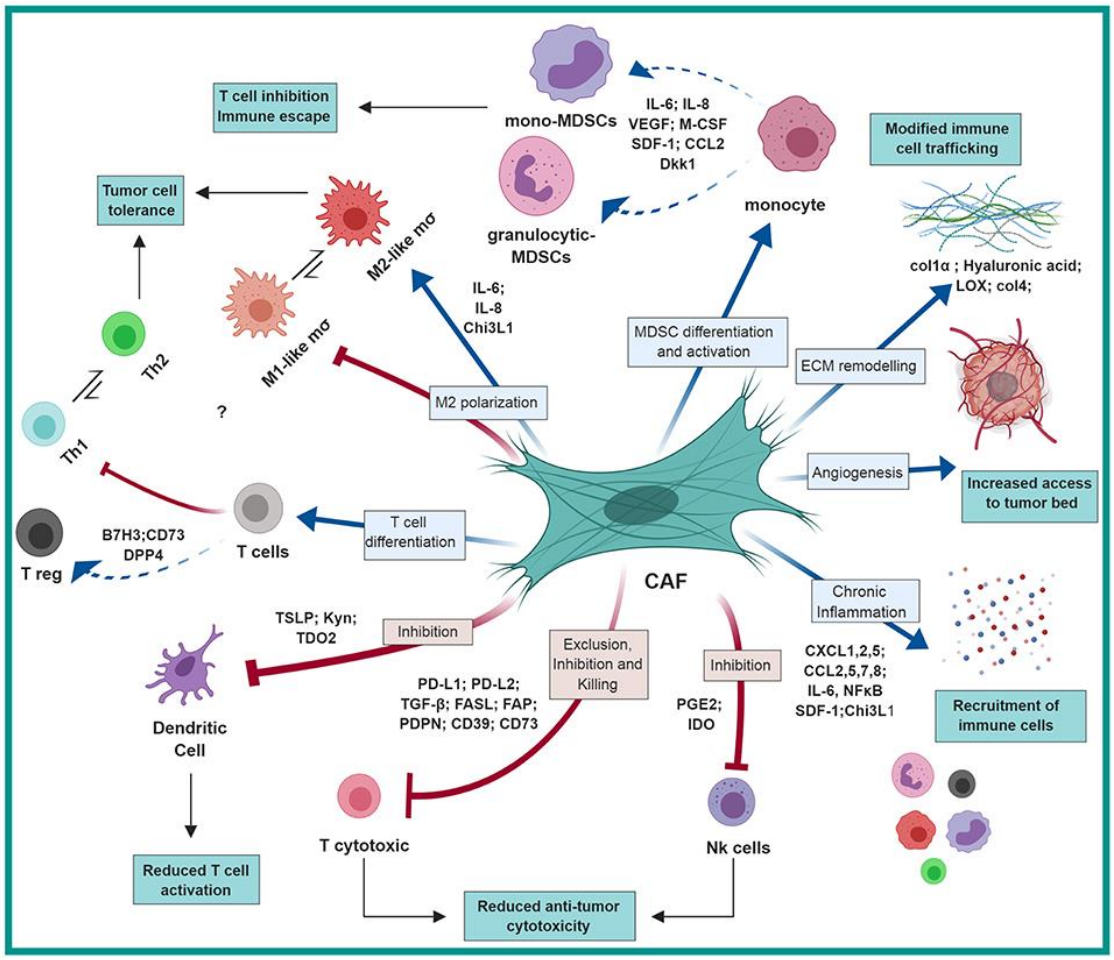

Figure 11. CAFs promote tumor growth by diverse intercellular interactions. *CAFs promote the maturation of M2 macrophages, inhibition of cytotoxic T-cells, NK-cells, and suppression of dendritic cells by secreting a plethora of cytokines. At the same time, CAFs maintain chronic inflammation in the tumor microenvironments, which recruits more immunomodulatory cells via chemokine ligand secretion (CXCL-1,2,5,7,8). CAFs also remodel the ECM through LOX and transglutaminase enzymes, which provide a stiff matrix, shielding the tumor from cytotoxic compounds. CAFs regulate angiogenesis and vasculogenic mimicry by VEGF and NOTCH-mediated intercellular signaling. Source: [140]*

CAFs also recruit immunosuppressive regulatory T-cells and regulatory dendritic cells into the tumor microenvironment through the secretion of IL-1 and IL-6, respectively, [145], [146]. CAFs influence the infiltration, survival, and differentiation of T-cell subsets

in multiple ways, such as, ECM thickening, immune-checkpoint blockade, programed cell death-ligands, anti-inflammatory cytokines, and antigen presentation, [147]. For example, CAFs upregulate the expression of CTLA4 on the surface of cytotoxic T-Cells through PGE-2, which inhibits inflammatory T-cell functions, [148]. CAFs also induce the expression of programmed cell death ligands PD-L1 and PD-L2 on adenocarcinoma cells, which inhibit CD8+ T-Cells by binding to PD-receptors, [149].

In addition to immune suppression, tumor-recruited CAFs mediate drug resistance of cancers by the upregulation of ABC-transporters [150], drug metabolic enzymes [152] or by the supplementation of cancer cells with antioxidant molecules [153]. For example, the upregulation of stress-responsive factor ATF-4 in CAFs from pancreatic cancer activates the transcription of multidrug-resistance gene ABCC1 in response to gemcitabine treatment [151]. Hypoxia and oxidative stress in the tumor microenvironment activate hypoxia-inducible factor-1 (HIF-1), which facilitates ECM-remodeling by upregulating the expression of MMPs and ECM crosslinking enzymes [154].

Another pro-tumorigenic function of CAFs is the maintenance of tumor microenvironment by facilitating angiogenesis [155] and regulating ECM-assembly [156]. The ECM is a key player in CAF-mediated tumor progression. CAFs synthetize thick, rigid ECM to shield the tumor from chemotherapeutic agents and limiting the infiltration of cytotoxic T-cells and NK-cells into the tumor microenvironment [157]. CAFs secrete transglutaminases [158] and lysyl-oxidase [159] to crosslink collagen and fibronectin fibrils within the tumor stroma. Cross-linked ECM fibrils promote increased cancer cell survival through focal adhesion/Srck signaling [160]. CAF-derived rigid ECM promotes cancer cell migration and invasion of cancer cells to the adjacent stromal niches. On the other hand, ECM-breakdown by CAFs enables cancer cell intravasation and invasion of cancer cells into pre-metastatic sites through the secretion of collagenases [161] and matrix-metalloproteinases (MMPs), [162]. Another implication of ECM-deposition, breakdown and assembly in the tumor environment is the promotion of tumor-angiogenesis.

CAFs fuel tumor-angiogenesis by secreting cytokines VEGF [163], HGF [164] and TGF-β [165], which promote endothelial progenitor-cell migration, activation of pro-angiogenic signaling pathways (HIF1α) and cancer-cell vascular mimicry. Furthermore,

CAF-secreted MMPs facilitate angiogenesis by releasing ECM-bound VEGFA [165] and bFGF [166] from ECM, recruiting pericytes and tumor-associated endothelial cells into the newly forming vessels.

Despite the pivotal importance of CAFs in tumor growth and progression was recognized in several solid tumors, limited information is available on the phenotypes and functions of CAFs in malignant metastatic melanomas.

1.8. Malignant Melanomas and Melanoma Stem cells:

Malignant metastatic melanoma is an aggressive, therapy-resistant skin cancer with poor survival and prognosis [167]. Although the primary tumors can be effectively eradicated by surgical dissection, they develop into metastatic stage rapidly, within a short period of time, (usually 2-6 months: [168]). Melanomas are cancers arising from the malignant transformation of melanocytes, pigment producing cells residing in the epidermal layer of skin. The most common driver mutations of melanomas occur in BRAF, NRAS, CDKN2A, CDK4 and p14ARF, frequently induced by prolonged exposure UV-B and UV-A [168]. Among them, the BrafV600E mutation gives rise to the most aggressively spreading, drug resistant, metastasizing cancers [170].

The early stage of melanoma spreading is characterized by a radial growth phase (RGP melanomas), where the survival and proliferation cancer cells are dependent on cell adhesion molecules and growth factors of their intraepithelial niche cells, (especially the keratinocytes) [171]. Upon the enrichment and selection of the more growth-factor-resistant cancer cell clones, melanomas transfer into vertical growth phase (VGP), where they spread into the dermal and subcutaneous layers. Furthermore, VGP melanomas facilitate the formation of cancerous microenvironments, which promote cancer immunosuppression, neo-angiogenesis, ECM remodeling and metastatic spreading.

Melanoma transformation involves the emergence of poorly differentiated, or de-differentiated cells, which acquire stem cell-like functions, such as drug-resistance, migratory phenotype, and high differentiation plasticity [173], (Fig.12).

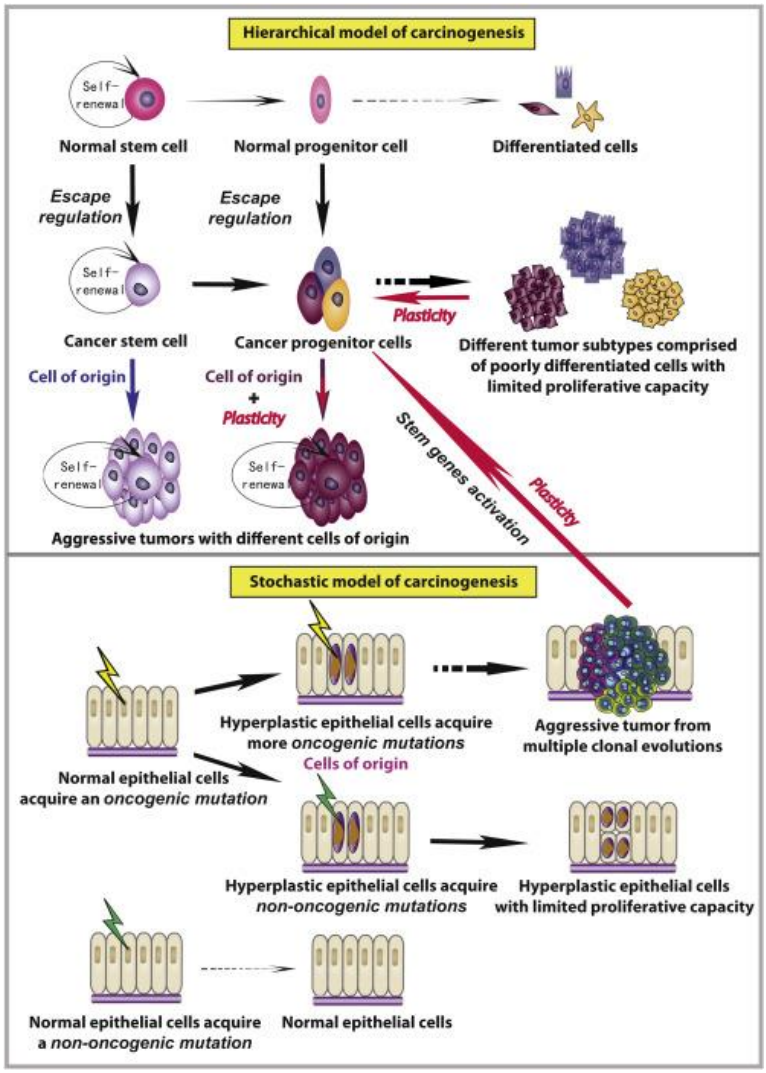

Figure 12. Hierarchical (top) and Stochastic (bottom) models of carcinogenesis and cancer growth. *According to the hierarchical model, cancerous cells arise from incompletely differentiated stem or progenitor cells of tissues. During their unregulated self-renewal, these stem/ progenitor cells acquire oncogenic mutations, which drive their transformation into cancer-initiating cells. Poorly differentiated cancer stem cells generate heterogeneous subclones of tumor cells to facilitate tumor growth and spreading. Conversely, the stochastic model emphasizes the effect of multiple oncogenic mutations occurring in the same cells. While the non-oncogenic mutations cause non-cancerous phenotypes, endowing the cells with a limited number of proliferations, cells with oncogenic mutations escape cell-cycle regulation, giving rise to the clonal evolution aggressive, resistant tumors. Furthermore, cancer cells engage in a stem-cell like phenotype through the reactivation of stemness genes. This de-differentiation process unifies the two models through the generation of tumor-initiating cancer stem cells. Source: [172]*

Although the de-differentiation of malignant cells is a complex process, which involves microenvironmental factors and cell-autonomous mechanisms, two different models were proposed to describe the process of cancerous transformation and spreading, (Fig.12.). According to the hierarchical model, normal tissue stem cells and their progenitors escape homeostatic cell cycle regulation and gain unlimited capacity for self-renewal. Besides, cancer stem cells and their progeny generate diverse tumor cell subsets to promote cancer growth and heterogeneity. The hierarchical model of carcinogenesis has been challenged by the observation that cancer cells with non-CSC characteristics can de-differentiate into CSCs (Fig.12, Fig.13). This phenomenon is driven by the stochastic acquisition of oncogenic mutations, which culminate in the activation of stemness genes. Although cellular subsets with stem cell properties were discovered in melanoma, several studies reported the non-hierarchical nature of melanoma genesis, and spontaneous de-differentiation of cancer cells into tumor-initiating CSCs [174]. These studies suggest that the emergence of tumor-initiating cells is not unidirectional, and CSCs can be induced and enriched by hypoxia and local inflammatory milieu of the melanoma microenvironment [175]. The immunosuppression in the tumor-microenvironment is not exclusively maintained by cancer cells, but also by tumor infiltrating macrophages, immunosuppressive regulatory T-cells, and melanoma-associated stromal cells (Fig.13.). On the other hand, stem cell subpopulations in melanoma were identified by the expression of hematopoietic (CD133), neural and neural crest stem cell (ABCB5, CD271) markers [176].

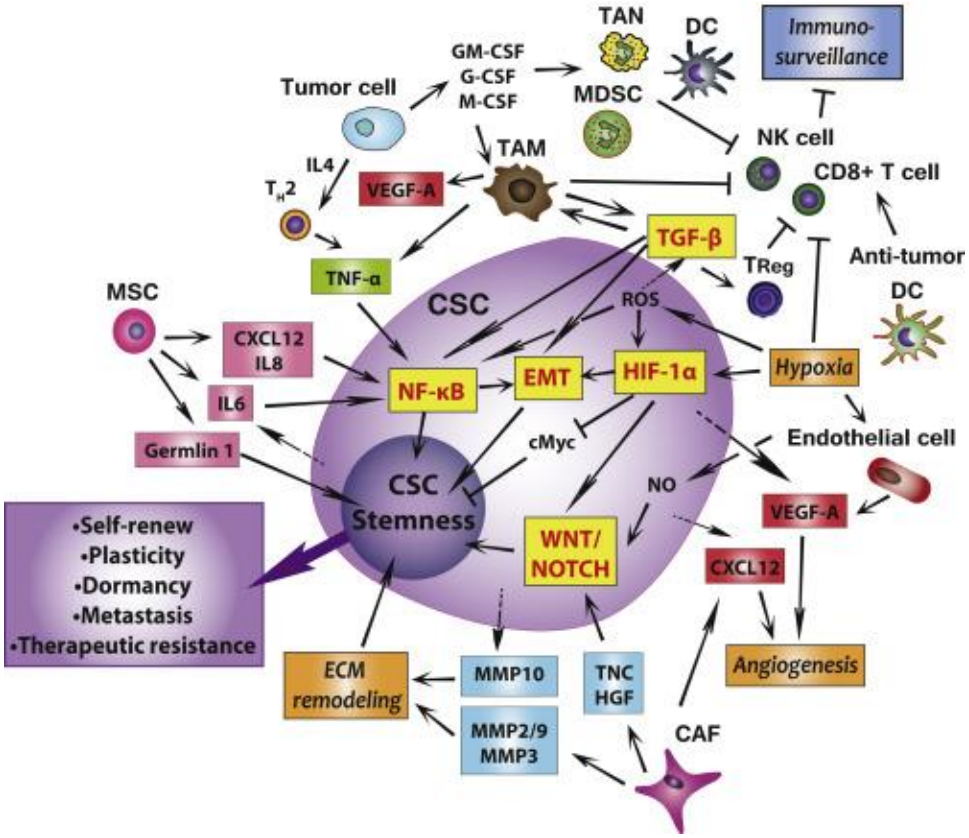

Figure 13. Cancer stem cells are maintained by the tumor microenvironment through diverse mechanisms, including hypoxia, inflammation, ECM remodeling and angiogenesis. *Tumor cells release macrophage-inducing cytokines (GM-CSF, M-CSF, G-CSF) to activate tumor-associated macrophages (TAMS). In turn, TAMS suppress CD8+ T-cells and NK-cells by producing TGF-β and IL-10. Furthermore, TGF-β activates epithelial-mesenchymal trans-differentiation of cancer cells, a phenotypic switch activating stemness genes. TNFα from tumor-infiltrating immune cells (TH2) activates the NFKβ pathway, which facilitates cancer stem cell self-renewal. Likewise, hypoxia in the tumor microenvironment leads to the generation of reactive oxygen species (ROS). ROS triggers the hypoxia-sensitive transcription factor HIF1a, which drives the transcription of stem-cell specific genes. Besides, HIF1a upregulates the NOTCH and Wnt signaling pathways to maintain cancer stem cells in an ESC-like state. CAF-mediated remodeling of the ECM by matrix-metalloproteinases (MMPs; MMP2/9, MMP3, MMP10,) triggers cancer stemness by focal adhesion-dependent signaling. Furthermore, cancer stemness is also facilitated by endothelial signaling molecules, such as nitrogen-monoxide. Source: [172]*

1.9. Melanoma-associated Fibroblasts

Several studies emerged reporting the critical role of melanoma stem cells in drug resistance [177], metastasis [178] and angiogenesis [179]. On the other hand, malignant melanoma niches contain reactive fibroblasts, termed 'melanoma associated fibroblasts' (MAFs), which regulate tumor growth, progression, and cancer stemness by intricate mechanisms.

In a study analyzing MAFs from both non-metastatic and metastatic melanomas, MAFs were described as myofibroblast cells, which express α-smooth muscle actin (αSMA), fibroblast activation protein (FASP), fibronectin, col11A and vimentin [180]. In addition, MAFs secreted significantly higher levels of IL-6, IL-8, tissue inhibitor of metalloproteinase-2 (TIMP2) and CCL11 chemokines compared to normal human fibroblasts. Despite the reported morphological characteristics and secretory profile, only limited information is available the cell surface markers identifying MAFs and their subsets.

MAFs suppress inflammatory immune cells by diverse mechanisms. Hypoxia in the melanoma microenvironment activates the secretion of several immunosuppressive factors, such as TGF-β, PD-L1 and IL-10 to inhibit T-cell-mediated cytotoxicity. Metastatic melanoma cells of the TF1 and TF2 cell lines inhibited NK-cell-mediated cell death through the downregulation of triggering receptors (DNAM-1, NKp30, NKp44) and cytolytic granules [181]. MAFs also inhibit anti-tumor immunity through the repression of immune checkpoint receptors. Conditioned medium of MAFs upregulated the expression of negative immune checkpoint receptors, TIGIT and BTLA on cytotoxic T-cells [182]. Furthermore, MAFs showed high L-arginase activity and increased expression of BTLA-ligands VISTA and HVEM. MAFs not only impede T-cell-mediated cytotoxicity, but also influence macrophage phenotypes in the tumor microenvironment [II]. MAFs induce the secretion of anti-inflammatory mediator IL-10 from macrophages in a cyclooxygenase- and indoleamine 2,3-dioxygenase-depentent manner.

MAFs interact with the tumor microenvironment not only by soluble messengers, but also through exosomes. Exosome release from melanoma cells melanoma is triggered by hypoxia and acidic pH within melanoma microenvironments [183]. Melanoma-derived exosomes are enriched in miRNAs, long non-coding, RNAs, metabolites, lipids, and heat-

shock proteins, which activate pro-angiogenic genes ('angiogenic switch') in MAFs through the NFKβ pathway [184]. Fox example, it was reported that cancer-derived exosomes are enriched in miR-155, which promote the expression of angiogenic factors VEGFa and MMP9 in MAFs [185].

Remodeling of the ECM plays a crucial role in immune-cell infiltration and metastasis of melanoma. Melanoma metastasis is facilitated by MMP-14 secreted by melanoma cells, which breaks down collagen XIV, [186]. Collagen XIV inhibits proliferation, adhesion, and migration of melanoma cells, thus the depletion of collagen XIV in melanoma promotes tumor progression. Likewise, Hyaluronan and Proteoglycan Link Protein 1 (HAPLN1) limits cell migration by crosslinking collagen fibers and facilitates immune-cell infiltration [187]. Depletion of HAPLN1 from ECM increases melanoma cell invasion and migration. Thus, age-dependent loss of HAPLN1 promotes remodeling of the ECM, which becomes permissive for melanoma invasion and metastasis.

1.10. Stem Cell Subsets of CAFs

Despite the lack of knowledge on the contribution of local stem cell subsets to melanoma growth, the significance of MSCs in malignant melanoma prognosis was reported. The pro-inflammatory milieu of the tumor microenvironment in melanoma produces MSCs, which are immunosuppressive and promote cancer cell spreading with diverse mechanisms, [II], [188]. MSCs in the tumor microenvironment suppress anti-tumor immune responses by inducing the secretion of soluble mediators (IL-10, PGE, IDO), which activate regulatory T-cells, M2 macrophages and inhibit B-cells, dendritic-cell maturation, NK-cell and CD8+ T-cell functions. In addition, MSCs secrete TGF-β, which enhances melanoma cell motility through the induction of EMT, [189].

MSCs in cancer niches promote angiogenesis by pro-angiogenic factors, such as TGF-β, VEGF and MIP-2, thus, they promote angiogenesis in tumor niches and pre-metastatic tissue environments [190]. Other MSC-derived pro-angiogenic factors, like MFG-E8 act indirectly, by facilitating the expression of VEGF and ET-1 in MSCs and polarizing macrophages towards M2 phenotypes [191]. Furthermore, MSCs from the cancer niche form capillary-like structures to promote tumor-cell angiogenesis by VEGF-A mediated manner in melanoma. Tumor-associated MSCs protect cancer cells directly from apoptosis

by the release of soluble factors activating pro-survival/ anti-apoptotic signaling molecules (Akt, BCl2), or by suppressing the anti-tumorigenic effects of p53.

Although several functions of CAFs and MSCs in the tumor microenvironment were reported, scant knowledge is available on the stem cell sources producing CAFs. In addition, the interaction of stromal stem cells of the human dermis (MUSE, SKP, DPSC, MSC) with melanoma cells has not been characterized yet. Neither the presence, proportion, and differentiation plasticity of MSC subsets and melanogenic MUSE cells are known in melanoma microenvironments.

2. Specific Aims

Malignant metastatic melanomas are the deadliest skin cancers due to high drug resistance and fast spreading of tumor cells. Melanoma cells have strikingly high differentiation plasticity, which endows them with the ability to generate genetically heterogeneous cancer stem cell populations in the tumor microenvironment. Conversely, cancer associated fibroblasts have stable genotype, which makes them attractive targets for anti-cancer therapies. Although, limited information is available on the specific cellular markers enabling the identification and targeting of MAFs. Furthermore, little is known on the differentiation plasticity of MAFs and its implications on melanoma growth and spreading.

The purpose of my doctoral research was to analyze and compare the molecular phenotype and the stem cell characteristics of MAFs. Given that cell surface markers and lineage differentiation potential of MAFs are incompletely characterized, here I set out to address the following questions.

(1) Which MSC markers do MAFs have?
(2) What is the difference between the tri-lineage differentiation potential of stromal stem cells in melanoma compared to normal skin?

Although, the presence of SSEA3+ fibroblasts in adult stromal niches were demonstrated [159], the presence, ratio, and pluripotency of those cells in melanoma has not been characterized yet. Furthermore, the generation of melanoma-competent melanocytic cells from SSEA3+ or other stromal stem cells in melanoma was not evaluated. Hence, I've sought to address, whether

(3) Pluripotent MUSE cells are present among MAFs, and
(4) If MUSE cells from melanoma undergo melanocyte lineage differentiation?

3. Experimental Procedures

3.1. Ethics Statement

Surgically removed tumors and naevi were obtained from patients at the Department of Dermatology, Venereology and Dermato-oncology, (Semmelweis University, Budapest, Hungary). Tissue samples were collected for research after obtaining the patient's informed consent. The study was conducted according to the Declaration of Helsinki principles and approved by the Hungarian Scientific and Research Ethics Committee of the Medical Research Council (ETT TUKEB; Decree No. 32/2007, supplements 32-2/2007 and 32-3/2007).

3.2. Isolation of Dermal Fibroblasts and Melanoma-associated Fibroblasts

Dermal fibroblasts (DFs) were isolated from non-tumorous skin tissue slices. Skin tissues pieces were exposed for 2 hours in dispase (Gibco, Gaithersburg, MT) at 37 °C. Then, the digested epidermis was removed by tweezers, and dermal tissue was digested in collagenase-dispase solution for 2 hours with vortexing every 15 minutes. The solution containing the digested tissue was flown through a 70 μm strainer to remove tissue aggregates. The obtained cell suspension was centrifuged, and resuspended in DMEM containing 20% FBS, 1% GlutaMax and 1% Pen/Strep (Gibco), followed by the seeding of the cells into tissue culture flasks. Cells were grown at 37 °C and 5% CO_2 and we changed half of the culture medium with fresh medium every third day.

In contrast to dermal fibroblasts, MAFs are encapsulated into the tumor core. Thus, thorough separation of subcutaneous melanoma tumors from the surrounding dermal or adipose tissue is required. The next major issue is the separation of cancer cells from cancer-associated stromal cells. Although most melanomas contain pigmented, mildly adherent cells, some melanoma subsets have higher adherence and motility, [191]. Differential adherence of melanoma cells can be addressed by transient (30 minutes) exposure of the cell suspension in DMEM containing 10% fetal bovine serum, and subsequent collection of the supernatant medium containing the floating tumor cells. Then, adherent cells are resuspended in DMEM with 20% FBS to provide the growth of MAFs. To ensure a pure fibroblast population, the culture must be checked regularly for

pigmented melanoma cells, expression of fibroblastic (FAP) and lack of melanocytic markers (MITF, GP100, DCT).

MAFs were isolated from surgically removed melanomas after obtaining the patients informed consent. Tumorous tissue was dissected from dermis, epidermis, and subcutaneous fat, chopped into smaller pieces by scalpels, then digested in collagenase-dispase solution for 2 hours to obtain single cells. Tissue slices were vortexed every 15 minutes during the incubation in collagenase-dispase solution (Gibco). To remove large cell aggregates, the solution with the digested tissue was flown through a 70 µm cell strainer (provided by Greiner Bio-one Ltd, Mosonmagyaróvár, Hungary), and centrifuged at 400 rpm for 5 minutes. Cellular pellet was resuspended in low glucose Dulbecco's modified eagle medium (DMEM, by Sigma Aldrich, St. Louis, MO) containing 10% fetal bovine serum (FBS; Corning, Tewksbury, MA) and incubated in a 25 cm^2 tissue culture flask (Corning, New York, USA) at 37 ^oC for 30 minutes to promote the attachment of fibroblast cells on the bottom of the flask, and the enrichment of cancer cells in the supernatant. Then, supernatant containing floating cells was removed by serological pipette and deposited into a new 25 cm^2 cell culture flask. Adhered cells were supplied with DMEM (Sigma Aldrich) containing 20% FBS, 1% Pen/Strep and 1% GlutaMax (Gibco) before putting back into the cell incubator (37 ^oC, 5% CO_2). We changed half of the cell culture medium on MAF cells every third day.

3.3. Methods for *in vitro* characterization

3.3.1. Immunocytochemistry

For immunocytochemical staining, we fixed cells in 4% paraformaldehyde (PFA) for 15 minutes, followed by permeabilization with 0.2% Trinton X-100 (Sigma) for 15 minutes and blocking in 2% bovine serum albumin (BSA, Corning) for 1 hour. Cells were incubated overnight with primary antibodies listed in table 3.2. at 4 ^oC. For secondary staining we used goat anti-mouse Cy3 conjugated antibody (purchased from Sigma), or donkey anti-rabbit Cy3 conjugated secondary antibody (purchased from Sigma). Nuclei were stained with the DNA-binding dye 4',6-diamidino-2-phenyl-indole (DAPI).

For setting up antibody staining for ectodermal and endodermal markers, we used immortalized cells or cancer cell lines originating from the given lineage, (Table 3.1). We choose cell lines with robust lineage marker expression, minimal cell culture requirements and fast growth kinetics. For the staining ectodermal neural markers MAP2, ENO2 and Nestin, we used A172 glioblastoma cell lines, while ectodermal melanocytic marker melan-A was assayed on SKMEL-28 and MALME-3M melanoma cell lines. We used HEP3B hepatocellular carcinoma cells to optimize the immunostaining of endodermal markers alpha-fetoprotein (AFP) and albumin. NTERA2 teratocarcinoma cells were used as positive control to assay pluripotency markers (OCT3/4, NANOG, TRA-1-60) expression.

Table 3.1. Cell Lines Used to Optimize Immunocytochemical Staining of Cellular Markers

Cell line	Tissue Origin	Disease	Markers	Reference
SKMEL-28	Skin	Melanoma	GP100, Melan-A, DCT, TYR, TRP-1	[193]
MALME-3M	Skin	Malignant Melanoma	GP100, Melan-A, DCT, TYR, TRP-1	[194]
A172	Brain	Glioblastoma	Nestin, Enolase-2, MAP2, mGLUR1	[195]
HEP-3B	Liver	Hepatocellular carcinoma	AFP, albumin, Cytokeratin-18	[196]
NTERA2/D1	Testis	Testis carcinoma	SOX2, OCT3/4, NANOG, TRA-1-60	[197]

Table 3.2. Antibodies Used for ICC					
Manufacturer/ Catalog no.	**Target**	**Host/ Clonality**	**Specificity**	**Isotype**	**Concentration**
Pluripotency					
Santa Cruz Sc-5279	Oct 3/4	Mouse, monoclonal (C10)	Mouse, Rat, Human	IgG2b	1:50
Merck Millipore AB5603	Sox2	Rabbit, Polyclonal	Human, Mouse	-	1:50
Abcam Ab16288	TRA-1-60	Human, Mouse Monoclonal (clone TRA-1-60)	Human	IgGM	1:100
Neuron					
Merck Millipore MAB5326	Nestin	Mouse, monoclonal (clone 10C2)	Human	IgG1	1:00
Melanocyte					
Abcam ab51061	Melan-A	Rabbit, monoclonal (clone EP1422Y)	Human	IgG	1:100
Hepatocyte					
MAB1368	Alfa-fetoprotein (AFP)	Mouse, monoclonal (Clone # 189502)	Human, Mouse	IgG1	1:50
sc-271605	Albumin	Mouse, monoclonal	Human, Mouse, Rat	IgG1	
Osteocyte					
ab95462	Alkaline Phosphatase (ALPL)	Rabbit, polyclonal	Human, Mouse, Rat	-	1:100
Adipocyte					
Cell Singlaing Technology	CEBPα	Rabbit, polyclonal	Human, Mouse, Rat	-	1:50
Secondary Antibodies					
Sigma Aldrich C2181	Anti-Mouse F(ab')2 fragment-Cy3	Sheep Polyclonal	Mouse	IgG	1:200
Sigma Aldrich C2306	Anti-Rabbit F(ab')2 fragment-Cy3	Sheep Polyclonal	Rabbit	IgG	1:100

3.3.2. Quantitative Real-time Polymerase Chain Reaction (RT-qPCR) with FAM-conjugated TaqMan Probes:

RNA extraction from 500.000-2000.000 cells was performed by using RNeasy mini kit of Qiagen, (Hilden, Germany). Briefly, cellular samples were lysed with RLT-buffer, and nucleic acids were precipitated by ethanol. Genomic DNA was eliminated by treating the samples with DNAse1 at room temperature for 30 minutes, followed by washing the samples through RNA-binding spin columns with washing buffers RW and RPE. RNA samples were eluted from the spin columns by adding nuclease-free dH_2O. For cDNA-synthesis we reverse-transcribed 1 µg RNA by using the MMLV reverse-transcriptase enzyme provided by Promega with oligo-dT primers, (Madison, USA). We measured qPCR in Lightcycler® 480. The FAM-MGB conjugated TaqMan Probes (by Thermo Fisher Scientific) used are listed in Table 3.3. below. We used GAPDH as a house-keeping control. Reaction mixes were incubated at 50 ^oC for 2 minutes, followed by denaturation (95 ^oC, 10 minutes). For the amplification we used 40 cycles starting with 95 ^oC, 15 seconds, followed by 60 ^oC for, 1 minutes and 72 ^oC, 1 second. Undifferentiated cells were used as internal, (normalization) controls for the calculation of C_T values.

Table 3.3. TaqMan Probes Used for qPCR Measurements			
Assay ID	**Gene**	**Assay design**	**Amplicon Length (bp)**
Pluripotency			
Hs01053049_s1	SOX2	Within a single exon	91
Hs00999634_gH	POU5F1	Spans exons	64
Hs02387400_g1	NANOG	Spans exons	109
Melanocyte			
Hs00173854_m1	PMEL	Spans exons	86
Hs01117294_m1	MITF	Spans exons	81
Hs01098278_m1	DCT	Spans exons	64
Hs00167051_m1	TYRP1	Spans exons	88
Neuron			
Hs04187831_g1	NES	Spans exons	58
Hs00258900_m1	MAP2	Spans exons	98
Hs00157360_m1	ENO2	Spans exons	77
Hepatocyte			
Hs00173490_m1	AFP	Spans exons	82
Hs00559840_m1	CK7	Spans exons	95
Mm01601704_g1	CK18	Spans exons	62
Hs00609411_m1	ALB	Spans exons	104
House keeping			
Hs99999905_m1	GAPDH	Amplicon spans exons/ probe does not span exons	122

3.3.3. Flow Cytometry and Fluorescence-activated Cell Sorting (FACS)

Flow cytometry and Fluorescence-activated Cell Sorting (FACS):

For flow cytometric analysis, 200.000 MAFs in flow cytometry tubes (Corning) were washed in phosphate-buffered saline (PBS), then the samples were centrifuged at 1000 rpm for 5 minutes and resuspended in flow cytometry buffer (PBS containing 2% FBS). MAFs were incubated with FC-receptor blocker (produced by Thermo Fischer) for 10 minutes, followed by incubation with primary antibodies for FITC-conjugated CD90, APC-

conjugated CD271, PE-conjugated SSEA3 (all from eBioScience, California, USA) and viability dye 7-amino-actinomycin-D (7AAD Thermo Fisher) for 30 minutes, (see Table 3.4. for the antibodies). After incubation of MAFs with antibodies, cells were washed with flow-cytometry buffer and resuspended in 500 µl flow cytometry buffer before the measurements. Single colored samples stained for CD90-PE (eBioScience), CD105-APC, CD90-FITC, and cells treated with 100 % methanol followed by incubation with 7AAD were used as compensation controls, while unstained cells were used to set signal thresholds for positive cell populations.

Table 3.4. Antibodies used for flow cytometry and FACS-sorting

Manufacturer /Catalog no.	Target	Host/ Clonality	Isotype	Conjugation	Dilution
BioLegend BZ-34003	CD73	Mouse, monoclonal (AD2)	IgG1	PE	1:50
BioLegend BZ-328107	CD90	Mouse, monoclonal (5E10)	IgG2b	FITC	1:50
Merck Millipore AB5603	CD105	Rabbit, Polyclonal	-	APC	1:50
Miltenyi Biotech BZ-345108	CD271	Mouse Monoclonal (clone ME20.4-1.H4)	IgG1	APC	1:100
Invitrogen 13-8833-82	SSEA3	Rat, Monoclonal (clone MC-631)	IgM	Biotin (used with PE-streptavidin)	1:300
EBioScience12-8833-42	SSEA3	Rat Monoclonal, (clone MC-631)	IgM	PE	1:50

For sorting SSEA3+ cells, we used biotinylated antibody against SSEA3 with PE-conjugated streptavidin, which binds biotin with high affinity, (Fig.14). 5-10 million MAF cells were used for FACS in single-cell suspension. Cells were washed in PBS and stained with fixable NIR viability dye (provided by Thermo Fischer) according to the manufacturer's instructions. Then, cells were washed in FACS buffer (0.5% BSA, 2mM EDTA, all from Sigma), and incubated with FC-receptor blocker (TruStain FcX Fc receptor blocker by BD Pharmingen, (San Diego, USA) for 10 minutes. FC-receptor blocking was followed by incubation with 10 ng/µl biotin-conjugated rat SSEA3 antibody (Thermo

Fischer Scientific, Waltham, Massachusetts, MA) and 4 ng/µl FITC-conjugated mouse CD90 antibody (eBioScience) for 30 minutes at 4 °C. Cells were washed with FACS buffer, and 750 ng/ml PE-streptavidin (eBioScience) was added for 30 minutes. Excess dye was removed by washing in FACS buffer, and cells were resuspended in 0.5 mL FACS buffer before the measurement. For FACS we used MA900 FACS-sorter of Sony Biotechnology (San Diego, USA). Live (nIR-negative) cells were gated out from the main population appearing on the forward scatter/ side-scatter (FSC/SSC) plot, followed by setting a gate on CD90+SSEA3+ double stained cells.

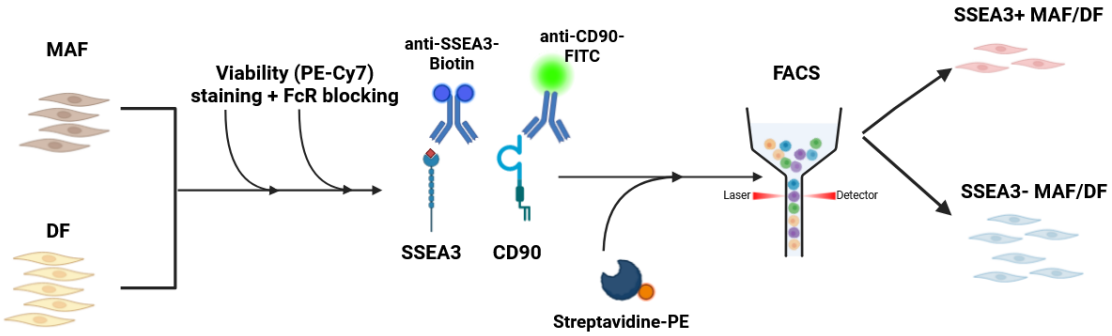

Figure 14. Labeling strategy for sorting SSEA3+CD90+ cells using FACS. *MAFs and DFs were stained for viability dye PE-Cy7, which was followed by FcR-blocking to avoid non-specific antibody binding to the Fc-receptors. After blocking, cells were incubated with biotin-conjugated anti-SSEA3 antibody and FITC-conjugated CD90+ antibody. To amplify the SSEA3 labeling, cells were incubated with PE-conjugated streptavidin. Both SSEA3+ and SSEA- cells were used for further experiments.*

3.4. *In Vitro* Differentiation Assays:

MAF and DF cells were stimulated to undergo ectodermal (neural, melanocytic), endodermal (hepatic) and mesodermal (osteocyte, adipocyte) differentiation, which was followed by assaying the lineage markers by ICC and RT-qPCR. For setting up the in vitro characterization assays of ectodermal and endodermal lineages we used immortalized cell lines of ectodermal and endodermal origins. A172 neuroblastoma cells were used for neural markers, while HEPG3 hepatocarcinoma cells were used for hepatic markers.

Pluripotent NTERA2 clone D1 cells were used to optimize in vitro tri-lineage (ectodermal, mesodermal, endodermal) differentiation, (see [197], [198] and results).

3.4.1. *In Vitro* Neural and Melanocyte Differentiation:

To induce neural differentiation, 10^5 cells/cm^2 were seeded on ultra-low attachment plates (Corning) in completed neurobasal medium comprising of Neurobasal medium with 1 X B27 supplement, 1XN2 supplement, 1% Pen/Strep (all from Gibco) with 30 ng/mL epidermal growth factor and 30 ng/mL basic fibroblast growth factor (bFGF) (all from Peprotech, London, UK) added, (Fig.15). Medium was changed every other day. After 14 days of cultivation, spheres were collected and plated into poly-D-lysine-coated dishes for 10 days of neural induction in α-MEM supplemented with 2% FBS, 1% Pen/Strep, 25 ng/ mL bFGF and 25 ng/mL brain-derived neurotrophic factor (BDNF) (Peprotech). At the end of neural induction samples were processed for immunocytochemistry (ICC) and quantitative real-time polymerase chain reaction (qRT-PCR). A172 glioblastoma cells were used as positive control for ICC experiments. Mean intensities of ICC stainings for Nestin in undifferentiated MAFs, differentiated MAFs and A172 cells were quantified using ImageJ and normalized to the mean intensities of DAPI staining.

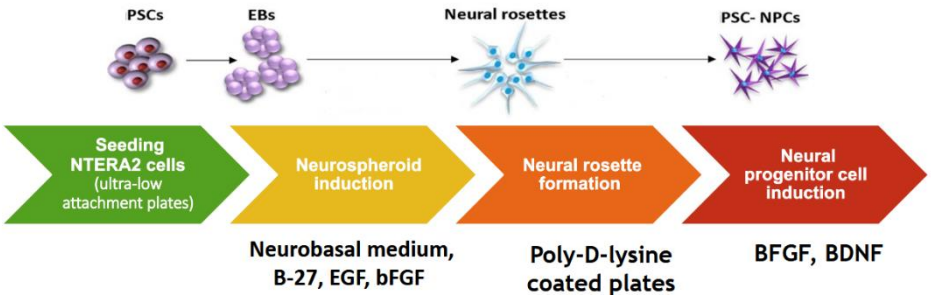

Figure 15. Overview of the differentiation protocol we devised for neural lineage differentiation of stem cells. *Pluripotent NTERA2 cells were used to optimize the in vitro neural differentiation assay. Embryoid bodies were generated from the cells on ultra-low attachment plates within 14 days in Neurobasal medium supplemented with B-27, N2 epidermal growth factor (EGF) and basic fibroblast growth factor (bFGF, FGF2). At day 14, spheres were transferred onto poly-D-lysine coated plates. Neural differentiation was induced by bFGF and BDNF in α-MEM medium containing 2% FBS.*

For melanocytic differentiation, we used the protocol by Yamauchi et al, (2013) [129], (Fig.16). Sorted SSEA3+ and SSEA3- cells were seeded into fibronectin-coated dishes in DMEM containing 20% FBS, 1% GlutaMax and 1% Pen/Strep. On the next day, medium was switched to melanocytes differentiation medium, which is 50% high-glucose DMEM, 30% low glucose DMEM, 20% MCDB201 medium containing 0.05 M dexamethasone (Sigma-Aldrich, St Louis, MO), 100 μM L-ascorbic acid, 1 mg/ml linoleic acid–BSA, 1 ×insulin–transferrin–selenium (Invitrogen), 50 ng/ml SCF (R&D Systems, Minneapolis, MN), 10 ng/mL endothelin-3 (ET-3, Sigma-Aldrich), 50 ng/mL Wnt3a, 20 pM cholera toxin (Wako, Osaka, Japan), 50 nM 12-O-tetradecanoyl-phorbol 13-acetate (Sigma-Aldrich), and 4 ng/ml bFGF. Cells were differentiated in this melanocyte medium for 42 days. At day 42 of differentiation, cellular samples were processed for ICC and qRT-PCR.

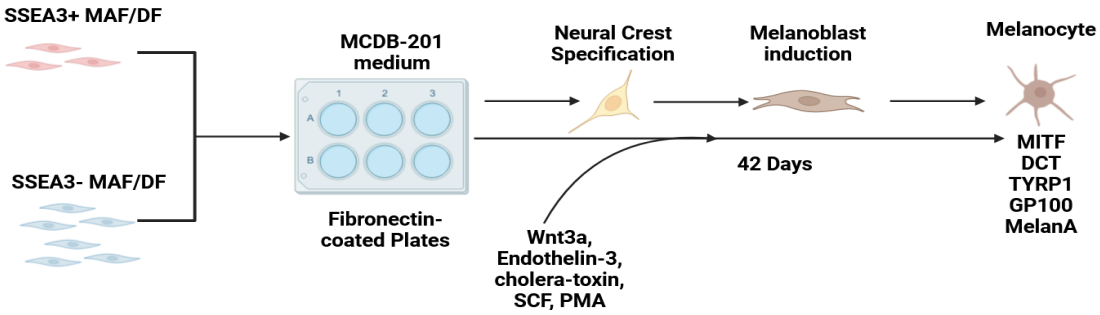

Figure 16. Method for in vitro melanocyte differentiation from SSEA+ and SSEA- cells, which were sorted from MAFs or DFs. *Cells were plated into fibronectin-coated plates and melanocytes differentiation was initiated by the addition of Wnt3a, Endothelin-3, SCF, PMA and cholera-toxin to the cell culture medium. Medium was changed every other day until day 42 of differentiation. On day 42, cells were characterized for the expression of melanocyte-specific markers.*

3.4.2. *In Vitro* Osteocyte and Adipocyte Differentiation:

To induce osteogenic differentiation, 1000.000 MAFs were seeded into tissue-culture treated 6-well plates with DMEM supplemented with 10 nM dexamethasone, 100 µM ascorbic acid, 2 mM β-glycerophosphate (all from Sigma), 20% FBS, 1% P/S and 1% GlutaMax (Gibco) for 21 days. Media was changed every 3rd day. At day 21, cells were fixed with 4% PFA for 15 minutes, and calcium-phosphate complexes were stained with Alizarin-Red S (ARS) for 30 minutes, followed by washing four times with double distilled water. ARS bound to calcium-phosphate complexes was extracted with 20 mM acetic acid, and the concentration of the extracted dye was calculated by measuring OD_{450}. In addition to the measurements of OD_{450} values of the extracted ARS, osteocyte markers were assayed by ICC and RT-qPCR.

Adipogenic differentiation was induced by plating 1000.000 MAFs into 6-well tissue culture-treated plates in low-glucose DMEM containing 0.5 mM 3-isobuthyl-2-methylxanthine (IBMX), 50 µM indomethacin, 0.5 µM hydrocortisone, 10 µM recombinant human insulin, 10 µM troglitazone, (all from Sigma), 20% FBS, 1% P/S and 1% GlutaMax. Medium was changed every third day until day 21 of differentiation. Lipid droplets were stained by fixing the cells in 4% PFA (15 minutes), rinsing them with 60% iso-propanol followed by 15 minutes incubation with the lipophilic dye Oil-Red O (ORO) in 2:3 ratio with double distilled water. ORO was extracted from the lipid droplets by using 60% isopropanol, and the intracellular ORO concentrations were calculated by measuring OD_{506} values of the extracted dye. Adipogenic markers were assayed by ICC and RT-qPCR.

3.4.3. *In Vitro* Hepatocyte Differentiation:

We used two methods for hepatocyte differentiation published by Mallana et al [40] and Wakao et al [132]. In the first method, we recapitulated hepatic differentiation in vitro by seeding $2x10^4$ cells/cm^2 on bovine collagen I-coated dishes (Gibco) in hepatic differentiation medium (HDM; DMEM supplemented with 10% FBS, 1X insulin-transferrin-selenium (Gibco), 10 nM dexamethasone (Sigma), 0.6 mg/mL nicotinamide (Sigma)), (Fig.17). Until the second day of differentiation, HDM was supplemented with 10 ng/mL bone-morphogenic protein-4 (BMP4 by RnD), 50 ng/mL fibroblast growth factor-4 (FGF4, by Peprotech) and 100 ng/mL activin-A (R&D). Between day 2 and day 5 cells were kept

in HDM supplemented with 100 ng/mL activin-A. From day 5 to day 10 HDM with 20 ng/mL BMP4 and 50 ng/mL FGF-4 was added, and medium was changed every other day. Between day 10 and day 15 cells were fed with HDM supplemented with 100 ng/mL hepatocyte growth factor (HGF) with medium changes every other day. From day 15 to day 20 we added HDM supplied with 20 ng/mL Oncostatin-M to the cells. At day 20 of differentiation cellular samples were processed for ICC and qRT-PCR. The hepatocarcinoma cell line Hep3B was used as positive control for the ICC experiments. Mean intensities of ICC stainings for albumin and AFP in undifferentiated, differentiated MAFS and HEP3B cells were quantified using ImageJ and normalized to the mean intensities of DAPI staining.

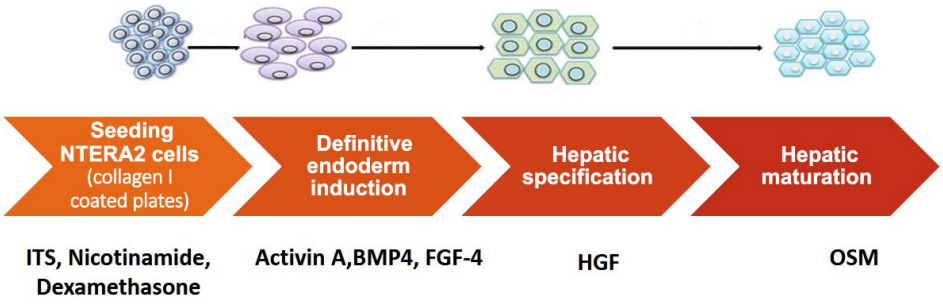

Figure 17. Optimized protocol for the in vitro differentiation of hepatocytes. *Cells were seeded into collagen-I-coated plates in hepatogenic differentiation medium (HDM) containing insulin-transferrin-selenium supplement, nicotinamide, and dexamethasone. DE-like cells were induced by activin A, BMP4 and FGF-4. Hepatic specification was promoted by the addition of HGF into the HDM, which was followed by maturation into hepatic cells with OSM. (For the exact timing of each cytokine and supplement, see the detailed description of our protocol below).*

Another method we tested for hepatic differentiation was published by Wakao et al, [132]. Briefly, cells were cultured on collagen-coated dishes with a seeding density of $2x10^4$ cells/cm^2. The hepatic differentiation medium (HDM) was DMEM containing, ITS supplement, 10 nM dexamethasone, 10% FBS and 100 ng/mL HGF and 50 ng/mL FGF-4. HDM was changed every 3rd day in 14 days. Hepatic marker expression was analyzed by RT-qPCR and ICC.

3.5. Statistical Analyses:

We used GraphPad Prism (version 5) for statistical analyses. For the statistical comparison of the relative mRNA expression values of multiple markers between control and differentiated samples we used two-way ANOVA with Bonferroni post-test. The same statistical test was used to compare the expression of CD146, CD271 and SSEA3 (measured by flow-cytometry) between MAFs and DFs. Paired Student's t-test was used to compare OR and ARS concentrations between control and differentiated samples during in vitro adipocyte and osteocyte differentiation assays, respectively. Normalized mean staining intensities for ALPL, CEBPα, Nestin and albumin were compared using Kruskal-Wallis test with Dunn's post hoc test. We chose 95% confidence interval for all statistical analyses.

4. Results

4.1. MSC Characteristics of MAFs

MSCs express characteristic cell surface markers and have mesodermal differentiation potential. Previous results published by our laboratory showed, that MAFs from primary and metastatic melanoma express fibroblast marker FAP, but not melanoma markers GP100 and MelanA [205]. These results suggested stromal cell characteristics of MAFs. To address whether MAFs have MSC characteristics, we isolated fibroblasts from healthy dermal tissues samples and subcutaneous metastatic melanomas. The stromal fibroblast phenotype was validated by the expression of stromal cell markers CD73, CD90 and CD105, (Fig.18), which were measured by flow-cytometry using FITC-conjugated antibodies. MAFs acquired spindle shaped morphology, and over 90% of the cells were positive for CD73, CD90 and CD105.

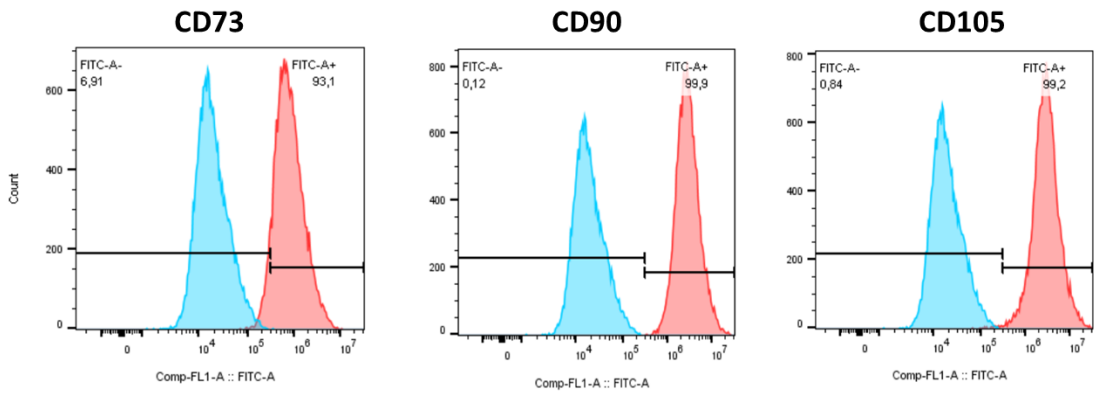

Figure 18. MAFs have a bone-marrow MSC-like phenotype. *Expression of canonical MSC markers CD73, CD90 and CD105 measured by flow cytometry. 200.000-300.000 cells/ sample were labeled with FITC-conjugated anti-CD73, anti-CD90 and anti-CD105 antibodies (N=5 MAFs and DFs from different donors were measured, experiments were repeated three times).*

In addition to the expression of canonical stromal markers (CD73, CD90, CD105) characterised here, our laboratory published the extended cell surface marker profiling of

MAFs by flow cytometry for an extended panel of bone-marrow MSC markers, including FITC-conjugated antibodies against CD9, CD10, CD44, CD51, CD54, CD56, CD61, CD81, CD102 and CD166, (results are from Anna Hajdara et al, [II]). Furthermore, our study revealed, that other MSC markers were expressed by a limited subset of MAFs (CD9, CD10, CD51, CD54), and rarely expressed MSC markers were also identified (CD56, CD61, CD102). Taken together the measurements from this publication -performed by Anna Hajdara- with the expression of canonical MSC markers by MAFs presented here, these results suggest the MSC-like surface marker profile of MAFs.

After the identification of the MSC-like phenotype of MAFs, we set out to address whether MAFs contain the stromal stem cell subsets, which reside in the dermis. It was previously reported that the human dermis contains diverse stem cell subsets from perivascular, papillary, and reticular dermal niches [85]. Thus, we stained healthy dermal fibroblasts and MAFs with antibodies against perivascular stem cell marker CD146 and bone marrow MSC-marker CD271, which are expressed on MSCs from the bone marrow and hypodermal adipose tissue. As stem cell subsets expressing pluripotent stem cell marker SSEA3 were also reported in the human bone marrow, adipose tissue, and dermis, we also included SSEA3 staining in our analyses. By using flow cytometric measurements, we showed that CD146, CD271 and SSEA3 were expressed in healthy DFs and MAFs (Fig.19). In addition, no double positive population was detected for SSEA3 and CD271 (Fig.19A, C), suggesting that the expression of these stem cell markers was not overlapping. Thus, CD271and SSEA3 marks distinct stem cell subsets in healthy fibroblasts and MAFs. Analysis of the expression of CD146, CD271 and SSEA3 showed, that MAFs have a significantly higher percentage of SSEA3+, CD146+, but not CD271+ cells compared to normal DFs (Fig.19E).

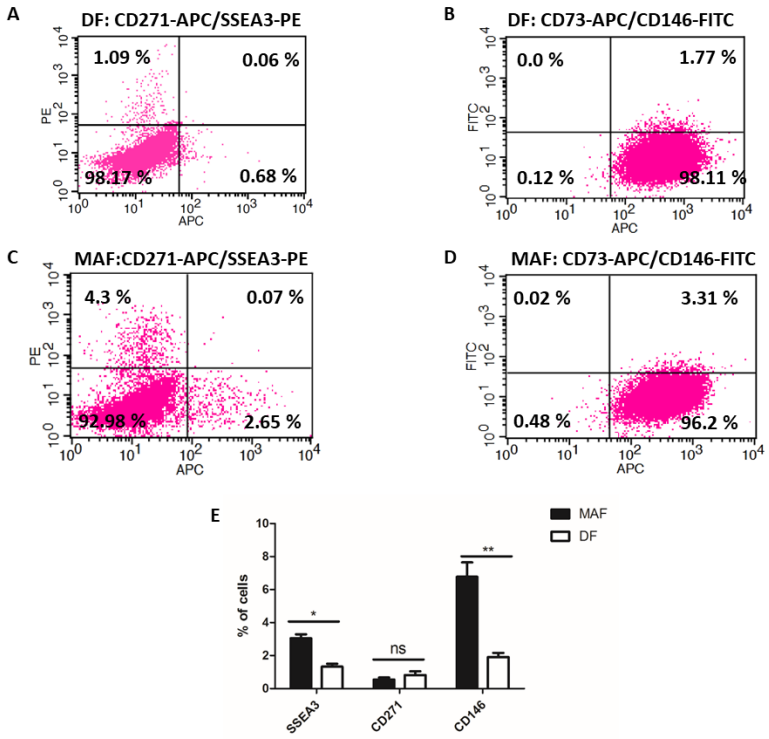

Figure 19. Stem-cell markers expression in normal dermal fibroblasts and MAFs. *Flow-cytometry dot plots made from measurements of DFs (A-B) and MAFs (C-D) double stained with SSEA3-PE/CD271-APC (A, C) and CD73-APC/CD146-FITC (B, D) antibodies. (E): Percentages of MAFs and DFs expressing SSEA3, CD271 and CD146. MAFs have significantly higher number of SSEA3+ and CD146+ cells. (**; 0.01< p < 0.05, *; p < 0.05, ns: non-significant. N=5 DF and MAF samples from different donors were measured, 20.000 events/sample were recorded. Experiments were repeated three times.).*

Next, we analyzed mesodermal lineage differentiation in MAFs, which is another hallmark of MSCs (Fig.20). We induced *in vitro* osteogenic and adipogenic differentiation in MAFs, followed by quantification of osteocyte-specific calcium deposits, and adipocyte-specific lipid droplets, respectively. To quantify osteogenic differentiation, we stained the cell cultures with Alizarin Red S (ARS), a water-soluble dye binding to calcium complexes deposited by osteocytes. ARS can be extracted from PFA-fixed cells using 10% acetic acid solution, and the concentration of the extracted dye can be calculated by measuring OD_{450} of the extracted dye. To quantify adipogenic differentiation we stained lipid droplets formed in the cells by using the lipophilic dye, Oil Red O (ORO), ORO was extracted from

the lipid droplets by using 60% isopropanol, and the intracellular ORO concentrations can be calculated by measuring OD_{506} value of the extracted dye.

Besides to their MSC-like cell surface marker profile, MAFs gave rise to calcium-depositing osteocytes and lipid-droplet containing adipocytes upon in vitro mesodermal lineage differentiation, as we demonstrated by Alizarin Red S and Oil Red O staining, respectively, (Fig.20A-B). Expression of osteocyte markers alkaline phosphatase (ALPL), BGLAP, and adipocyte markers CEBPα and PPARγ were confirmed by RT-qPCR (Fig.20C-D) and ICC, (Fig.21). Taken together, these features suggest bone-marrow MSC-like phenotype and differentiation potential of MAFs.

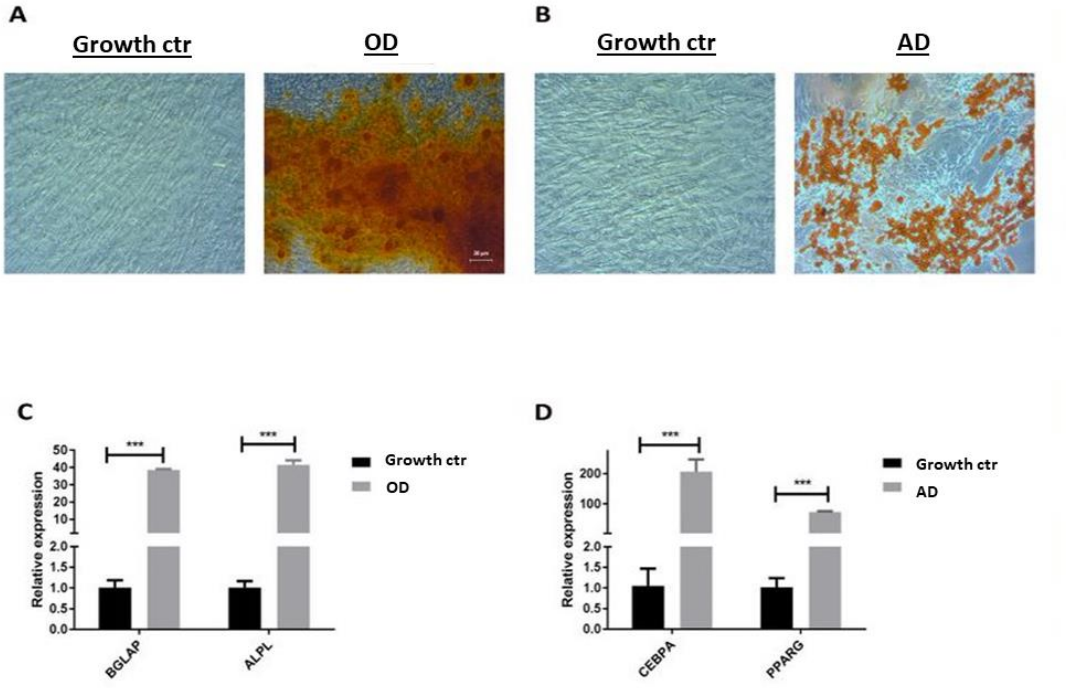

Figure 20. MAFs have a bone marrow MSC-like mesodermal differentiation potential *MAFs generate mesodermal lineage cells, osteocytes, and adipocytes. Representative images showing calcium-phosphate complexes of osteocytes stained with Alizarin Red S (A), while adipocyte-specific lipid droplets were stained with Oil Red O (B), respectively, (scalebar; 20 μM). Osteocyte and adipocyte differentiation were also characterized by RT-qPCR measurements for osteocyte markers (BGLAP, ALPL, C) and adipocyte markers (CEBPα, PPARγ, D). Relative mRNA expression values are shown compared. (GAPDH was used as housekeeping control, and undifferentiated samples were used as normalization controls. ***: $p < 0.001$). (OD: osteocyte differentiation, AD: adipocyte differentiation. All experiments with MAFs from N=5 different donors were repeated three times).*

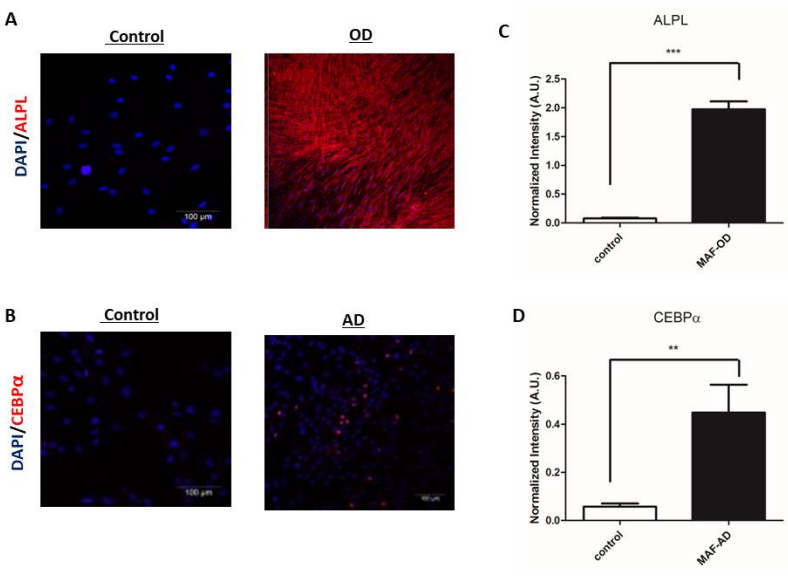

Figure 21. Expression of osteocyte marker ALPL and adipocyte marker CEBPα in MAFs upon osteogenic and adipogenic differentiation, respectively. *(A) Immunocytochemical staining of osteogenic marker alkaline phosphatase in undifferentiated MAFs and MAF-derived osteocytes. (B) Immunocytochemical staining of the adipogenic marker CEBPα in undifferentiated MAFs and MAF-derived adipocytes (B), (scalebar; 100 µm). Mean Intensities of ALPL staining in MAF derived osteocytes (C), and CEBPα in MAF-derived adipocytes normalized to DAPI. (***: P < 0.01; **: 0.01< p < 0.05) (OD: osteocyte differentiation, AD: adipocyte differentiation. All experiments with MAFs from N=5 different donors were repeated three times).*

4.2. Optimizing in vitro Ectodermal and Endodermal Lineage Characterizations Assays Using Immortalized Cell Lines

In vitro differentiation produces cell types with morphological, functional characteristics and cellular markers of a given lineage. Thus, the reliable *in vitro* characterization of lineage markers is an essential step, which must be optimized for *in vitro* differentiation protocols. For the validation of ectodermal and endodermal lineage markers we sought for immortalized cell lines, which robustly express neural, melanocytic, and hepatic lineage markers, though, they can be easily maintained in feeder-free cultures with minimal amounts of supplements (see; Table 3.1. by Methods),

such as FBS. While A172 glioblastoma cell lines were used to optimize the detection of neural markers Nestin, MAP2, ENO2, (Fig.22A, Fig.24B-C), we used hepatocellular carcinoma line HEP3B to set up the characterization of endodermal/hepatic markers α-fetoprotein (AFP) and albumin (ALB) by ICC and qPCR (Fig.22B, Fig.25A-B). Immunocytochemical staining of melanocytic marker melan-A was assayed on malignant melanoma cell line SKMEL-28, (Fig.22C).

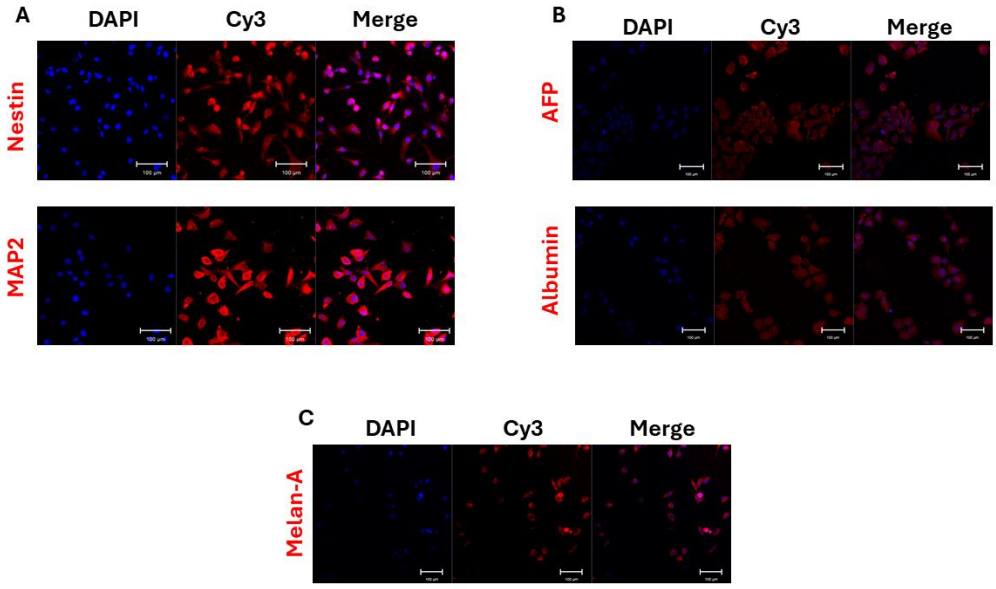

Figure 22. Immunocytochemical staining of neural (MAP2, Nestin) markers on A172 cells (A) and hepatic (AFP, albumin) (B) lineage markers on Hep3B cells. *(C) Staining of melanocyte differentiation marker Melan-A on SKMEL-28 cells. Nuclei were stained with DAPI. (Scalebar: 100 µm. Experiments were repeated three times)*

4.3. Optimizing *in vitro* Ectodermal, Endodermal and Mesodermal Lineage Differentiation Using the NTERA2 (clone D1) cell line

To optimize our in vitro ectodermal and endodermal differentiation assays we utilized the NTERA2 embryonic teratocarcinoma cell line as a positive control. Though NTERA2 cells are pluripotent, and their capacity for neural differentiation was reported [197] [198], their differentiation towards other specific cell types, such as hepatocytes and osteocytes

has not been characterized yet. We validated the expression of pluripotent stem cell markers Oct3/4, NANOG, Sox2, TRA-1-60 and SSEA3 in cultured NTERA2 cells by flow-cytometry, ICC and RT-qPCR (Fig.23) [I].

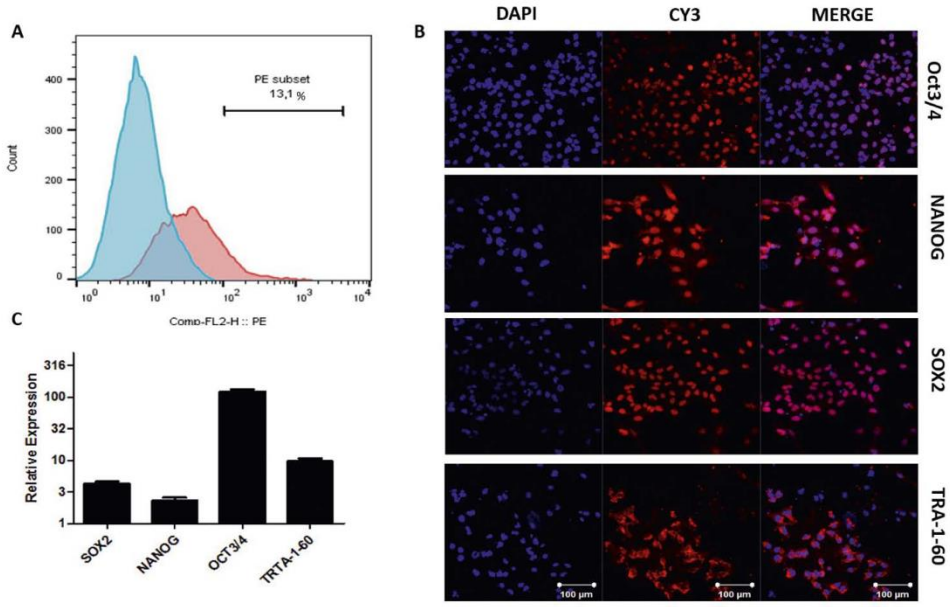

Figure 23. Pluripotent stem cell markers expression on NTERA2 clone D1 cells were analyzed by flow-cytometry, ICC, and qRT-PCR. *(A) 200.000-500.000 NTERA2 cells were stained with biotin-conjugated anti-SSEA3 antibody, which was followed by incubation with PE-conjugated streptavidin. Percentage of SSEA3+ cells (red histogram) were analyzed by flow cytometry, NTERA2 cells without primary antibody staining were used as control (blue histogram). (B) Immunocytochemical staining of NTERA2 cells with antibodies against pluripotency markers Oct3/4, NANOG, Sox2 and TRA-1-60. Nuclei were stained with DAPI, (scalebar; 100 µm). (C) Relative mRNA expression of the pluripotency markers was measured by qRT-PCR. TaqMan probe for GAPDH was used as housekeeping control, and normal dermal fibroblast samples were used as normalization control for the measurements. (Experiments were repeated three times)*

Next, we optimized our in vitro neural and hepatic differentiation methods by using NTERA2 cells (Fig.24, Fig.25). Several different approaches were published for neural differentiation of pluripotent stem cells, including feeder cell layers [199], chemical [200], [201] and recombinant vector-based methods [202], although these methods generate neural cells with highly variable time demands, yields and phenotypic compositions. On

the other hand, many PSC-based methods rely on the induction of multipotent neural stem cells in 2D and 3D cultures, which can be further differentiated to variable neural subtypes, [203], [17], [133].

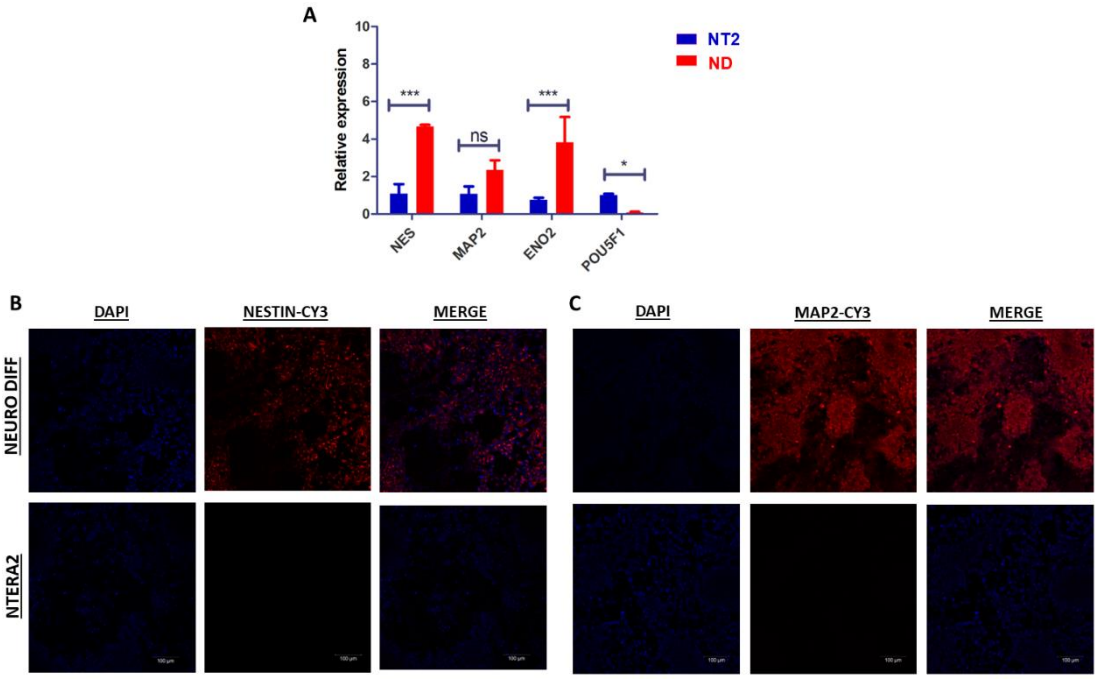

Figure 24. Neural lineage differentiation of NTERA2 cells. *Significant increase in neural lineage markers and decrease in the relative mRNA expression of pluripotency marker POU5F1 were measured by qRT-PCR. (GAPDH was used as a housekeeping control, and undifferentiated NTERA2 cells were used as normalization control for the experiments). (B) Expression of MAP2 and Nestin (C) were detected in differentiated and positive control (A172) cells, but not in undifferentiated NTERA2 cells, (scalebar; 100µm). (NT2: NTERA2 cells, ND: neural differentiation. *: $p < 0.05$, ***: $p < 0.001$, ns: non-significant. Three repeated experiments were made.).*

Instead of deriving specific neural cell types, our goal was to analyze the general neural lineage differentiation potential of MAFs, and their commitment towards neural lineages. Therefore, we used the neural induction method in 3D cultures of cells with cytokines stimulating neural lineage specification. (Fig.15, Fig.24) For neural lineage differentiation, NTERA2-derived neural-like spheroids were generated from NTERA2 cells in ultra-low adherent cell culture dishes for 14 days in supplemented neurobasal medium containing EGF and bFGF, cytokines maintaining the self-renewal of neural stem cells,

(see Methods). Neurospheres at day 14 were seeded into poly-D-Lysine-coated dishes. To induce the generation of neuronal cells from neural stem cells, we used neuronal induction medium without EGF and bFGF but supplemented with neuronal differentiation activating cytokine BMP4. We observed the expression of Nestin and MAP2 in differentiated NTERA2 cells, but not in undifferentiated NTRERA2 cells by ICC, (Fig.24B-C). Although the upregulation of neuronal marker MAP2 was not significant on the mRNA level, NES and neuronal lineage marker *ENO2* were significantly upregulated. In addition, we observed significant downregulation of pluripotency marker *POU5F1,* (Fig.24A*)*. These results suggest a neural progenitor cell-like phenotype of the differentiated NTERA2 cells, which shows similarity to the neural progenitor cells derived from PSCs, [17], [18]. Taken together with the expression of Nestin, MAP2 and ENO2, our results highlight the neuronal lineage commitment of NTERA2 cells in our *in vitro* neural differentiation assay.

Although hepatic differentiation was induced from PSCs through the generation of definitive endoderm cells *in vivo* [40], time-effective *in vitro* approaches using stimulation with HGF, FGF-4 and OSM on skin fibroblasts were also published [132], [206]. Therefore, to induce hepatic differentiation *in vitro*, we used two different protocols. In the first method (referred from here as 'HEP1 method') published by Wakao et al [132] we used stimulation of fibroblasts with hepatic differentiation medium containing all cytokines for endoderm induction (FGF-4) hepatic induction (HGF), and hepatic maturation (OSM) for 14 days, (Fig.17). The second approach (referred from here as 'HEP2 method') was the slightly modified method published by Mallana et al [40]. This method is based on the induction of a definitive endoderm by hepatic differentiation medium containing Activin A FGF-4, and BMP-4 [40], which is followed by a switch in the cytokine content of the medium to induce hepatic specification (HGF) and hepatic cell maturation (OSM), (Fig.17). *In vitro* hepatogenic differentiation method HEP2 produced cells, which were positive for AFP and albumin (ALB) (Fig.25A), and POU5F1 was significantly downregulated by the end of the differentiation (Fig.25C). In addition, definitive endoderm induction by Activin-A and BMP-4 resulted in significant upregulation of CK7 and CK18, cytokeratin family proteins expressed by bile duct epithelial cells and hepatocytes, respectively, (Fig.25C). Conversely, the HEP1 method failed to induce the expression of ALB and CK18, and the expression of POU5F1 was not changed significantly by the end of differentiation, indicating incomplete hepatic lineage differentiation, (Fig25.D).

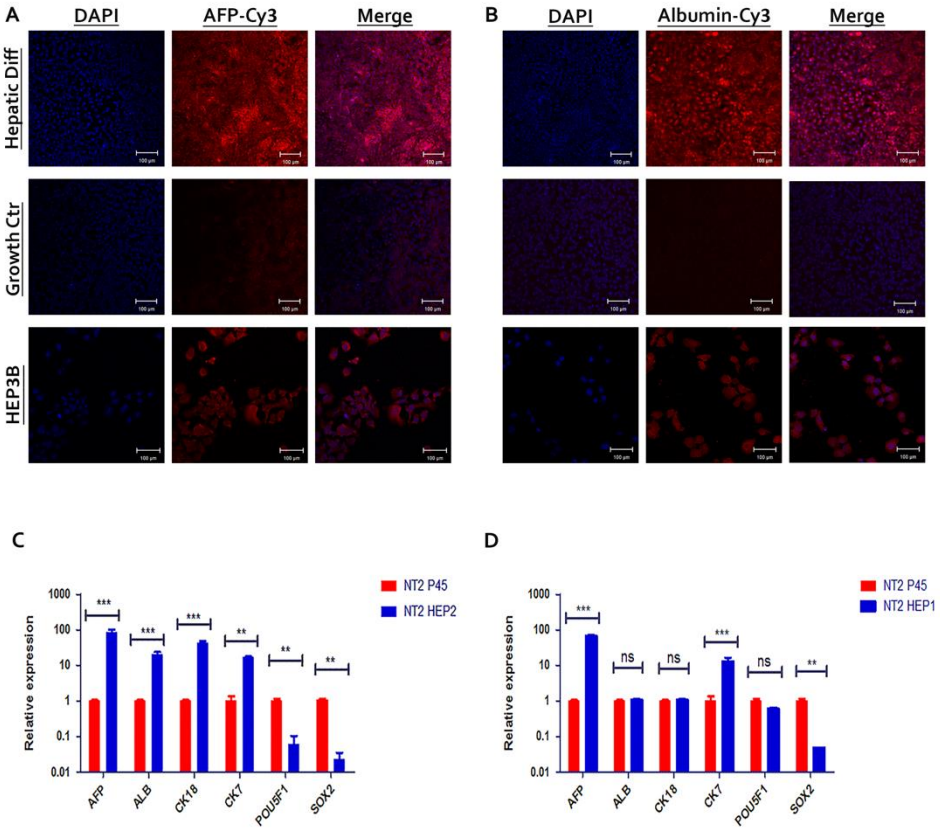

Figure 25. In vitro differentiation of NTERA2 cells towards hepatic lineages. *(A) Expression of AFP and albumin (B) were detected in NTERA2 cells differentiated by HEP2 method, and positive control (HEP3B) cells, but not in undifferentiated NTERA2 cells, (scalebar; 100µm). (C) Significant increase in hepatic lineage markers (AFP, ALB, CK18, CK7) and significant decrease in the relative mRNA expression of pluripotency markers POU5F1 and SOX2 were measured by qRT-PCR. (D) In contrast, no significant difference in the expression of ALB, CK18 and POU5F1 were detected when we utilized the HEP1 method. (***: $p < 0.01$, **: $0.01 < p < 0.05$. Experiments were repeated three times).*

Our results are in accordance with the published methods using definitive endoderm induction [40], [204], highlighting the importance of this step by hepatogenic differentiation of NTERA2 cells.

Despite the upregulation of mesodermal markers Brachyury, Msx1, MyoD and HAND1 was reported for NTERA2 cells upon *in vitro* mesodermal lineage differentiation [204],

limited information is available on their differentiation to osteocyte lineage cells. To analyze osteogenic differentiation of NTERA2 cells, we adopted the in vitro osteogenic differentiation protocol from Vaculik et al, [85] using ascorbic acid, and β-glycerophosphate to activate osteogenic gene expression, collagen synthesis and matrix mineralization, (Fig.26).

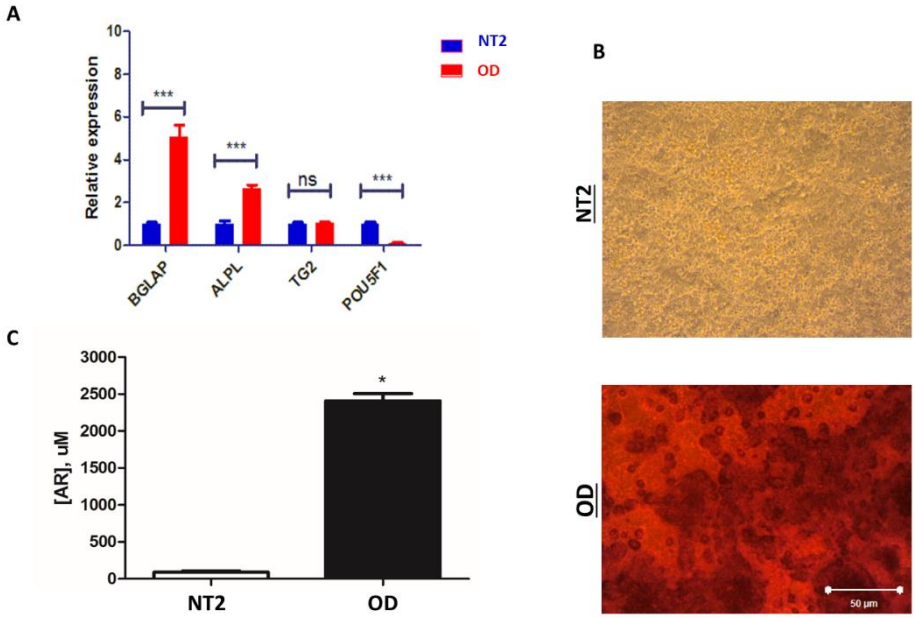

Figure 26. Osteocyte lineage differentiation of NTERA2 cells. *(A) Significant increase in osteocyte lineage markers (BGLAP2, ALPL, TG2), and decrease in the relative mRNA expression of pluripotency marker POU5F1 were measured by qRT-PCR. (B) ARS staining revealed an increased number of calcium-phosphate deposits in differentiated NTERA2 cells, but not in undifferentiated NTERA2 cells, (scalebar; 100µm). (NT2: NTERA2 cells, OD osteocyte differentiation. *: p < 0.05, ***: p < 0.001, ns: non-significant. Three repeated experiments were made.).*

In vitro osteogenic differentiation of NTERA2 cells produced cells with upregulated expression of osteocyte markers (BGLAP2, ALPL, but not TG2 Fig24.A), downregulation of pluripotency marker POU5F1, and significantly increased concentration of ARS extracted from calcium-phosphate complexes of differentiated NTERA2 cells compared to undifferentiated NTERA2 cells, (Fig26.B-C)

In conclusion, by utilizing the protocols described above, we optimized and published methods for the in the *in vitr*o neural (Fig.24), hepatogenic (Fig.25) and osteogenic (Fig.26) lineage differentiation of NTERA2 cells, [I].

4.4. MAFs Have Enhanced Mesodermal Differentiation Potential Compared to Normal Dermal Fibroblasts

Given our optimized *in vitro* differentiation assays, we set out to characterize the in vitro differentiation potential melanoma stromal cells compared to normal dermal fibroblasts. Firstly, we compared, osteogenic (Fig.27) and adipogenic (Fig.28) differentiation of healthy fibroblasts and MAFs derived from five different patients

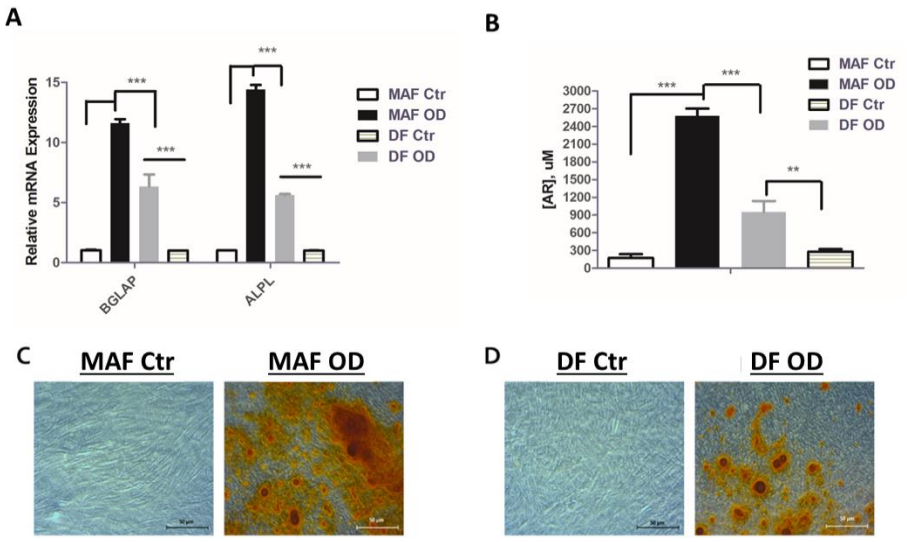

Figure 27. MAFs have significantly higher osteogenic differentiation potential than DFs. *(A) Relative mRNA expression of osteogenic markers BGLAP and ALP in control and differentiated (OD) MAFs and DFs, measured by qRT-PCR. GAPDH was used as housekeeping control, expression values were normalized to control/undifferentiated samples. (B) Concentration of ARS dye extracted from calcium phosphate complexes of control and differentiated MAFs and DFs, (given in µM). Representative images showing ARS staining of calcium-phosphate complexes of DF- (C) and MAF-derived osteocytes (D) compared to their undifferentiated controls, (scalebar; 50 µm). (Ctr: undifferentiated cells, OD: osteocyte differentiation. ***: $p < 0.01$, **: $0.01 < p < 0.05$. N= 5 MAFs and DFs from different donors were used for the experiments, experiments were repeated three times).*

. MAF-derived osteocytes displayed significantly higher concentrations of ARS, than normal DFs (Fig.27B-D). In addition, osteocyte specific genes *BGLAP2* and *ALPL* were expressed significantly higher in MAFs compared to DFs, (Fig.27A). Likewise, MAF-derived adipocytes had a significantly higher ORO extracted from lipid droplets than normal DFs (Fig.28B-D), and MAF-adipocytes expressed adipocyte-specific genes PPARγ and CEBPα at significantly higher levels compared to DFs, (Fig.28A). Taken together with the results from 4.1, MAFs contain stromal stem cell subsets and have an enhanced differentiation plasticity compared to normal skin fibroblasts.

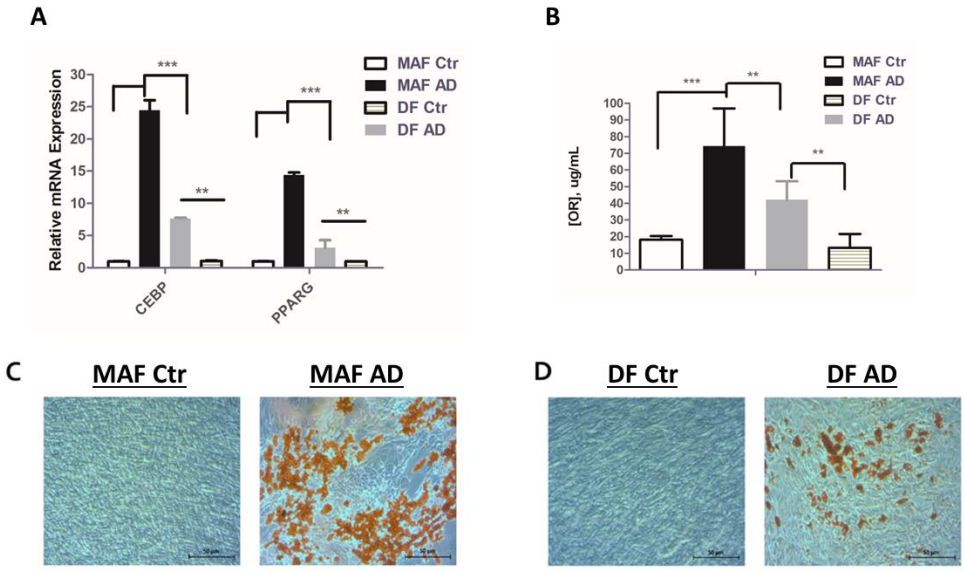

Figure 28. MAFs have significantly higher adipogenic differentiation potential than DFs. *(A) Relative mRNA expression of adipogenic markers PPARG and CEBPα in control and differentiated MAFs and DFs, measured by qRT-PCR. GAPDH was used as housekeeping control, expression values were normalized to control/undifferentiated samples. (B) Concentration of lipophilic dye Oil Red O (ORO) dye extracted from lipid droplets of control and differentiated MAFs and DFs, (given in µg/mL). Representative images showing ORO staining of lipid droplets in DF- (C) and MAF-derived adipocytes (D) compared to their undifferentiated controls, (scalebar; 50 µm). (Ctr: undifferentiated cells, AD: adipocyte differentiation. ***: $p < 0.01$, **: $0.01 < p < 0.05$. N= 5 MAFs and DFs from different donors were used for the experiments, experiments were repeated three times).*

4.5. Differentiation of MAFs Into Ectodermal and Endodermal Lineage Cells

Given the elevated mesodermal lineage generation capacity of MAFs, we furthered characterized MAFs for their ability to generate ectodermal and mesodermal lineage cells. We used our *in vitro* ectodermal and endodermal lineage differentiation methods, which we optimized for NTERA2 cells in 4.2, (for detailed description of the methods, see 3.4.3).

MAFs showed neurogenic and hepatogenic differentiation (Fig.29). Intriguingly, neurogenic differentiation of MAFs generated Nestin-positive cells, (Fig.29A), and neural markers Nestin, MAP2 and enolase-2 were slightly, (though significantly) upregulated in MAFs following in vitro neural differentiation, (Fig.29B). A possible explanation could be for this observation that skin fibroblasts originate from both mesodermal and neural crest precursor cells [61], and the latter precursor cells retain their capacity for neural lineage differentiation, [93], [101]. Likewise, MAFs gave rise to endodermal lineage-like cells expressing albumin (ALB) and α-fetoprotein (AFP), but not CK18 (Fig.29C-D).

These results suggest that certain stem cell subsets of MAFs within the bulk MAF population are endowed with ectodermal (neural) and endodermal lineage differentiation potentials. Next, we sought to address whether MAFs contain MUSE cells, multipotent stem cells of stromal niches.

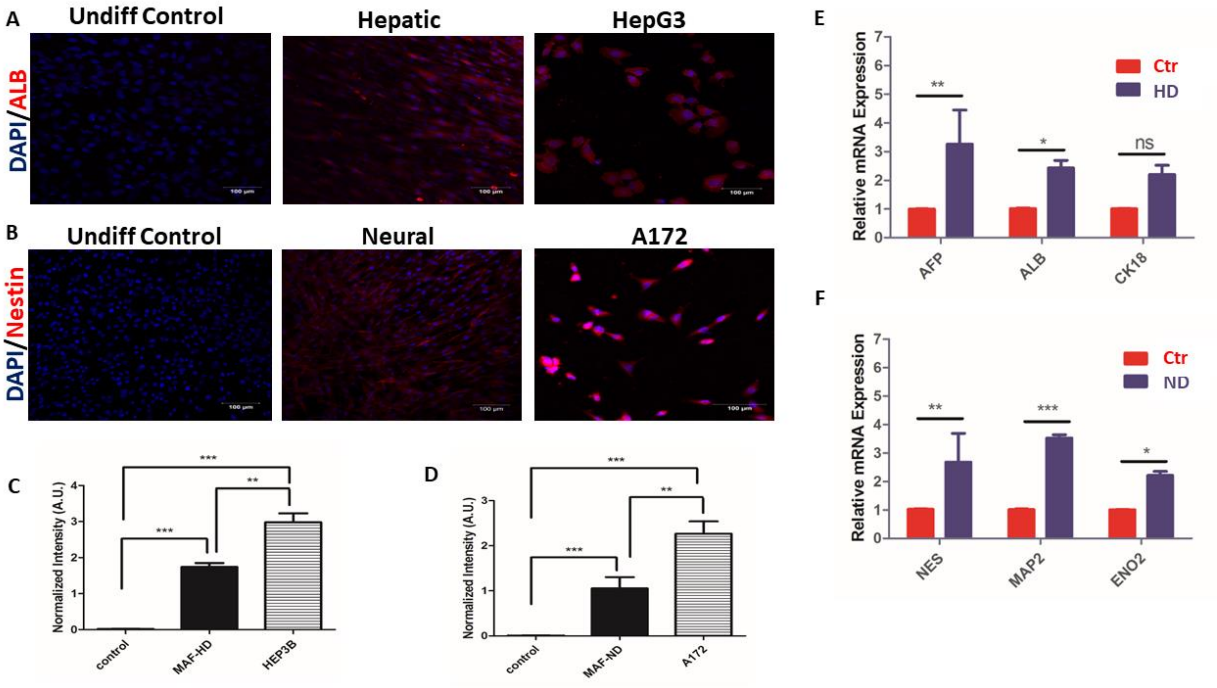

Figure 29. In vitro neural and hepatic differentiation of MAFs. *(A) MAFs were differentiated towards neural lineage cells and characterized for the expression of Nestin by ICC. Nuclei were stained with DAPI. Left: undifferentiated control MAFs, middle: differentiated MAFs, right: A172 cells (positive control), (scalebar; 100 um). (B) MAFs were differentiated towards hepatic lineage cells and characterized for the expression of albumin (ALB) by ICC. Nuclei were stained with DAPI. Left: undifferentiated control MAFs, middle: differentiated MAFs, right: HEP3B cells (positive control), (scalebar; 100 µM). (C) Quantitation of the mean staining intensities for ALB in undifferentiated controls, hepatic differentiation of MAFs and HEP3B cells, normalized for mean staining intensity of DAPI (arbitrary units). (Control: undifferentiated cells, ND: neural differentiation, HD: hepatic differentiation. ND***: $p < 0.01$, **: $0.01 < p < 0.05$). (D) Quantitation of the mean staining intensities for Nestin in undifferentiated controls, neural differentiation of MAFs and A172 cells, normalized for mean staining intensity of DAPI (arbitrary units). (***: $p < 0.01$, **: $0.01 < p < 0.05$). (E) Neural markers Nestin, MAP2 and ENO2 were upregulated, as shown by qRT-PCR. (GAPDH was used as housekeeping control, samples were normalized to undifferentiated controls.) (F) Hepatic markers AFP, ALB and CK18 were upregulated, as shown by qRT-PCR. (GAPDH was used as housekeeping control, samples were normalized to undifferentiated controls). (***: $p < 0.01$, **: $0.01 < p < 0.05$, *: $p \leq 0.05$, ns: non-significant. N=3 MAFS from different donors were used, experiments were repeated two times).*

4.6. MAFs Harbor SSEA3+ Pluripotent Cells

MUSE cells were described in stromal tissues (skin, adipose tissue, bone marrow) as an SSEA3+ cell subset expressing both stromal markers (CD29, CD90, CD105) and pluripotent stem cell markers (Oct3/4, NANOG, TRA-1-60, Sox2), [123]-[127]. Our previous measurements identified SSEA3+ cells among MAFs and DFs, (Fig.19). On the other hand, diverse fibroblast subsets with variable lineage differentiation potentials were identified, which express stage specific embryonic antigens [85], [227], [228]. To address whether SSEA3+ stromal cells in MAFs and dermal fibroblasts are MUSE cells, we isolated CD90+SSEA3+ fibroblasts from dermal and MAFs by FACS (Fig.30), and we analyzed pluripotency marker (Oct3/4, NANOG, Sox2, TRA-1-60) expression in the sorted cells by ICC and RT-qPCR.

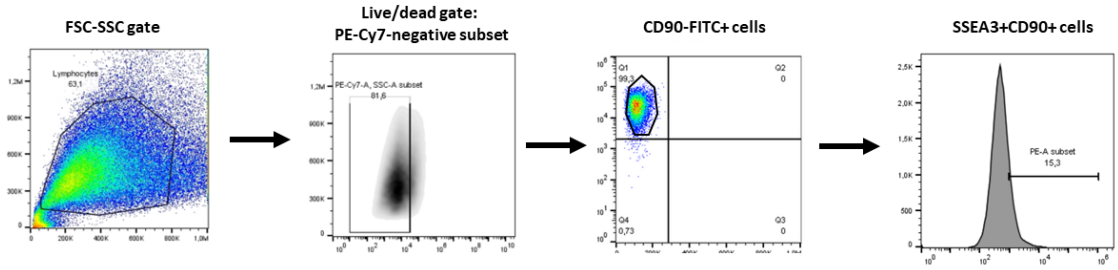

Figure 30. Gating strategy for analyzing SSEA3+CD90+ cells. *Viable cells were selected from cells within the FSC-SSC gate, which are negative for the PE-cy7 viability dye staining. Then, a gate for living CD90+ cells was set to obtain percentages of viable, CD90+SSEA3+ cells.*

As the SSEA3+ cells constituted a minor fraction within MAFs and DFs, we amplified the fluorescent signal from SSEA3+-labelling by using a biotinylated SSEA3+ antibody, which binds with high affinity to PE-conjugated streptavidin, (chapter 3.3.3, Fig.14). After gating out cells in the FSC-SSC-gate, we set a gate to the cell population, which is negative for the PE-Cy7-conjugated viability dye, (live/dead gate). SSEA3+ cells were then selected from gating out all cells within the live/dead gate, which were positive for CD90, (Fig.30). Sorted SSEA3+ cells were plated for ICC or processed for RT-QPCR. SSEA3+ cells from MAFs and DFs expressed SOX2, OCT ¾, TRA-1-60 and NANOG as shown by ICC and RT-qPCR, (Fig.31B, C, D). On the other hand, SSEA3- cells lacked the expression of any pluripotency markers. Thus, similarly to DFs, MAFs contain SSEA3+ MUSE cells.

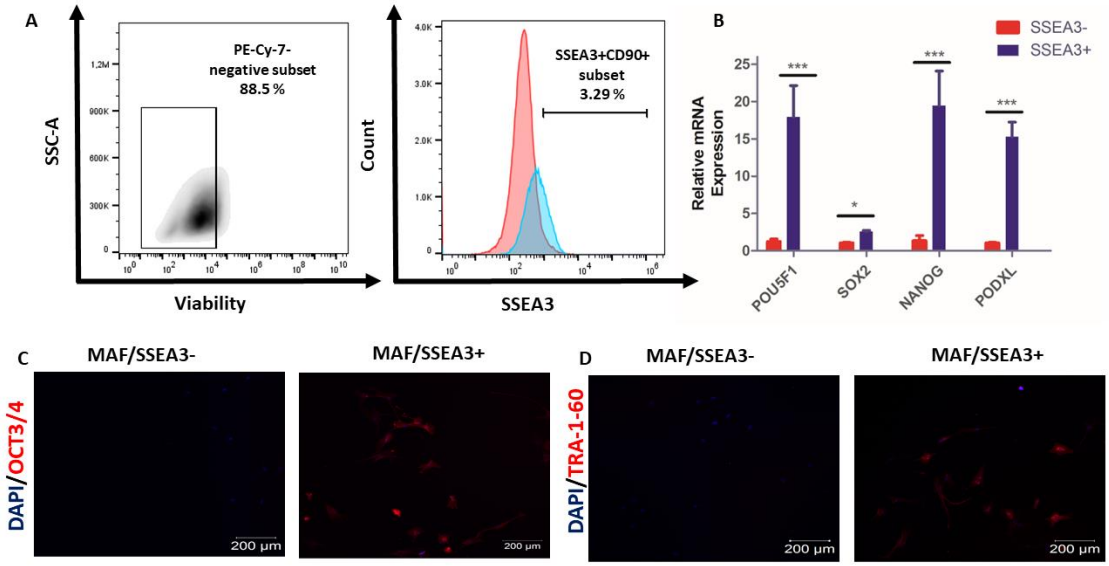

Figure 31. MAFs encompass MUSE cells. *(A) Isolation of MUSE cells by* FACS. *Cytometry gates were set to viable cells (lacking PE-Cy-7 staining), and then for SSEA3+ population. (5-10 million cells from N=3 MAFs from different donors were used. Red histogram represents unstained control, and the blue histogram shows SSEA+ cells before FACS). (B) Relative mRNA expression of pluripotent stem cell markers POU5F1, SOX2, NANOG and PODXL were analyzed by qRT-PCR. (GAPDH was used as housekeeping control, expression values were normalized to SSEA3- sorted samples). (C) Sorted SSEA3+ cells, but not SSEA3-negative cells express Oct3/4 and TRA-1-60, as demonstrated by ICC. (scalebar; 200 µm, nuclei were stained with DAPI). (***: $p < 0.01$, *: $p \leq 0.05$, N= 5 MAFs from different donors were used, experiments were repeated two-times).*

4.7. SSEA3+ MAFS, but not SSEA3- MAFs Have *In Vitro* Melanocyte Lineage Differentiation Potential

It was reported that dysregulated melanocyte differentiation in malignant melanoma microenvironments highly contributes to the generation of novel melanoma cells [207]. As melanocytes can emerge from both melanocyte stem cells and dermal stem cells, [208] we sought to address melanocyte differentiation of MUSE cells sorted from MAFs.

Melanocyte differentiation methods published on PSCs aim to recapitulate basic steps of in vivo melanocyte development, such as neural crest induction, melanoblast

differentiation, melanocyte specification and maturation [210]. Although many approaches using PSCs are based on embryoid body formation [211], 2D differentiation methods for MUSE cells were published using fibronectin-coated dishes [128], [129]. These methods used Wnt3a for neural crest patterning of MUSE cells, which was followed by melanoblast induction by Endothelin.3, and melanocyte specification using cholera-toxin, which mimics the effects of melanocyte stimulating hormone, MSH. Melanocytes differentiated from dermis- and adipose tissue-derived MUSE cells acquired long dendrites, and they expressed pre-melanosome protein PMEL, melanocyte-specific transcription factor MITF (microphthalmia-associated transcription factor). In addition, MUSE-cell derived melanocytes displayed positivity for melanin biosynthetic enzymes dopachrome-tautomerase (DCT) and tyrosinase-related protein-1 (TYRP1), and showed positivity for the L-DOPA reaction assay.

To analyze the *in vitro* melanocyte differentiation of MAF-derived MUSE cells ('MAF-MUSE'), we isolated MUSE cells from MAFs, and plated the cells into fibronectin-coated dishes. We used the *in vitro* melanocyte differentiation protocol published for MUSE cells by Yamauchi et al, [129], (Fig.16). Melanocyte differentiation was initiated by medium supplemented with melanocyte inducing factors phorbol-myristyl-acetate (PMA), basic fibroblast growth factor (bFGF), cholera toxin, stem cell factor (SCF), endothelin-3 (ET-3) and Wnt-3. Differentiated MAF-MUSE cells acquired dendritic melanocyte-like morphology (Fig.32B), and the expression of PMEL, MITF, DCT and TYRP-1 were confirmed by ICC and RT-qPCR, (Fig.32A, C), similarly to the results published for adipose tissue fibroblasts and dermal fibroblasts [128], [129]. In contrast, SSEA3- cells from MAFs failed to upregulate any melanocyte marker after in vitro melanocyte induction, (Fig.32A).

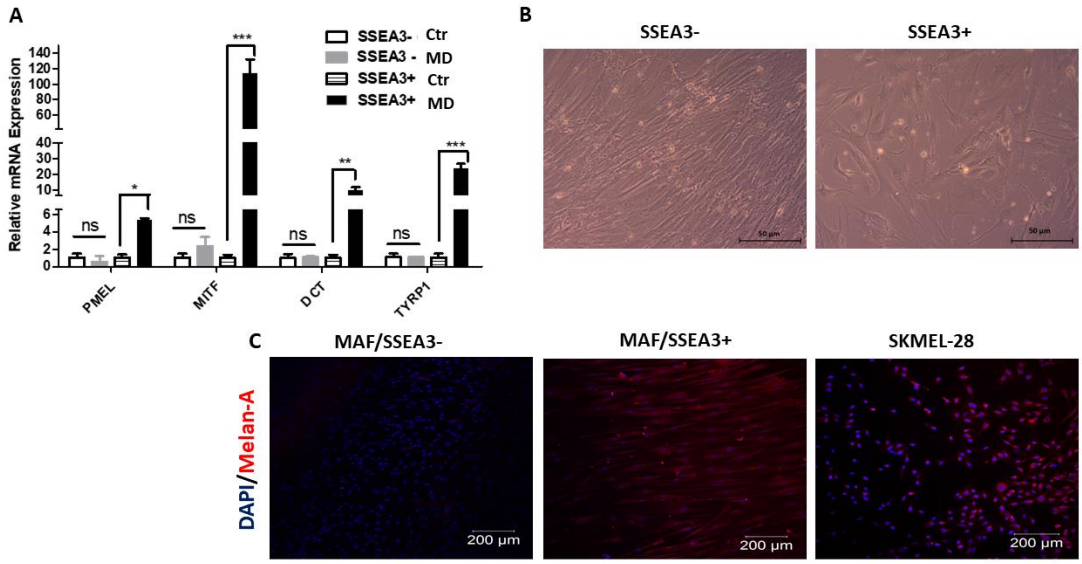

Figure 32. MAF-MUSE cells give rise to melanocyte lineage cells in vitro. *MUSE cells from MAFs were separated as viable CD90+SSEA3+ cells from viable CD90+SSEA3- cells by FACS-sorting. Sorted SSEA3+ and SSEA3- cells were seeded into fibronectin-coated plates, and melanocyte lineage cells were induced within 6 weeks. (A) Upregulation of melanocyte markers PMEL, MITF, DCT and TYRP1 were observed in sorted and differentiated SSEA+ MAFs by qRT-PCR. GAPDH was used as housekeeping control, and relative mRNA expressions values were normalized to undifferentiated control samples. (Ctr: undifferentiated control, MD: melanocyte differentiation. ***: p< 0.01, **; 0.01< p < 0.05, *; p < 0.05). (B) SSEA3+, but not SSEA3- cells acquired elongated, dendritic morphology. (Light microscopic images at day 42 of differentiation, scalebar; 50 µm). (C) Expression of Melan-A was confirmed in SSEA3+ cells (up/ middle), but not in SSEA3- cells (down/middle) by ICC, compared to undifferentiated control (left panel) and positive control (SKMEL-28 cells, right side image). (Nuclei were stained with DAPI, scalebar; 200 µm). (N= 5 MAFs from different donors were used for the experiments).*

To compare the melanocyte differentiation potential of MAF-MUSE cells with MUSE cells isolated from healthy DFs ('DF-MUSE cells'), we differentiated MUSE cells isolated from MAFs and DFs into melanocyte lineage cells, and we analyzed melanocyte marker expression in undifferentiated, and differentiated SSEA3-negative MAFs, SSEA3-negative

DFs, MAF-MUSE and DF-MUSE cells. Melanocyte-specific markers (*MITF*, *PMEL*, *DCT* and *TYRP1*) were expressed at significantly higher levels in MAF-MUSE cell-derived melanocytes compared to melanocytes generated from DF-MUSE cells, (Fig.33). This suggests that MUSE cells residing in melanoma microenvironments have increased capacity for melanocyte differentiation and might be possible stem-cell sources for dysregulated melanocytes generation in melanoma niches.

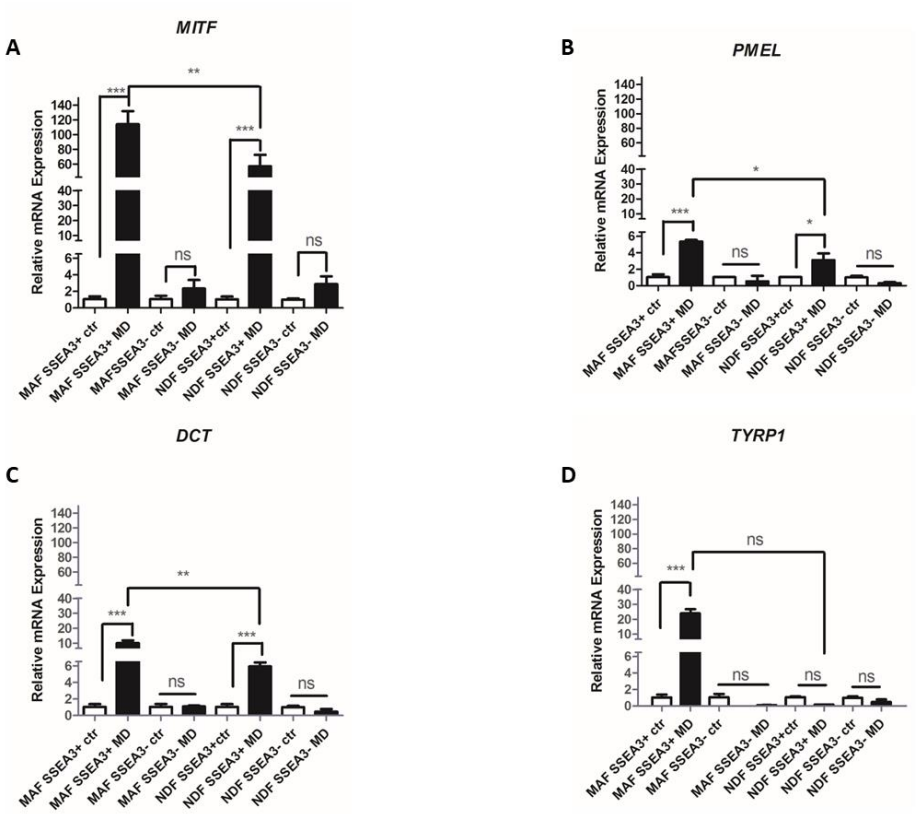

Figure 33. MUSE cells from MAFs express higher level of melanocyte markers upon melanocyte differentiation, than MUSE cells from DFs. *Melanocyte marker MITF (A), PMEL (B), DCT (C) and TYRP1 (D) were observed in sorted SSEA+ MAFs by qRT-PCR. GAPDH was used as housekeeping control, and relative mRNA expressions values were normalized to undifferentiated control samples. (Ctr: undifferentiated control, MD: melanocyte differentiation. ***: p< 0.01, **; 0.01< p < 0.05, *; p < 0.05). (N= 5 MAFs from different donors were used for the experiments)*

5. Discussion

Dysregulation of stem cell homeostasis in skin leads to carcinogenesis, and subsequent formation of cancer cell micro-niches [7],[172]. Cancers constitute a unique stromal microenvironment, which includes cancer-infiltrating immune cells [145]-[147], CAFs and cancer stem cells [145]. CAFs are highly heterogeneous cells of the tumor microenvironment contributing to cancer drug-resistance [134]-[136], cancer-stemness [137], immunosuppression [137], [140]-[143] and metastasis.

Malignant metastatic melanomas are the deadliest skin cancers with high mortality rate and poor prognosis worldwide, [167]-[169]. Aggressiveness, drug-resistance, and high metastatic potential of malignant melanomas stems from enhanced differentiation plasticity and heterogeneity of melanoma cell subsets [174]-[179]. On the other hand, cancer growth, survival and stemness are also supplied by stromal cells of the tumor-microenvironment. Several studies analyzed the origin, functional and phenotypic heterogeneity of CAFs in hepatocellular carcinoma [147], pancreatic cancer [151], and breast cancers [153], [214], although, less is known on the functions and phenotype of stromal cells in metastatic melanoma niches. The identification and targeting of specific MAF subsets promoting melanoma metastasis, immunosuppression and drug-resistance would greatly impede tumor growth and progression.

Our previous studies revealed that MAFs have MSC-like characteristics [II]. By analyzing the cell surface markers of MAFs *in vitro* by flow cytometry, we showed that metastatic melanoma-derived MAFs express canonical markers of MSCs; CD73, CD90 and CD105. Furthermore, MAFs also expressed cell surface molecules CD9, CD44, CD51, CD54 and CD81, which were shown to be specifically involved in cancer cell motility and migration [212]- [214], melanoma growth [216] and drug-resistance [215]. Intriguingly, it was reported by others that the UV3 monoclonal antibody blocking CD54 decreased melanoma growth in C.B.-17 SCID/beige immunocompromised mice [217]. Furthermore, another study demonstrated that CD9-containing exosomes released by CAF inhibited the proliferation of melanoma cells, [214]. Thus, our analysis demonstrated the presence of cell-surface molecules on MAFs, which serve as candidate targets for future anti-melanoma therapies.

Here, we demonstrated that CAFs express canonical stromal markers CD73, CD90 and CD105 (Fig.18) have distinct cell subsets with dermal stem cell markers CD146, CD271 and SSEA3. CD146 is expressed on perivascular MSCs of the human dermis, while CD271 cells are localized to the hypodermal adipose tissue and nerve terminals. Both CD146+ and CD271+ stem cells are highly immunogenic and stimulate angiogenesis in damaged stromal tissue. Given their elevated immunomodulatory [218] and angiogenic potential [219], it would be interesting to analyze how CD146+ and CD271+ MAFs contribute to cancer-angiogenesis and immunosuppression in metastatic melanomas.

After the identification of stem cell subsets in MAFs, we aimed to analyze tri-lineage differentiation of stromal cells in melanomas by optimizing the induction methods for in vitro ectodermal, endodermal, and mesodermal lineage differentiation (chapter 4.3, Fig.24-26). The published methods for in vitro ectodermal, endodermal, and mesodermal differentiation show high variability in terms of the cell types and tissue sources used, the applied growth factor combinations, characterization methods and reproducibility. The cellular models differ in their maturity stage, gene expression profile, and lineage generation potential, which hampers the elaboration of standardized stem cell differentiation protocols. Thus, the optimization of *in vitro* differentiation assays requires not only a careful choice of cell culture conditions (extracellular matrix substrates, culture medium supplements, growth factors), but also the utilization of cellular positive controls for optimizing differentiation and in vitro characterization. Immortalized cell lines from various tissue sources provide efficient tools for optimizing characterization experiments of in vitro differentiation assays, due to their indefinite proliferation and abundant expression of lineage-specific markers, [193]-[197]. To set up the *in vitro* characterization of ectodermal (neural, melanocyte) and endodermal (hepatocyte) and markers expression, we used immortalized cells lines which abundantly express neural (A172 cells from glioblastoma, [195]), melanocyte (SKMEL-28, [193] and MALME-3, [194] melanoma cells) and hepatocyte markers (HEP3B hepatocellular carcinoma cells, [196]). Pluripotent stem cells and pluripotent cell lines are suitable model systems for testing and optimization of *in vitro* differentiation protocols, as they undergo tri-lineage differentiation to generate ectodermal, mesodermal, and endodermal lineage cells. On the other hand, the differentiation capacity of pluripotent stem cell lines can be changed or reduced over maintenance due to spontaneous differentiation, genetic mutations, or acquisition of

epigenetic aberrations causing lineage-biased differentiation [220]. Thus, quality control over pluripotent stem cell lines through regular characterization for pluripotency must be exerted. In addition, the maintenance of ESC and iPSC lines require specialized cell culture medium, extracellular matrix supply or feeder cell layer. NTERA2 clone D1 cells have the advantage of recapitulating embryonic stem cell functions throughout long-term *in vitro* culturing, including their high clonogenic potential, and their capacity to generate ectodermal, endodermal, and mesodermal lineage daughter cells [196]. On the other hand, the NTERA2 clone D1 cell line does not require extracellular matrix, neither feeder cell layer nor timely regulated addition of growth factors for their long-term culturing. NTERA2 cells can be easily cultivated in plastic culture dishes containing DMEM supplemented with FBS. We used NTERA2 cells to optimize *in vitro* ectodermal (neural), mesodermal (osteogenic) and endodermal (hepatic) differentiation.

Although the chemical, genetic and feeder cell-based methods are commonly used for neural differentiation of pluripotent cell lines, they are time-demanding and producing neural cells with highly variable phenotypes. For example, the use of retinoic acid and Shh predominantly generate caudal phenotypes of the developing neural tube [221]. On the other hand, effective 3D induction methods for neural stem cells from PSCs were published [222], which more reliably recapitulate in vivo neural development. Cells obtained with these methods express classical neural stem cell markers (Nestin) and neuronal lineage markers (ENO2, MAP2). To analyze neural lineage differentiation of MAFs, we chose the 3D neural differentiation method published by Wakao et al, which is followed by 2D culturing with medium containing the neurogenic factor BDNF. NTERA2-derived neural cell cultures expressing Nestin, MAP2 and ENO2, (Fig.24) similarly to the methods published for NSC differentiation from PSCs.

Hepatic differentiation from PSCs were reported both in 2D and 3D cultures. Although the generation of functional hepatocytes by cytokines [223], small molecule chemicals [224], [225] and metabolites [226] were also reported, most of the 2D approaches follow a stepwise protocol utilizing definitive endoderm induction, hepatic specification, and hepatocyte maturation. By utilizing bona fide cytokines for definitive endoderm induction, hepatic endoderm specification, hepatic specification, and maturation we obtained hepatic-like cells expressing hepatic markers AFP, albumin, Cytokeratin 7 and Cytokeratin 18, (Fig.25). Although we did not assay our cells for endodermal progenitor makers, it was

reported that AFP is expressed in hepatocyte progenitor cells, while albumin and Cytokeratin 18 are reported to be expressed in hepatocytes. Our results suggest that our *in vitro* hepatocyte differentiation method carried out on NTERA2 cells produced hepatocyte lineage cells. On the other hand, hepatocyte-specific functions, such as CYP450 enzyme activity and urea production were also reported for PSC-derived hepatocytes [223]. We are planning to implement these functional assays to further complement the cellular phenotypes obtained upon *in vitro* hepatic differentiation. Our results showed that NTERA2 cells provide an efficient, cost-effective source of pluripotent cells to study not just neurogenic, but also osteogenic and hepatogenic differentiation.

After identifying stem cell subsets from MAFs, we analyzed their differentiation potential. Our results showed that MAFs contain multipotent stem cell subsets, for which the mesodermal lineage differentiation was reported. Furthermore, MAFs had significantly higher osteogenic and adipogenic lineage differentiation potential, than normal dermal fibroblasts. Our results suggest a higher differentiation plasticity of MAFs acquired in the melanoma microenvironment. It would be intriguing to reveal how the tumor microenvironment regulates the differentiation of MAFs to promote cancer growth and spreading. On the other hand, the utility of targeting MAFs for differentiation therapy to eliminate their cancer-promoting functions needs more investigation. In the case of leukemia and breast cancer, a dramatic decrease in tumorigenicity was observed upon targeted differentiation of tumor cells [209]. Despite the beneficial effects of induced differentiation reported for cancer cells, the effects of targeted differentiation of CAFs on cancer growth, immunosuppression, and metastasis need more investigation. In addition, MAFs displayed not only MSC-like mesodermal lineage differentiation, but also neural and hepatic lineage differentiation. The fraction of differentiated ectodermal and endodermal lineage cells show donor-to-donor variabilities, which might arise from patient-specific differences of subcutaneous melanoma samples, such as mutation status, tumor stage, age, and gender. Nevertheless, the ectodermal and endodermal differentiation potential observed in MAFs suggest the presence of multipotent stromal stem cell subsets in the melanoma microenvironment, which can give rise to heterogeneous CAFs.

Adult multipotent MSCs and MUSE cells are non-tumorigenic stem cells with immunomodulatory potential. They suppress inflammatory responses, including pro-inflammatory cytokine production, M1 macrophage and CD8+ T-Cell activation [106],

[133]. The regulation of local immune-homeostasis is necessary for these stem cells to exert their beneficial activities during tissue repair by homing and tissue-specific cell production by differentiation. On the other hand, MAFs cells contribute to immunosuppression and evasion of anti-tumor immunity in malignant melanomas. Given the immunomodulatory potential of MUSE cells, their presence in the stromal compartments of malignant melanomas and their contribution to MAF-mediated immunosuppression remains an intriguing question. MUSE cells were identified as multipotent adult stem cells, which reside in various stromal compartments, including bone-marrow, adipose tissue, and skin. On the other hand, little is known on their presence among CAFs. We showed a small fraction of SSEA3+ cells among MAFs, which were also positive for MSC markers CD90 and CD105. Diverse cell subsets of the dermis were reported to express stage-specific embryonic antigens, although not all SSEA-expressing cell showed pluripotent stem cell marker expression [227], [85], as it was published for MUSE cells by Wakao et al [132]. Thus, we addressed whether MAF-derived SSEA3+ cells express pluripotency markers and the ability to generate cells beyond mesodermal lineages, such as melanocytes. We detected the expression of embryonic stem cell factors OCT3/4, NANOG, and TRA-1-60 FACS-sorted SSEA3+ cells, (Fig.31), suggesting their intrinsic ability for multilineage differentiation. These results suggest, that MAFs contain MUSE cells. MAF-derived MUSE cells differentiated into melanocyte-like cells with dendritic morphology, and they expressed melanocyte-specific markers (MITF, DCT, PMEL, melan-A, TYRP1). In addition, MUSE cells from MAFs differentiated into melanocytes more efficiently, than MUSE cells isolated from dermal fibroblasts, (Fig.33). These results raise the intriguing question whether tumor competent melanocytes can emerge from MAF-derived MUSE cells. Although CAFs have a stable genotype it is still unknown whether MAF- and MUSE-cell-derived melanocytes retain their genomic stability in the melanoma microenvironment. Regarding that the tumor microenvironment is characterized by hypoxia, inflammation and growth-factor enrichment, there is a possibility of oncogenic transformation of MUSE cell-derived melanocytes within melanoma niches. Thus, the differentiation plasticity of MAFs and MUSE cells within melanoma necessitates further investigation.

In conclusion, we found that MAFs have an MSC-like molecular phenotype and diverse stromal stem cell subsets. Besides MAFs have a higher differentiation plasticity compared

to dermal fibroblasts, which includes their elevated mesodermal, ectodermal, and endodermal lineage differentiation potential. This increased ability to generate ectodermal, mesodermal, and endodermal lineage cells can be ascribed to the presence of SSEA3+ cells among MAFs, which express pluripotent stem cell markers and differentiate into melanocyte lineage cells, such as MUSE cells. Further experiments are required to see if SSEA3+ MAFs and their melanocyte derivatives contribute to melanoma growth, progression, drug resistance and metastasis.

6. New Scientific Results

Thesis 1: MAFs have a Bone-marrow Mesenchymal Stromal/Stem Cell-like Phenotype.

MAFs isolated from subcutaneous melanoma metastases displayed mesenchymal stromal cell (MSC)-like features, such as spindle shaped morphology, and high adherence to non-coated cell culture plates. To further dissect the MSC-like phenotype of MAFs, we analyzed the expression of MSC-specific cell surface molecules by flow cytometry. We showed that MAFs are MSC-like cells expressing canonical MSC markers CD73, CD90, and CD105. To address whether MAFs have MSC-like mesodermal lineage differentiation, we exposed MAFs to *in vitro* osteogenic and adipogenic differentiation media. *In vitro* differentiation was followed by the detection of osteocyte-specific calcium deposits and adipocite-specific lipid droplets by Alizarin Red S and Oil Red O staining, respectively. MAFs accumulated calcium-phosphate deposits upon *in vitro* osteogenic differentiation, and lipid droplets were enriched in MAF cultures during *in vitro* adipocite differentiation. By conducting RT-qPCR measurements, we detected the osteocyte markers *ALPL* and *BGLAP* (Fig.6C), and adipocyte markers *PPARG* and *CEBPA* in differentiated MAFs, (Fig.6D). Furthermore, we detected the expression of osteogenic marker alkaline phosphatase (ALPL, Fig.1C), and adipogenic marker CCAAT enhancer binding protein α (CEBPα, Fig.1D) in differentiated MAFs. These results indicate, that MAFs generate osteocytes and adipocytes *in vitro*.

Thesis 2: NTERA2 cells undergo *in vitro* neural, hepatic and osteogenic differentiation.

We showed, that NTERA2 cells express pluripotency markers ($Oct_{3/4}$, NANOG, TRA-160, Sox2). By using NTERA2 cells, we optimized our methods for in vitro neural, hepatocyte and osteogenic lineage differentiation. By using the A172 and HEP3B immortalized cell lines as positive controls for *in vitro* characterizations, we demonstrated the generation of neural and hepatic lineage cells from NTERA2 cells. NTERA2-derived neural lineage cells expressed markers of neural stem cells, such as Nestin, MAP2 and neuronal progenitor cell marker ENO2. NTERA-derived hepatic lineage cells displayed markers of fetal hepatocytes, including albumin, AFP and CK18. In addition, osteogenic differentiation of NTERA2 cells produced calcium-phosphate deposits in the cell cultures, and cells expressing osteogenic markers BGLAP and ALPL. Our results underpin the potential of

NTERA2 clone D1 cells to serve as a cost-effective source of cellular positive control for studying pluripotent stem cell traits of induced pluripotent stem cells and adult tissue stem cells, such as MUSE cells.

Thesis 3: MAFs Have Enhanced Tri-lineage Differentiation Potential Compared to Normal Dermal Fibroblasts.

We compared mesodermal lineage differentiation potential of MAFs to normal dermal fibroblasts by using our *in vitro* osteogenic and adipogenic differentiation assays.

MAFs generated significantly higher number of mesodermal lineage cells, than normal dermal fibroblasts. Next, we analyzed multilineage differentiation of MAFs in our *in vitro* ectodermal (neural) and endodermal (hepatic) lineage differentiation assays, which were optimized on pluripotent NTERA2 cells. In addition to their enhanced mesodermal lineage generation potential, melanoma associated fibroblasts generated MAP+Nestin+ ectodermal, and AFP+albumin+ endodermal lineage cells.

Thesis 4: MAFs harbor MUSE cells, CD146+ and CD271+ stem cell subsets.

By utilizing flow-cytometric measurements, we showed that MAFs contain stromal stem cell subsets, such as CD271+, CD146+ and SSEA3+ cells. SSEA3+ cells were described as multi-lineage differentiating, stress enduring cells, which express pluripotent stem cell markers [125], modulate inflammatory immune responses [133], and give rise to melanocytes [128]. To further characterize the SSEA3+ cell subset in melanomas, we isolated SSEA3+CD90+ stromal cells from MAFs by fluorescence-activated cell sorting and analyzed the expression of pluripotency markers in these cells. We showed by ICC staining and qRT-PCR measurements that SSEA3+ MAF cells express pluripotent stem cell marker $Oct_{3/4}$, SOX2, NANOG and TRA-1-60. In conclusion, MAFs encompass SSEA3+ MUSE cells, which express not only the canonical stromal markers (CD90, CD105), but also pluripotent stem cell markers ($Oct_{3/4}$, Sox2, NANOG, TRA-1-60).

Thesis 5: MUSE cells from MAFs Generate Melanocyte Lineage Cells.

After the identification of MUSE cells in MAFs, we examined their ability to generate melanocyte lineage cells *in vitro*. MUSE cells were isolated by FACS using SSEA3/CD90 double staining. MUSE cells from MAFs, but not SSEA3- non-MUSE cells differentiate into melanocyte lineage cells in vitro, which have elongated, dendritic morphology and express GP100 and Melan A., (Fig.32). Furthermore, additional melanocyte lineage markers, such as MITF, DCT and TYRP1 were also upregulated in SSEA3+ cells, but not in SSEA3- (non-MUSE) cells upon *in vitro* melanocytic differentiation.

7. Potential Application of the Results

CAFs are the most abundant cells of the tumor-microenvironment, and through intricate interactions with the tumor-microenvironment they play central roles in orchestrating cancer growth, immunosuppression, metastasis, and drug resistance. Although molecular targeting strategies abrogating CAF functions have emerged [208], specific markers enabling the identification of CAFs are still missing. In contrast to the cancer cells, CAFs have a lower proliferation rate, therefore they are less targetable by conventional chemotherapeutic approaches. On the other hand, the identification of CAF-specific molecular markers would greatly enhance the selective elimination of tumor-promoting CAF subsets. Given the high heterogeneity of CAFs, elucidating the stem cell sources of CAFs is an important step in the effective targeting and abrogation of the stromal supply of cancers.

Malignant melanoma is an extremely aggressive and drug-resistant cancer associated with high mortality and poor prognosis. In concert with similar studies our lab reported the immunosuppressive action of MAFs, [229], [II], yet limited information is available on the phenotypic composition, stem cell sources and differentiation plasticity of MAFs. Here, I demonstrated that melanoma associated fibroblasts have an MSC-like molecular phenotype (Fig.18-20, chapter 4.1), and enhanced capacity for in vitro multilineage differentiation. The advanced differentiation potential of MAFs raises the possibility of targeting these cells by chemical agents promoting their differentiation to other cell types, (for e.g., adipocytes) with subsequent loss of their pro-tumorigenic functions [209].

To analyze the ectodermal (neural, melanocyte), mesodermal (osteocyte, adipocyte) and endodermal (hepatocyte) lineage differentiation of MAFS, we optimized the *in vitro* tri-lineage differentiation assays by using the NTERA2 clone D1 cel line, (chapter 4.3). We showed, that NTERA2 cells express pluripotent stem cell markers (Fig.23), and they generate neural, hepatocyte and osteocyte lineage cells, (Fig.24-26). Therefore, our results support NTERA2 cells as a model system, which is suitable for analyzing tri-lineage differentiation of pluripotent cell lines and subtypes, such as MUSE cells.

In addition to their MSC-like phenotype, we identified stem cell subsets in MAFs, which might be possible sources of the tumor stroma due to their self-renewal and differentiation potential. We showed, that MAFs harbor the CD146+ and CD271+ stem cell

subsets, (Fig.19), which are implicated in immunomodulation and angiogenesis in homeostatic tissues, [218], [219]. It remains to be seen how the targeting of these cell subsets affects immunosuppression and angiogenesis in melanoma. In addition to the CD146+ and CD271+ cells, we also demonstrated the presence of multi-lineage differentiating, stress enduring cells in MAFs, (Fig.19, Fig.32), a multipotent stem cell subpopulation awakened by cellular stress, inflammatory and tissue damage signals. Given their ability to suppress inflammatory T-cell responses [8], the significance of MUSE cells in tumor growth and resistance remains an intriguing question, which warrants further studies. Furthermore, the implications of enhanced melanocytic differentiation of MUSE cells from MAFs (Fig.32, Fig.33) needs further investigation in the context of melanoma growth.

Taken together, our results showed that specific stromal cell subsets reside in human malignant melanomas with stem cell properties. We identified three stromal stem cell subsets among MAFs: CD146+ cells, CD271+ cells and MUSE cells. These stem cell subsets might contribute to the enhanced capacity of MAFs for the generation of mesodermal lineage cells and multilineage differentiation. Contribution of these MAF subpopulations to the growth and spreading of melanomas requires further studies, as well as their suitability as cellular targets for novel anti-cancer therapies.

8. Acknowledgements

I would like to express my gratitude to the Roska Tamás Doctoral School of Science and Technology, its Directorate and the PhD student's registry office for allowing my PhD research in the Stem Cell Laboratory of the Clinics of Dermatology, Venerology and Dermato-oncology, (University of Semmelweis). I am deeply thankful to Professor Dr. Sarolta Kárpáti and Dr. Krisztián Németh to allow me to participate the Stem Cell Research Group. I would like to express my gratitude to my supervisors, Dr. Krisztián Németh and Dr. Miklós Gyöngy for their contribution to study design, supervision, and manuscripts preparation. I am grateful to Dr. Balázs Mayer, Dr. Zoltán Pos, Dr. Barbara Molnár-Érsek and Dr. Gábor Barna for their great amount of help in learning flow cytometry, cell sorting techniques, statistical analysis, and data interpretation. I would like to thank dr. Pálma Silló, Mercédesz Mazán, Adrien Suba for providing me training and methodological insight into fibroblast isolation and real-time quantitative PCR measurements. I'm also thankful to my former and current colleagues, dr. Melinda Fábián, Szilvia Barsi, Anna Hajdara and Dr. Cakir Ugur for their helpful, cooperative, and friendly attitude and all support in my scientific work.

This work was supported by the Hungarian National Research, Development, and Innovation Office (Grant NN 114460 to Prof. Sarolta Kárpáti). The research has been supported by the ÚNKP-19-3 New National Excellence Programme of the Ministry of Human Capacities, Hungary (Grant ÚNKP-19-3-III-PPKE-30). The research project has been partially supported by the European Union, co-financed by the European Social Fund (EFOP-3.6.3-VEKOP-16-2017-00002). Preparation of frozen cell biobanks from MAFs, DFs and all cell lines were supported by the NKFIA TKP2021-NVA-15 programme of the University of Semmelweis.

9. References

[1]: Zakrzewski, W., Dobrzyński, M., Szymonowicz, M., & Rybak, Z. (2019). Stem cells: past, present, and future. *Stem cell research & therapy*, *10*(1), 68

[2]: Joung, J., Ma, S., Tay, T., Geiger-Schuller, K. R., Kirchgatterer, P. C., Verdine, V. K., Guo, B., Arias-Garcia, M. A., Allen, W. E., Singh, A., Kuksenko, O., Abudayyeh, O. O., Gootenberg, J. S., Fu, Z., Macrae, R. K., Buenrostro, J. D., Regev, A., & Zhang, F. (2023). A transcription factor atlas of directed differentiation. *Cell*, *186*(1), 209–229.e26.

[3]: Gökbuget, D., & Blelloch, R. (2019). Epigenetic control of transcriptional regulation in pluripotency and early differentiation. *Development (Cambridge, England)*, *146*(19), dev164772.

[4]: Berdasco, M., & Esteller, M. (2011). DNA methylation in stem cell renewal and multipotency. *Stem cell research & therapy*, *2*(5), 42.

[5]: Watt, F. M., & Huck, W. T. (2013). Role of the extracellular matrix in regulating stem cell fate. *Nature reviews. Molecular cell biology*, *14*(8), 467–473.

[6]: Mathur, A. N., Zirak, B., Boothby, I. C., Tan, M., Cohen, J. N., Mauro, T. M., Mehta, P., Lowe, M. M., Abbas, A. K., Ali, N., & Rosenblum, M. D. (2019). Treg-Cell Control of a CXCL5-IL-17 Inflammatory Axis Promotes Hair-Follicle-Stem-Cell Differentiation During Skin-Barrier Repair. *Immunity*, *50*(3), 655–667.e4

[7]: Gómez-López S, Lerner RG, Petritsch C. Asymmetric cell division of stem and progenitor cells during homeostasis and cancer. Cell Mol Life Sci. 2014 Feb;71(4):575-97.

[8]: Shitamukai, A., & Matsuzaki, F. (2012). Control of asymmetric cell division of mammalian neural progenitors. *Development, growth & differentiation*, *54*(3), 277–286.

[9]: Liu, S., Dontu, G., & Wicha, M. S. (2005). Mammary stem cells, self-renewal pathways, and carcinogenesis. *Breast cancer research: BCR*, *7*(3), 86–95.

[10]: Snippert, H. J., van der Flier, L. G., Sato, T., van Es, J. H., van den Born, M., Kroon-Veenboer, C., Barker, N., Klein, A. M., van Rheenen, J., Simons, B. D., & Clevers, H. (2010). Intestinal crypt homeostasis results from neutral competition between symmetrically dividing Lgr5 stem cells. *Cell*, *143*(1), 134–144.

[11]: Fortunel, N. O., Chadli, L., Coutier, J., Lemaître, G., Auvré, F., Domingues, S., Bouissou-Cadio, E., Vaigot, P., Cavallero, S., Deleuze, J. F., Roméo, P. H., & Martin, M. T. (2019). KLF4 inhibition promotes the expansion of keratinocyte precursors from adult human skin and of embryonic-stem-cell-derived keratinocytes. *Nature biomedical engineering*, *3*(12), 985–997.

[12]: Yao, C., Yao, R., Luo, H., & Shuai, L. (2022). Germline specification from pluripotent stem cells. *Stem cell research & therapy*, *13*(1), 74.

[13]: Jiménez-Rojo, L., Granchi, Z., Graf, D., & Mitsiadis, T. A. (2012). Stem Cell Fate Determination during Development and Regeneration of Ectodermal Organs. *Frontiers in physiology*, *3*, 107.

[14]: Nikolopoulou, E., Galea, G. L., Rolo, A., Greene, N. D., & Copp, A. J. (2017). Neural tube closure: cellular, molecular, and biomechanical mechanisms. *Development (Cambridge, England)*, *144*(4), 552–566.

[15]: Conti, L., & Cattaneo, E. (2010). Neural stem cell systems: physiological players or in vitro entities? *Nature reviews. Neuroscience*, *11*(3), 176–187.

[16]: Schirò, G., Iacono, S., Ragonese, P., Aridon, P., Salemi, G., & Balistreri, C. R. (2022). A Brief Overview on BDNF-Trk Pathway in the Nervous System: A Potential Biomarker or Possible Target in Treatment of Multiple Sclerosis? *Frontiers in neurology*, *13*, 917527.

[17]: Chambers, S. M., Fasano, C. A., Papapetrou, E. P., Tomishima, M., Sadelain, M., & Studer, L. (2009). Highly efficient neural conversion of human ES and iPS cells by dual inhibition of SMAD signaling. *Nature biotechnology*, *27*(3), 275–280.

[18]: Liu, D. D., He, J. Q., Sinha, R., Eastman, A. E., Toland, A. M., Morri, M., Neff, N. F., Vogel, H., Uchida, N., & Weissman, I. L. (2023). Purification and characterization of human neural stem and progenitor cells. *Cell*, *186*(6), 1179–1194.e15.

[19]: Li, M., Knapp, S. K., & Iden, S. (2020). Mechanisms of melanocyte polarity and differentiation: What can we learn from other neuroectoderm-derived lineages? *Current opinion in cell biology*, *67*, 99–108.

[20]: Lowdon, R. F., Zhang, B., Bilenky, M., Mauro, T., Li, D., Gascard, P., Sigaroudinia, M., Farnham, P. J., Bastian, B. C., Tlsty, T. D., Marra, M. A., Hirst, M., Costello, J. F., Wang, T., & Cheng, J. B. (2014). Regulatory network decoded from epigenomes of surface ectoderm-derived cell types. *Nature communications*, *5*, 5442.

[21]: Hida, T., Kamiya, T., Kawakami, A., Ogino, J., Sohma, H., Uhara, H., & Jimbow, K. (2020). Elucidation of Melanogenesis Cascade for Identifying Pathophysiology and Therapeutic Approach of Pigmentary Disorders and Melanoma. *International journal of molecular sciences*, *21*(17), 6129.

[22]: Mirea, M. A., Eckensperger, S., Hengstschläger, M., & Mikula, M. (2020). Insights into Differentiation of Melanocytes from Human Stem Cells and Their Relevance for Melanoma Treatment. *Cancers*, *12*(9), 2508.

[23]: Ge, C., Cawthorn, W. P., Li, Y., Zhao, G., Macdougald, O. A., & Franceschi, R. T. (2016). Reciprocal Control of Osteogenic and Adipogenic Differentiation by ERK/MAP Kinase Phosphorylation of Runx2 and PPARγ Transcription Factors. *Journal of cellular physiology*, *231*(3), 587–596.

[24]: Xu, J., Li, Z., Hou, Y., & Fang, W. (2015). Potential mechanisms underlying the Runx2 induced osteogenesis of bone marrow mesenchymal stem cells. *American journal of translational research*, *7*(12), 2527–2535.

[25]: Wang, S., Lin, Y., Gao, L., Yang, Z., Lin, J., Ren, S., Li, F., Chen, J., Wang, Z., Dong, Z., Sun, P., & Wu, B. (2022). PPAR-γ integrates obesity and adipocyte clock through epigenetic regulation of *Bmal1*. *Theranostics*, *12*(4), 1589–1606.

[26]: Zhou, X., Beilter, A., Xu, Z., Gao, R., Xiong, S., Paulucci-Holthauzen, A., Lozano, G., de Crombrugghe, B., & Gorlick, R. (2021). Wnt/ß-catenin-mediated p53 suppression is indispensable for osteogenesis of mesenchymal progenitor cells. *Cell death & disease*, *12*(6), 521.

[27]: Xiong, J., Almeida, M., & O'Brien, C. A. (2018). The YAP/TAZ transcriptional co-activators have opposing effects at different stages of osteoblast differentiation. *Bone*, *112*, 1–9.

[28]: Talele, N. P., Fradette, J., Davies, J. E., Kapus, A., & Hinz, B. (2015). Expression of α-Smooth Muscle Actin Determines the Fate of Mesenchymal Stromal Cells. *Stem cell reports*, *4*(6), 1016–1030.

[29]: Kovar, H., Bierbaumer, L., & Radic-Sarikas, B. (2020). The YAP/TAZ Pathway in Osteogenesis and Bone Sarcoma Pathogenesis. *Cells*, *9*(4), 972.

[30]: Kawai, M., & Rosen, C. J. (2010). PPARγ: a circadian transcription factor in adipogenesis and osteogenesis. *Nature reviews. Endocrinology*, *6*(11), 629–636.

[31]: Hamidouche, Z., Haÿ, E., Vaudin, P., Charbord, P., Schüle, R., Marie, P. J., & Fromigué, O. (2008). FHL2 mediates dexamethasone-induced mesenchymal cell differentiation into osteoblasts by activating Wnt/β-catenin signaling-dependent Runx2 expression. *FASEB journal: official publication of the Federation of American Societies for Experimental Biology*, *22*(11), 3813–3822.

[32]: Hong, D., Chen, H. X., Xue, Y., Li, D. M., Wan, X. C., Ge, R., & Li, J. C. (2009). Osteoblastogenic effects of dexamethasone through upregulation of TAZ expression in rat mesenchymal stem cells. *The Journal of steroid biochemistry and molecular biology*, *116*(1-2), 86–92.

[33]: Franceschi, R. T., Iyer, B. S., & Cui, Y. (1994). Effects of ascorbic acid on collagen matrix formation and osteoblast differentiation in murine MC3T3-E1 cells. *Journal of bone and mineral research: the official journal of the American Society for Bone and Mineral Research*, *9*(6), 843–854.

[34]: Tada, H., Nemoto, E., Foster, B. L., Somerman, M. J., & Shimauchi, H. (2011). Phosphate increases bone morphogenetic protein-2 expression through cAMP-dependent protein kinase and ERK1/2 pathways in human dental pulp cells. *Bone*, *48*(6), 1409–1416.

[35]: Tafuri S. R. (1996). Troglitazone enhances differentiation, basal glucose uptake, and Glut1 protein levels in 3T3-L1 adipocytes. *Endocrinology*, *137*(11), 4706–4712.

[36]: Yang, D. C., Tsay, H. J., Lin, S. Y., Chiou, S. H., Li, M. J., Chang, T. J., & Hung, S. C. (2008). cAMP/PKA regulates osteogenesis, adipogenesis and ratio of RANKL/OPG mRNA expression in mesenchymal stem cells by suppressing leptin. *PloS one*, *3*(2), e1540.

[37]: Sahabian, A., Dahlmann, J., Martin, U., & Olmer, R. (2021). Production and cryopreservation of definitive endoderm from human pluripotent stem cells under defined and scalable culture conditions. *Nature protocols*, *16*(3), 1581–1599.

[38]: Ikonomou, L., & Kotton, D. N. (2015). Derivation of Endodermal Progenitors From Pluripotent Stem Cells. *Journal of cellular physiology*, *230*(2), 246–258.

[39]: Carpentier, A., Nimgaonkar, I., Chu, V., Xia, Y., Hu, Z., & Liang, T. J. (2016). Hepatic differentiation of human pluripotent stem cells in miniaturized format suitable for high-throughput screen. *Stem cell research*, *16*(3), 640–650.

[40]: Mallana, S. K., & Duncan, S. A. (2013). Differentiation of hepatocytes from pluripotent stem cells. *Current protocols in stem cell biology*, *26*, 1G.4.1–1G.4.13.

[41]: Miyajima, A., Tanaka, M., & Itoh, T. (2014). Stem/progenitor cells in liver development, homeostasis, regeneration, and reprogramming. *Cell stem cell*, *14*(5), 561–574.

[42]: Jones, D. L., & Wagers, A. J. (2008). No place like home: anatomy and function of the stem cell niche. *Nature reviews. Molecular cell biology*, *9*(1), 11–21.

[43]: Cui KW, Engel L, Dundes CE, Nguyen TC, Loh KM, Dunn AR. Spatially controlled stem cell differentiation via morphogen gradients: A comparison of static and dynamic microfluidic platforms. J Vac Sci Technol A. 2020 May;38(3):033205. doi: 10.1116/1.5142012. Epub 2020 Mar 24. PMID: 32255900; PMCID: PMC7093209.

[44]: Zhang, J., Klos, M., Wilson, G. F., Herman, A. M., Lian, X., Raval, K. K., Barron, M. R., Hou, L., Soerens, A. G., Yu, J., Palecek, S. P., Lyons, G. E., Thomson, J. A., Herron, T. J., Jalife, J., & Kamp, T. J. (2012). Extracellular matrix promotes highly efficient cardiac differentiation of human pluripotent stem cells: the matrix sandwich method. *Circulation research*, *111*(9), 1125–1136.

[45]: Chen, S., Zheng, Y., Ran, X., Du, H., Feng, H., Yang, L., Wen, Y., Lin, C., Wang, S., Huang, M., Yan, Z., Wu, D., Wang, H., Ge, G., Zeng, A., Zeng, Y. A., & Chen, J. (2021). Integrin $\alpha E\beta 7^{+}$ T cells direct intestinal stem cell fate decisions via adhesion signaling. *Cell research*, *31*(12), 1291–1307.

[46]: Mohyeldin, A., Garzón-Muvdi, T., & Quiñones-Hinojosa, A. (2010). Oxygen in stem cell biology: a critical component of the stem cell niche. *Cell stem cell*, *7*(2), 150–161.

[47]: Roberts KJ, Kershner AM, Beachy PA. The Stromal Niche for Epithelial Stem Cells: A Template for Regeneration and a Brake on Malignancy. Cancer Cell. 2017 Oct 9;32(4):404-410.

[48]: Lamaison, C., & Tarte, K. (2021). B cell/stromal cell crosstalk in health, disease, and treatment: Follicular lymphoma as a paradigm. *Immunological reviews*, *302*(1), 273–285.

[49]: Blanpain, C., & Fuchs, E. (2009). Epidermal homeostasis: a balancing act of stem cells in the skin. *Nature reviews. Molecular cell biology*, *10*(3), 207–217.

[50]: Hsu, Y. C., Li, L., & Fuchs, E. (2014). Emerging interactions between skin stem cells and their niches. *Nature medicine*, *20*(8), 847–856.

[51]: Rahmani, W., Abbasi, S., Hagner, A., Raharjo, E., Kumar, R., Hotta, A., Magness, S., Metzger, D., & Biernaskie, J. (2014). Hair follicle dermal stem cells regenerate the dermal

sheath, repopulate the dermal papilla, and modulate hair type. *Developmental cell*, *31*(5), 543–558.

[52]: Feldman, A., Mukha, D., Maor, I. I., Sedov, E., Koren, E., Yosefzon, Y., Shlomi, T., & Fuchs, Y. (2019). Blimp1^{+} cells generate functional mouse sebaceous gland organoids in vitro. *Nature communications*, *10*(1), 2348.

[53]: Heitman, N., Sennett, R., Mok, K. W., Saxena, N., Srivastava, D., Martino, P., Grisanti, L., Wang, Z., Ma'ayan, A., Rompolas, P., & Rendl, M. (2020). Dermal sheath contraction powers stem cell niche relocation during hair cycle regression. *Science (New York, N.Y.)*, *367*(6474), 161–166.

[54]: Lim, X., Tan, S. H., Yu, K. L., Lim, S. B., & Nusse, R. (2016). Axin2 marks quiescent hair follicle bulge stem cells that are maintained by autocrine Wnt/β-catenin signaling. *Proceedings of the National Academy of Sciences of the United States of America*, *113*(11), E1498–E1505.

[55]: Malakpour-Permlid, A., Buzzi, I., Hegardt, C., Johansson, F., & Oredsson, S. (2021). Identification of extracellular matrix proteins secreted by human dermal fibroblasts cultured in 3D electrospun scaffolds. *Scientific reports*, *11*(1), 6655.

[56]: Cattaneo, P., Mukherjee, D., Spinozzi, S., Zhang, L., Larcher, V., Stallcup, W. B., Kataoka, H., Chen, J., Dimmeler, S., Evans, S. M., & Guimarães-Camboa, N. (2020). Parallel Lineage-Tracing Studies Establish Fibroblasts as the Prevailing In Vivo Adipocyte Progenitor. *Cell reports*, *30*(2), 571–582.

[57]: Foster, D. S., Januszyk, M., Yost, K. E., Chinta, M. S., Gulati, G. S., Nguyen, A. T., Burcham, A. R., Salhotra, A., Ransom, R. C., Henn, D., Chen, K., Mascharak, S., Tolentino, K., Titan, A. L., Jones, R. E., da Silva, O., Leavitt, W. T., Marshall, C. D., des Jardins-Park, H. E., Hu, M. S., … Longaker, M. T. (2021). Integrated spatial multiomics reveals fibroblast fate during tissue repair. *Proceedings of the National Academy of Sciences of the United States of America*, *118*(41)

[58]: Díaz-García D, Filipová A, Garza-Veloz I, Martinez-Fierro ML. A Beginner's Introduction to Skin Stem Cells and Wound Healing. Int J Mol Sci. 2021 Oct 13;22(20)

[59]: Jevtić, M., Löwa, A., Nováčková, A., Kováčik, A., Kaessmeyer, S., Erdmann, G., Vávrová, K., & Hedtrich, S. (2020). Impact of intercellular crosstalk between epidermal keratinocytes and dermal fibroblasts on skin homeostasis. *Biochimica et biophysica acta. Molecular cell research*, *1867*(8), 118722.

[60]: Nowarski, R., Jackson, R., & Flavell, R. A. (2017). The Stromal Intervention: Regulation of Immunity and Inflammation at the Epithelial-Mesenchymal Barrier. *Cell*, *168*(3), 362–375.

[61]: Driskell, R. R., & Watt, F. M. (2015). Understanding fibroblast heterogeneity in the skin. *Trends in cell biology*, *25*(2), 92–99.

[62]: Driskell, R. R., Lichtenberger, B. M., Hoste, E., Kretzschmar, K., Simons, B. D., Charalambous, M., Ferron, S. R., Herault, Y., Pavlovic, G., Ferguson-Smith, A. C., & Watt, F.

M. (2013). Distinct fibroblast lineages determine dermal architecture in skin development and repair. *Nature*, *504*(7479), 277–281.

[63]: Walker, J. T., Flynn, L. E., & Hamilton, D. W. (2021). Lineage tracing of Foxd1-expressing embryonic progenitors to assess the role of divergent embryonic lineages on adult dermal fibroblast function. *FASEB bioAdvances*, *3*(7), 541–557.

[64]: Rinn, J. L., Bondre, C., Gladstone, H. B., Brown, P. O., & Chang, H. Y. (2006). Anatomic demarcation by positional variation in fibroblast gene expression programs. *PLoS genetics*, *2*(7), e119.

[65]: Plikus, M. V., Wang, X., Sinha, S., Forte, E., Thompson, S. M., Herzog, E. L., Driskell, R. R., Rosenthal, N., Biernaskie, J., & Horsley, V. (2021). Fibroblasts: Origins, definitions, and functions in health and disease. *Cell*, *184*(15), 3852–3872.

[66]: Chang, Y., Li, H., & Guo, Z. (2014). Mesenchymal stem cell-like properties in fibroblasts. *Cellular physiology and biochemistry: international journal of experimental cellular physiology, biochemistry, and pharmacology*, *34*(3), 703–714.

[67]: Wong, C. W., LeGrand, C. F., Kinnear, B. F., Sobota, R. M., Ramalingam, R., Dye, D. E., Raghunath, M., Lane, E. B., & Coombe, D. R. (2019). In Vitro Expansion of Keratinocytes on Human Dermal Fibroblast-Derived Matrix Retains Their Stem-Like Characteristics. *Scientific reports*, *9*(1), 18561

[68]: Onursal, C., Dick, E., Angelidis, I., Schiller, H. B., & Staab-Weijnitz, C. A. (2021). Collagen Biosynthesis, Processing, and Maturation in Lung Ageing. *Frontiers in medicine*, *8*, 593874.

[69]: Westermarck, J., Li, S., Jaakkola, P., Kallunki, T., Grénman, R., & Kähäri, V. M. (2000). Activation of fibroblast collagenase-1 expression by tumor cells of squamous cell carcinomas is mediated by p38 mitogen-activated protein kinase and c-Jun NH2-terminal kinase-2. *Cancer research*, *60*(24), 7156–7162.

[70]: Freitas-Rodríguez, S., Folgueras, A. R., & López-Otín, C. (2017). The role of matrix metalloproteinases in aging: Tissue remodeling and beyond. *Biochimica et biophysica acta. Molecular cell research*, *1864*(11 Pt A), 2015–2025.

[71]: Herchenhan, A., Uhlenbrock, F., Eliasson, P., Weis, M., Eyre, D., Kadler, K. E., Magnusson, S. P., & Kjaer, M. (2015). Lysyl Oxidase Activity Is Required for Ordered Collagen Fibrillogenesis by Tendon Cells. *The Journal of biological chemistry*, *290*(26), 16440–16450.

[72]: Mao, Y., & Schwarzbauer, J. E. (2005). Fibronectin fibrillogenesis, a cell-mediated matrix assembly process. *Matrix biology: journal of the International Society for Matrix Biology*, *24*(6), 389–399.

[73]: Fortunati, D., Chau, D. Y., Wang, Z., Collighan, R. J., & Griffin, M. (2014). Cross-linking of collagen I by tissue transglutaminase provides a promising biomaterial for promoting bone healing. *Amino acids*, *46*(7), 1751–1761.

[74]: Watt, F., Huck, W. Role of the extracellular matrix in regulating stem cell fate. *Nat Rev Mol Cell Biol* **14**, 467–473 (2013).

[75]: Trappmann, B., Gautrot, J. E., Connelly, J. T., Strange, D. G., Li, Y., Oyen, M. L., Cohen Stuart, M. A., Boehm, H., Li, B., Vogel, V., Spatz, J. P., Watt, F. M., & Huck, W. T. (2012). Extracellular-matrix tethering regulates stem-cell fate. *Nature materials*, *11*(7), 642–649.

[76]: Schuster, R., Rockel, J. S., Kapoor, M., & Hinz, B. (2021). The inflammatory speech of fibroblasts. *Immunological reviews*, *302*(1), 126–146.

[77]: Davidson, S., Coles, M., Thomas, T. *et al.* Fibroblasts as immune regulators in infection, inflammation, and cancer. *Nat Rev Immunol* **21**, 704–717 (2021).

[78]: Moretti, L., Stalfort, J., Barker, T. H., & Abebayehu, D. (2022). The interplay of fibroblasts, the extracellular matrix, and inflammation in scar formation. *The Journal of biological chemistry*, *298*(2), 101530.

[79]: Gomes, R.N., Manuel, F. & Nascimento, D.S. The bright side of fibroblasts: molecular signature and regenerative cues in major organs. *npj Regen Med* **6**, 43 (2021).

[80]: Takahashi, M., Umehara, Y., Yue, H., Trujillo-Paez, J. V., Peng, G., Nguyen, H. L. T., Ikutama, R., Okumura, K., Ogawa, H., Ikeda, S., & Niyonsaba, F. (2021). The Antimicrobial Peptide Human β-Defensin-3 Accelerates Wound Healing by Promoting Angiogenesis, Cell Migration, and Proliferation Through the FGFR/JAK2/STAT3 Signaling Pathway. *Frontiers in immunology*, *12*, 712781.

[81]: Rogler, G., Gelbmann, C. M., Vogl, D., Brunner, M., Schölmerich, J., Falk, W., Andus, T., & Brand, K. (2001). Differential activation of cytokine secretion in primary human colonic fibroblast/myofibroblast cultures. *Scandinavian journal of gastroenterology*, *36*(4), 389–398.

[82]: Shen, Y., Ning, J., Zhao, L. *et al.* Matrix remodeling associated 7 proteins promote cutaneous wound healing through vimentin in coordinating fibroblast functions. *Inflamm Regener* **43**, 5 (2023).

[83]: Shams, F., Moravvej, H., Hosseinzadeh, S. *et al.* Overexpression of *VEGF* in dermal fibroblast cells accelerates the angiogenesis and wound healing function: in vitro and in vivo studies. *Sci Rep* **12**, 18529 (2022).

[84]: Pakshir, P., Alizadehgiashi, M., Wong, B. *et al.* Dynamic fibroblast contractions attract remote macrophages in fibrillar collagen matrix. *Nat Commun* **10**, 1850 (2019).

[85]: Vaculik, C., Schuster, C., Bauer, W., Iram, N., Pfisterer, K., Kramer, G., Reinisch, A., Strunk, D., & Elbe-Bürger, A. (2012). Human dermis harbors distinct mesenchymal stromal cell subsets. *The Journal of investigative dermatology*, *132*(3 Pt 1), 563–574.

[86]: Amini-Nik, S., Dolp, R., Eylert, G., Datu, A. K., Parousis, A., Blakeley, C., & Jeschke, M. G. (2018). Stem cells derived from burned skin - The future of burn care. *EBioMedicine*, *37*, 509–520.

[87]: Díaz-García, D., Filipová, A., Garza-Veloz, I., & Martinez-Fierro, M. L. (2021). A Beginner's Introduction to Skin Stem Cells and Wound Healing. *International journal of molecular sciences*, *22*(20), 11030.

[88]: Chen, Z., Pradhan, S., Liu, C., & Le, L. Q. (2012). Skin-derived precursors as a source of progenitors for cutaneous nerve regeneration. *Stem cells (Dayton, Ohio)*, *30*(10), 2261–2270.

[89]: Huang, S., Hu, Z., Wang, P. *et al*. Rat epidermal stem cells promote the angiogenesis of full-thickness wounds. *Stem Cell Res Ther* **11**, 344 (2020).

[90]: Wang, P., Theocharidis, G., Vlachos, I. S., Kounas, K., Lobao, A., Shu, B., Wu, B., Xie, J., Hu, Z., Qi, S., Tang, B., Zhu, J., & Veves, A. (2022). Exosomes Derived from Epidermal Stem Cells Improve Diabetic Wound Healing. *The Journal of investigative dermatology*, *142*(9), 2508–2517.

[91]: Tan, L., Dai, T., Liu, D., Chen, Z., Wu, L., Gao, L., Wang, Y., & Shi, C. (2016). Contribution of dermal-derived mesenchymal cells during liver repair in two different experimental models. *Scientific reports*, *6*, 25314.

[92]: Friedenstein AJ. Osteogenic stem cells in bone marrow. In: Heersche JNM, Kanis JA, editors. Bone and Mineral Research. Amsterdam: Elsevier; 1990. pp. 243–272.

[93]: Konstantinov I. E. (2000). In search of Alexander A. Maximow: the man behind the unitarian theory of hematopoiesis. *Perspectives in biology and medicine*, *43*(2), 269–276.

[94]: Földes, A., Reider, H., Varga, A., Nagy, K. S., Perczel-Kovach, K., Kis-Petik, K., DenBesten, P., Ballagi, A., & Varga, G. (2021). Culturing and Scaling up Stem Cells of Dental Pulp Origin Using Microcarriers. *Polymers*, *13*(22), 3951.

[95]: Zhou, L., Song, Q., Shen, J., Xu, L., Xu, Z., Wu, R., Ge, Y., Zhu, J., Wu, J., Dou, Q., & Jia, R. (2017). Comparison of human adipose stromal vascular fraction and adipose-derived mesenchymal stem cells for the attenuation of acute renal ischemia/reperfusion injury. *Scientific reports*, *7*, 44058.

[96]: Xiao, X., Li, W., Rong, D., Xu, Z., Zhang, Z., Ye, H., Xie, L., Wu, Y., Zhang, Y., & Wang, X. (2021). Human umbilical cord mesenchymal stem cells-derived extracellular vesicles facilitate the repair of spinal cord injury via the miR-29b-3p/PTEN/Akt/mTOR axis. *Cell death discovery*, *7*(1), 212.

[97]: Dominici, M., Le Blanc, K., Mueller, I., Slaper-Cortenbach, I., Marini, F., Krause, D., Deans, R., Keating, A., Prockop, D.j, & Horwitz, E. (2006). Minimal criteria for defining multipotent mesenchymal stromal cells. The International Society for Cellular Therapy position statement. *Cytotherapy*, *8*(4), 315–317.

[98]: Krawczenko, A., & Klimczak, A. (2022). Adipose Tissue-Derived Mesenchymal Stem/Stromal Cells and Their Contribution to Angiogenic Processes in Tissue Regeneration. *International journal of molecular sciences*, *23*(5), 2425.

[99]: Mohamed-Ahmed, S., Fristad, I., Lie, S. A., Suliman, S., Mustafa, K., Vindenes, H., & Idris, S. B. (2018). Adipose-derived and bone marrow mesenchymal stem cells: a donor-matched comparison. *Stem cell research & therapy*, *9*(1), 168.

[100]: Chen, Q., Shou, P., Zheng, C., Jiang, M., Cao, G., Yang, Q., Cao, J., Xie, N., Velletri, T., Zhang, X., Xu, C., Zhang, L., Yang, H., Hou, J., Wang, Y., & Shi, Y. (2016). Fate decision of mesenchymal stem cells: adipocytes or osteoblasts? *Cell death and differentiation*, *23*(7), 1128–1139.

[101]: Maharlooei, M. K., Bagheri, M., Solhjou, Z., Jahromi, B. M., Akrami, M., Rohani, L., Monabati, A., Noorafshan, A., & Omrani, G. R. (2011). Adipose tissue derived mesenchymal stem cell (AD-MSC) promotes skin wound healing in diabetic rats. *Diabetes research and clinical practice*, *93*(2), 228–234.

[102]: Zhou, X. B., Li, H., Li, F., Song, X. K., Liu, T., Ma, T., Guo, H. Y., Wu, N., & Li, J. (2020). Generation and characterization of two iPSC lines from human adipose tissue-derived stem cells of healthy donors. *Stem cell research*, *48*, 101973.

[103]: Hoang, D. H., Nguyen, T. D., Nguyen, H. P., Nguyen, X. H., Do, P. T. X., Dang, V. D., Dam, P. T. M., Bui, H. T. H., Trinh, M. Q., Vu, D. M., Hoang, N. T. M., Thanh, L. N., & Than, U. T. T. (2020). Differential Wound Healing Capacity of Mesenchymal Stem Cell-Derived Exosomes Originated From Bone Marrow, Adipose Tissue and Umbilical Cord Under Serum- and Xeno-Free Condition. *Frontiers in molecular biosciences*, *7*, 119.

[104]: Mishra, P. J., Mishra, P. J., & Banerjee, D. (2016). Keratinocyte Induced Differentiation of Mesenchymal Stem Cells into Dermal Myofibroblasts: A Role in Effective Wound Healing. *International journal of translational science*, *2016*(1), 5–32.

[105]: Tan, L., Dai, T., Liu, D., Chen, Z., Wu, L., Gao, L., Wang, Y., & Shi, C. (2016). Contribution of dermal-derived mesenchymal cells during liver repair in two different experimental models. *Scientific reports*, *6*, 25314.

[106]: Bernardo, M. E., & Fibbe, W. E. (2013). Mesenchymal stromal cells: sensors and switchers of inflammation. *Cell stem cell*, *13*(4), 392–402.

[107]: Wang, Y. K., & Chen, C. S. (2013). Cell adhesion and mechanical stimulation in the regulation of mesenchymal stem cell differentiation. *Journal of cellular and molecular medicine*, *17*(7), 823–832.

[108]: Moniz, I., Ramalho-Santos, J., & Branco, A. F. (2022). Differential Oxygen Exposure Modulates Mesenchymal Stem Cell Metabolism and Proliferation through mTOR Signaling. *International journal of molecular sciences*, *23*(7), 3749.

[109]: Noronha, N. C., Mizukami, A., Caliári-Oliveira, C., Cominal, J. G., Rocha, J. L. M., Covas, D. T., Swiech, K., & Malmegrim, K. C. R. (2019). Correction to: Priming approaches to improve the efficacy of mesenchymal stromal cell-based therapies. *Stem cell research & therapy*, *10*(1), 132.

[110]: Fernández-Francos, S., Eiro, N., Costa, L. A., Escudero-Cernuda, S., Fernández-Sánchez, M. L., & Vizoso, F. J. (2021). Mesenchymal Stem Cells as a Cornerstone in a Galaxy

of Intercellular Signals: Basis for a New Era of Medicine. *International journal of molecular sciences*, *22*(7), 3576.

[111]: Guarnerio, J., Coltella, N., Ala, U., Tonon, G., Pandolfi, P. P., & Bernardi, R. (2014). Bone marrow endosteal mesenchymal progenitors depend on HIF factors for maintenance and regulation of hematopoiesis. *Stem cell reports*, *2*(6), 794–809.

[112]: Zhao, Y., Sun, Q., & Huo, B. (2021). Focal adhesion regulates osteogenic differentiation of mesenchymal stem cells and osteoblasts. *Biomaterials translational*, *2*(4), 312–322.

[113]: Lorthongpanich, C., Thumanu, K., Tangkiettrakul, K., Jiamvoraphong, N., Laowtammathron, C., Damkham, N., U-Pratya, Y., & Issaragrisil, S. (2019). YAP as a key regulator of adipo-osteogenic differentiation in human MSCs. *Stem cell research & therapy*, *10*(1), 402.

[114]: Mays, R. W., van't Hof, W., Ting, A. E., Perry, R., & Deans, R. (2007). Development of adult pluripotent stem cell therapies for ischemic injury and disease. *Expert opinion on biological therapy*, *7*(2), 173–184.

[115]: Ahangar, P., Mills, S. J., Smith, L. E., Strudwick, X. L., Ting, A. E., Vaes, B., & Cowin, A. J. (2020). Human multipotent adult progenitor cell-conditioned medium improves wound healing through modulating inflammation and angiogenesis in mice. *Stem cell research & therapy*, *11*(1), 299.

[116]: D'Ippolito, G., Diabira, S., Howard, G. A., Menei, P., Roos, B. A., & Schiller, P. C. (2004). Marrow-isolated adult multilineage inducible (MIAMI) cells, a unique population of postnatal young and old human cells with extensive expansion and differentiation potential. *Journal of cell science*, *117*(Pt 14), 2971–2981.

[117]: Ratajczak, M. Z., Zuba-Surma, E., Wojakowski, W., Suszynska, M., Mierzejewska, K., Liu, R., Ratajczak, J., Shin, D. M., & Kucia, M. (2014). Very small embryonic-like stem cells (VSELs) represent a real challenge in stem cell biology: recent pros and cons in the midst of a lively debate. *Leukemia*, *28*(3), 473–484.

[118]: Petrenko, Y., Vackova, I., Kekulova, K., Chudickova, M., Koci, Z., Turnovcova, K., Kupcova Skalnikova, H., Vodicka, P., & Kubinova, S. (2020). A Comparative Analysis of Multipotent Mesenchymal Stromal Cells derived from Different Sources, with a Focus on Neuroregenerative Potential. *Scientific reports*, *10*(1), 4290.

[119]: Sart, S., Tsai, A. C., Li, Y., & Ma, T. (2014). Three-dimensional aggregates of mesenchymal stem cells: cellular mechanisms, biological properties, and applications. *Tissue engineering. Part B, Reviews*, *20*(5), 365–380.

[120]: Heneidi, S., Simerman, A. A., Keller, E., Singh, P., Li, X., Dumesic, D. A., & Chazenbalk, G. (2013). Awakened by cellular stress: isolation and characterization of a novel population of pluripotent stem cells derived from human adipose tissue. *PloS one*, *8*(6), e64752.

[121]: Alessio, N., Squillaro, T., Özcan, S., Di Bernardo, G., Venditti, M., Melone, M., Peluso, G., & Galderisi, U. (2018). Stress and stem cells: adult Muse cells tolerate extensive

genotoxic stimuli better than mesenchymal stromal cells. *Oncotarget*, *9*(27), 19328–19341.

[122]: Mao, X. Q., Cheng, Y., Zhang, R. Z., Liu, Y. B., Li, Y., Ge, K., & Jin, H. L. (2022). RNA-seq and ATAC-seq analyses of multilineage differentiating stress enduring cells: Comparison with dermal fibroblasts. *Cell biology international*, *46*(9), 1480–1494.

[123]: Kuroda, Y., Wakao, S., Kitada, M., Murakami, T., Nojima, M., & Dezawa, M. (2013). Isolation, culture, and evaluation of multilineage-differentiating stress-enduring (Muse) cells. *Nature protocols*, *8*(7), 1391–1415.

[124]: Dezawa M. (2016). Muse Cells Provide the Pluripotency of Mesenchymal Stem Cells: Direct Contribution of Muse Cells to Tissue Regeneration. *Cell transplantation*, *25*(5), 849–861.

[125]: Ogura, F., Wakao, S., Kuroda, Y., Tsuchiyama, K., Bagheri, M., Heneidi, S., Chazenbalk, G., Aiba, S., & Dezawa, M. (2014). Human adipose tissue possesses a unique population of pluripotent stem cells with nontumorigenic and low telomerase activities: potential implications in regenerative medicine. *Stem cells and development*, *23*(7), 717–728.

[126]: Chen, X., Yin, X. Y., Zhao, Y. Y., Wang, C. C., Du, P., Lu, Y. C., Jin, H. B., Yang, C. C., & Ying, J. L. (2021). Human Muse cells-derived neural precursor cells as the novel seed cells for the repair of spinal cord injury. *Biochemical and biophysical research communications*, *568*, 103–109.

[127]: Iseki, M., Kushida, Y., Wakao, S., Akimoto, T., Mizuma, M., Motoi, F., Asada, R., Shimizu, S., Unno, M., Chazenbalk, G., & Dezawa, M. (2017). Muse Cells, Nontumorigenic Pluripotent-Like Stem Cells, Have Liver Regeneration Capacity Through Specific Homing and Cell Replacement in a Mouse Model of Liver Fibrosis. *Cell transplantation*, *26*(5), 821–840.

[128]: Tsuchiyama, K., Wakao, S., Kuroda, Y., Ogura, F., Nojima, M., Sawaya, N., Yamasaki, K., Aiba, S., & Dezawa, M. (2013). Functional melanocytes are readily reprogrammable from multilineage-differentiating stress-enduring (muse) cells, distinct stem cells in human fibroblasts. *The Journal of investigative dermatology*, *133*(10), 2425–2435.

[129]: Yamauchi, T., Yamasaki, K., Tsuchiyama, K., Koike, S., & Aiba, S. (2017). A quantitative analysis of multilineage-differentiating stress-enduring (Muse) cells in human adipose tissue and efficacy of melanocytes induction. *Journal of dermatological science*, *86*(3), 198–205

[130]: Yamauchi, T., Kuroda, Y., Morita, T., Shichinohe, H., Houkin, K., Dezawa, M., & Kuroda, S. (2015). Therapeutic effects of human multilineage-differentiating stress enduring (MUSE) cell transplantation into infarct brain of mice. *PloS one*, *10*(3), e0116009.

[131]: Katagiri, H., Kushida, Y., Nojima, M., Kuroda, Y., Wakao, S., Ishida, K., Endo, F., Kume, K., Takahara, T., Nitta, H., Tsuda, H., Dezawa, M., & Nishizuka, S. S. (2016). A Distinct Subpopulation of Bone Marrow Mesenchymal Stem Cells, Muse Cells, Directly Commit to the Replacement of Liver Components. *American journal of transplantation: official journal*

of the American Society of Transplantation and the American Society of Transplant Surgeons, *16*(2), 468–483.

[132]: Wakao, S., Kitada, M., Kuroda, Y., Shigemoto, T., Matsuse, D., Akashi, H., Tanimura, Y., Tsuchiyama, K., Kikuchi, T., Goda, M., Nakahata, T., Fujiyoshi, Y., & Dezawa, M. (2011). Multilineage-differentiating stress-enduring (Muse) cells are a primary source of induced pluripotent stem cells in human fibroblasts. *Proceedings of the National Academy of Sciences of the United States of America*, *108*(24), 9875–9880.

[133]: Gimeno, M. L., Fuertes, F., Barcala Tabarrozzi, A. E., Attorressi, A. I., Cucchiani, R., Corrales, L., Oliveira, T. C., Sogayar, M. C., Labriola, L., Dewey, R. A., & Perone, M. J. (2017). Pluripotent Nontumorigenic Adipose Tissue-Derived Muse Cells have Immunomodulatory Capacity Mediated by Transforming Growth Factor-β1. *Stem cells translational medicine*, *6*(1), 161–173.

[134]: Manoukian, P., Bijlsma, M., & van Laarhoven, H. (2021). The Cellular Origins of Cancer-Associated Fibroblasts and Their Opposing Contributions to Pancreatic Cancer Growth. *Frontiers in cell and developmental biology*, *9*, 743907.

[135]: Kayamori, K., Katsube, K., Sakamoto, K., Ohyama, Y., Hirai, H., Yukimori, A., Ohata, Y., Akashi, T., Saitoh, M., Harada, K., Harada, H., & Yamaguchi, A. (2016). NOTCH3 Is Induced in Cancer-Associated Fibroblasts and Promotes Angiogenesis in Oral Squamous Cell Carcinoma. *PloS one*, *11*(4)

[136]: Mao, X., Xu, J., Wang, W., Liang, C., Hua, J., Liu, J., Zhang, B., Meng, Q., Yu, X., & Shi, S. (2021). Crosstalk between cancer-associated fibroblasts and immune cells in the tumor microenvironment: new findings and future perspectives. *Molecular cancer*, *20*(1), 131.

[137]: Calvo, F., Ege, N., Grande-Garcia, A., Hooper, S., Jenkins, R. P., Chaudhry, S. I., Harrington, K., Williamson, P., Moeendarbary, E., Charras, G., & Sahai, E. (2013). Mechanotransduction and YAP-dependent matrix remodelling is required for the generation and maintenance of cancer-associated fibroblasts. *Nature cell biology*, *15*(6), 637–646.

[138]: Giannoni, E., Bianchini, F., Calorini, L., & Chiarugi, P. (2011). Cancer associated fibroblasts exploit reactive oxygen species through a proinflammatory signature leading to epithelial mesenchymal transition and stemness. *Antioxidants & redox signaling*, *14*(12), 2361–2371.

[139]: Mueller, A. C., Piper, M., Goodspeed, A., Bhuvane, S., Williams, J. S., Bhatia, S., Phan, A. V., Van Court, B., Zolman, K. L., Peña, B., Oweida, A. J., Zakem, S., Meguid, C., Knitz, M. W., Darragh, L., Bickett, T. E., Gadwa, J., Mestroni, L., Taylor, M. R. G., Jordan, K. R., … Karam, S. D. (2021). Induction of ADAM10 by Radiation Therapy Drives Fibrosis, Resistance, and Epithelial-to-Mesenchyal Transition in Pancreatic Cancer. *Cancer research*, *81*(12), 3255–3269.

[140]: Monteran, L., & Erez, N. (2019). The Dark Side of Fibroblasts: Cancer-Associated Fibroblasts as Mediators of Immunosuppression in the Tumor Microenvironment. *Frontiers in immunology*, *10*, 1835.

[141]: Gok Yavuz, B., Gunaydin, G., Gedik, M. E., Kosemehmetoglu, K., Karakoc, D., Ozgur, F., & Guc, D. (2019). Cancer associated fibroblasts sculpt tumour microenvironment by recruiting monocytes and inducing immunosuppressive PD-1^{+} TAMs. *Scientific reports*, *9*(1), 3172.

[142]: Yamada, K., Uchiyama, A., Uehara, A., Perera, B., Ogino, S., Yokoyama, Y., Takeuchi, Y., Udey, M. C., Ishikawa, O., & Motegi, S. (2016). MFG-E8 Drives Melanoma Growth by Stimulating Mesenchymal Stromal Cell-Induced Angiogenesis and M2 Polarization of Tumor-Associated Macrophages. *Cancer research*, *76*(14), 4283–4292.

[143]: Bruch-Oms, M., Olivera-Salguero, R., Mazzolini, R., Del Valle-Pérez, B., Mayo-González, P., Beteta, Á., Peña, R., & García de Herreros, A. (2023). Analyzing the role of cancer-associated fibroblast activation on macrophage polarization. *Molecular oncology*, *17*(8), 1492–1513.

[144]: Gunaydin G. (2021). CAFs Interacting With TAMs in Tumor Microenvironment to Enhance Tumorigenesis and Immune Evasion. *Frontiers in oncology*, *11*, 668349.

[145]: Haist, M., Stege, H., Grabbe, S., & Bros, M. (2021). The Functional Crosstalk between Myeloid-Derived Suppressor Cells and Regulatory T Cells within the Immunosuppressive Tumor Microenvironment. *Cancers*, *13*(2), 210.

[146]: Chen, L., Huang, H., Zheng, X., Li, Y., Chen, J., Tan, B., … Jiang, J. (2022). IL1R2 increases regulatory T cell population in the tumor microenvironment by enhancing MHC-II expression on cancer-associated fibroblasts.

[147]: Cheng, J. T., Deng, Y. N., Yi, H. M., Wang, G. Y., Fu, B. S., Chen, W. J., Liu, W., Tai, Y., Peng, Y. W., & Zhang, Q. (2016). Hepatic carcinoma-associated fibroblasts induce IDO-producing regulatory dendritic cells through IL-6-mediated STAT3 activation. *Oncogenesis*, *5*(2), e198.

[148]: Mao, X., Xu, J., Wang, W., Liang, C., Hua, J., Liu, J., Zhang, B., Meng, Q., Yu, X., & Shi, S. (2021). Crosstalk between cancer-associated fibroblasts and immune cells in the tumor microenvironment: new findings and future perspectives. *Molecular cancer*, *20*(1), 131.

[149]: Inoue, C., Miki, Y., Saito, R., Hata, S., Abe, J., Sato, I., Okada, Y., & Sasano, H. (2019). PD-L1 Induction by Cancer-Associated Fibroblast-Derived Factors in Lung Adenocarcinoma Cells. *Cancers*, *11*(9), 1257.

[150]: Zhang, Q., Yang, J., Bai, J., & Ren, J. (2018). Reverse of non-small cell lung cancer drug resistance induced by cancer-associated fibroblasts via a paracrine pathway. *Cancer science*, *109*(4), 944–955.

[151]: Wei, L., Lin, Q., Lu, Y., Li, G., Huang, L., Fu, Z., Chen, R., & Zhou, Q. (2021). Cancer-associated fibroblasts-mediated ATF4 expression promotes malignancy and gemcitabine resistance in pancreatic cancer via the TGF-β1/SMAD2/3 pathway and ABCC1 transactivation. *Cell death & disease*, *12*(4), 334.

[152]: Qiao, Y., Zhang, C., Li, A., Wang, D., Luo, Z., Ping, Y., Zhou, B., Liu, S., Li, H., Yue, D., Zhang, Z., Chen, X., Shen, Z., Lian, J., Li, Y., Wang, S., Li, F., Huang, L., Wang, L., Zhang, B.,

Zhang, Y. (2018). IL6 derived from cancer-associated fibroblasts promotes chemoresistance via CXCR7 in esophageal squamous cell carcinoma. *Oncogene*, *37*(7), 873–883.

[153]: Domogauer, J. D., de Toledo, S. M., Howell, R. W., & Azzam, E. I. (2021). Acquired radioresistance in cancer associated fibroblasts is concomitant with enhanced antioxidant potential and DNA repair capacity. *Cell communication and signaling: CCS*, *19*(1), 30.

[154]: Gilkes, D. M., Bajpai, S., Chaturvedi, P., Wirtz, D., & Semenza, G. L. (2013). Hypoxia-inducible factor 1 (HIF-1) promotes extracellular matrix remodeling under hypoxic conditions by inducing P4HA1, P4HA2, and PLOD2 expression in fibroblasts. *The Journal of biological chemistry*, *288*(15), 10819–10829.

[155]: Wang, F. T., Sun, W., Zhang, J. T., & Fan, Y. Z. (2019). Cancer-associated fibroblast regulation of tumor neo-angiogenesis as a therapeutic target in cancer. *Oncology letters*, *17*(3), 3055–3065.

[156]: Bruni, S., Mercogliano, M. F., Mauro, F. L., Cordo Russo, R. I., & Schillaci, R. (2023). Cancer immune exclusion: breaking the barricade for a successful immunotherapy. *Frontiers in oncology*, *13*, 1135456.

[157]: Lu, P., Weaver, V. M., & Werb, Z. (2012). The extracellular matrix: a dynamic niche in cancer progression. *The Journal of cell biology*, *196*(4), 395–406.

[158]: Delaine-Smith, R., Wright, N., Hanley, C., Hanwell, R., Bhome, R., Bullock, M., Drifka, C., Eliceiri, K., Thomas, G., Knight, M., Mirnezami, A., & Peake, N. (2019). Transglutaminase-2 Mediates the Biomechanical Properties of the Colorectal Cancer Tissue Microenvironment that Contribute to Disease Progression. *Cancers*, *11*(5), 701.

[159]: Liu, X., Li, J., Yang, X., Li, X., Kong, J., Qi, D., Zhang, F., Sun, B., Liu, Y., & Liu, T. (2023). Carcinoma-associated fibroblast-derived lysyl oxidase-rich extracellular vesicles mediate collagen crosslinking and promote epithelial-mesenchymal transition via p-FAK/p-paxillin/YAP signaling. *International journal of oral science*, *15*(1), 32.

[160]: Levental, K. R., Yu, H., Kass, L., Lakins, J. N., Egeblad, M., Erler, J. T., Fong, S. F., Csiszar, K., Giaccia, A., Weninger, W., Yamauchi, M., Gasser, D. L., & Weaver, V. M. (2009). Matrix crosslinking forces tumor progression by enhancing integrin signaling. *Cell*, *139*(5), 891–906.

[161]: Noël, A., Emonard, H., Polette, M., Birembaut, P., & Foidart, J. M. (1994). Role of matrix, fibroblasts and type IV collagenases in tumor progression and invasion. *Pathology, research, and practice*, *190*(9-10), 934–941.

[162]: Johansson, A. C., Ansell, A., Jerhammar, F., Lindh, M. B., Grénman, R., Munck-Wikland, E., Östman, A., & Roberg, K. (2012). Cancer-associated fibroblasts induce matrix metalloproteinase-mediated cetuximab resistance in head and neck squamous cell carcinoma cells. *Molecular cancer research: MCR*, *10*(9), 1158–1168.

[163]: Li, J., Liu, X., Zang, S., Zhou, J., Zhang, F., Sun, B., Qi, D., Li, X., Kong, J., Jin, D., Yang, X., Luo, Y., Lu, Y., Lin, B., Niu, W., & Liu, T. (2020). Small extracellular vesicle-bound

vascular endothelial growth factor secreted by carcinoma-associated fibroblasts promotes angiogenesis in a bevacizumab-resistant manner. *Cancer letters*, *492*, 71–83.

[164]: Jia, T., Jacquet, T., Dalonneau, F., Coudert, P., Vaganay, E., Exbrayat-Héritier, C., Vollaire, J., Josserand, V., Ruggiero, F., Coll, J. L., & Eymin, B. (2021). FGF-2 promotes angiogenesis through a SRSF1/SRSF3/SRPK1-dependent axis that controls VEGFR1 splicing in endothelial cells. *BMC biology*, *19*(1), 173.

[165]: Ren, Y., Cao, B., Law, S., Xie, Y., Lee, P. Y., Cheung, L., Chen, Y., Huang, X., Chan, H. M., Zhao, P., Luk, J., Vande Woude, G., & Wong, J. (2005). Hepatocyte growth factor promotes cancer cell migration and angiogenic factors expression: a prognostic marker of human esophageal squamous cell carcinomas. *Clinical cancer research: an official journal of the American Association for Cancer Research*, *11*(17), 6190–6197.

[166]: Yang, J., Lu, Y., Lin, Y. Y., Zheng, Z. Y., Fang, J. H., He, S., & Zhuang, S. M. (2016). Vascular mimicry formation is promoted by paracrine TGF-β and SDF1 of cancer-associated fibroblasts and inhibited by miR-101 in hepatocellular carcinoma. *Cancer letters*, *383*(1), 18–27.

[167]: Huang, A. C., & Zappasodi, R. (2022). A decade of checkpoint blockade immunotherapy in melanoma: understanding the molecular basis for immune sensitivity and resistance. *Nature immunology*, *23*(5), 660–670.

[168]: Tejera-Vaquerizo, A., Nagore, E., Meléndez, J. J., López-Navarro, N., Martorell-Calatayud, A., Herrera-Acosta, E., Traves, V., Guillén, C., & Herrera-Ceballos, E. (2012). Chronology of metastasis in cutaneous melanoma: growth rate model. *The Journal of investigative dermatology*, *132*(4), 1215–1221.

[169]: Hodis, E., Watson, I. R., Kryukov, G. V., Arold, S. T., Imielinski, M., Theurillat, J. P., Nickerson, E., Auclair, D., Li, L., Place, C., Dicara, D., Ramos, A. H., Lawrence, M. S., Cibulskis, K., Sivachenko, A., Voet, D., Saksena, G., Stransky, N., Onofrio, R. C., Winckler, W., … Chin, L. (2012). A landscape of driver mutations in melanoma. *Cell*, *150*(2), 251–263.

[170]: Vasudevan, S., Flashner-Abramson, E., Alkhatib, H., Roy Chowdhury, S., Adejumobi, I. A., Vilenski, D., Stefansky, S., Rubinstein, A. M., & Kravchenko-Balasha, N. (2021). Overcoming resistance to $BRAF^{V600E}$ inhibition in melanoma by deciphering and targeting personalized protein network alterations. *NPJ precision oncology*, *5*(1), 50.

[171]: Hussein, M. R., Haemel, A. K., Sudilovsky, O., & Wood, G. S. (2005). Genomic instability in radial growth phase melanoma cell lines after ultraviolet irradiation. *Journal of clinical pathology*, *58*(4), 389–396.

[172]: Plaks, V., Kong, N., & Werb, Z. (2015). The cancer stem cell niche: how essential is the niche in regulating stemness of tumor cells? *Cell stem cell*, *16*(3), 225–238.

[173]: Jamal, S. M. E., Alamodi, A., Wahl, R. U., Grada, Z., Shareef, M. A., Hassan, S. Y., Murad, F., Hassan, S. L., Santourlidis, S., Gomez, C. R., Haikel, Y., Megahed, M., & Hassan, M. (2020). Melanoma stem cell maintenance and chemo-resistance are mediated by CD133 signal to PI3K-dependent pathways. *Oncogene*, *39*(32), 5468–5478.

[174]: Quintana, E., Shackleton, M., Foster, H. R., Fullen, D. R., Sabel, M. S., Johnson, T. M., & Morrison, S. J. (2010). Phenotypic heterogeneity among tumorigenic melanoma cells from patients that is reversible and not hierarchically organized. *Cancer cell*, *18*(5), 510–523.

[175]: Wouters, J., Stas, M., Govaere, O., Barrette, K., Dudek, A., Vankelecom, H., Haydu, L. E., Thompson, J. F., Scolyer, R. A., & van den Oord, J. J. (2014). A novel hypoxia-associated subset of FN1 high MITF low melanoma cells: identification, characterization, and prognostic value. *Modern pathology: an official journal of the United States and Canadian Academy of Pathology, Inc*, *27*(8), 1088–1100.

[176]: Széky, B., Silló, P., Fábián, M., Mayer, B., Kárpáti, S., & Németh, K. (2016). Tumorőssejtek szerepe a melanoma progressziójában és heterogenitásában [Role of cancer stem cells in the progression and heterogeneity of melanoma]. *Orvosi hetilap*, *157*(34), 1339–1348.

[177]: Lionetti, M. C., Fumagalli, M. R., & La Porta, C. A. M. (2020). Cancer stem cells, plasticity, and drug resistance. *Cancer drug resistance (Alhambra, Calif.)*, *3*(2), 140–148.

[178]: Li, X., Liu, D., Chen, H., Zeng, B., Zhao, Q., Zhang, Y., Chen, Y., Wang, J., & Xing, H. R. (2022). Melanoma stem cells promote metastasis via exosomal miR-1268a inactivation of autophagy. *Biological research*, *55*(1), 29.

[179]: Kumar, D., Kumar, S., Gorain, M., Tomar, D., Patil, H. S., Radharani, N. N. V., Kumar, T. V. S., Patil, T. V., Thulasiram, H. V., & Kundu, G. C. (2016). Notch1-MAPK Signaling Axis Regulates $CD133^{+}$ Cancer Stem Cell-Mediated Melanoma Growth and Angiogenesis. *The Journal of investigative dermatology*, *136*(12), 2462–2474.

[180]: Papaccio, F., Kovacs, D., Bellei, B., Caputo, S., Migliano, E., Cota, C., & Picardo, M. (2021). Profiling Cancer-Associated Fibroblasts in Melanoma. *International journal of molecular sciences*, *22*(14), 7255.

[181]: Balsamo, M., Scordamaglia, F., Pietra, G., Manzini, C., Cantoni, C., Boitano, M., Queirolo, P., Vermi, W., Facchetti, F., Moretta, A., Moretta, L., Mingari, M. C., & Vitale, M. (2009). Melanoma-associated fibroblasts modulate NK cell phenotype and antitumor cytotoxicity. *Proceedings of the National Academy of Sciences of the United States of America*, *106*(49), 20847–20852.

[182]: Érsek, B., Silló, P., Cakir, U., Molnár, V., Bencsik, A., Mayer, B., Mezey, E., Kárpáti, S., Pós, Z., & Németh, K. (2021). Melanoma-associated fibroblasts impair CD8+ T cell function and modify expression of immune checkpoint regulators via increased arginase activity. *Cellular and molecular life sciences: CMLS*, *78*(2), 661–673.

[183]: Boussadia, Z., Gambardella, A. R., Mattei, F., & Parolini, I. (2021). Acidic and Hypoxic Microenvironment in Melanoma: Impact of Tumour Exosomes on Disease Progression. *Cells*, *10*(12), 3311.

[184]: Tang, H., Zhou, X., Zhao, X., Luo, X., Luo, T., Chen, Y., Liang, W., Jiang, E., Liu, K., Shao, Z., & Shang, Z. (2022). HSP90/IKK-rich small extracellular vesicles activate pro-angiogenic

melanoma-associated fibroblasts via the NF-κB/CXCL1 axis. *Cancer science*, *113*(4), 1168–1181.

[185]: Zhou, X., Yan, T., Huang, C., Xu, Z., Wang, L., Jiang, E., Wang, H., Chen, Y., Liu, K., Shao, Z., & Shang, Z. (2018). Melanoma cell-secreted exosomal miR-155-5p induce proangiogenic switch of cancer-associated fibroblasts via SOCS1/JAK2/STAT3 signaling pathway. *Journal of experimental & clinical cancer research: CR*, *37*(1), 242.

[186]: Pach, E., Kümper, M., Fromme, J. E., Zamek, J., Metzen, F., Koch, M., Mauch, C., & Zigrino, P. (2021). Extracellular Matrix Remodeling by Fibroblast-MMP14 Regulates Melanoma Growth. *International journal of molecular sciences*, *22*(22), 12276.

[187]: Kaur, A., Ecker, B. L., Douglass, S. M., Kugel, C. H., 3rd, Webster, M. R., Almeida, F. V., Somasundaram, R., Hayden, J., Ban, E., Ahmadzadeh, H., Franco-Barraza, J., Shah, N., Mellis, I. A., Keeney, F., Kossenkov, A., Tang, H. Y., Yin, X., Liu, Q., Xu, X., Fane, M., … Weeraratna, A. T. (2019). Remodeling of the Collagen Matrix in Aging Skin Promotes Melanoma Metastasis and Affects Immune Cell Motility. *Cancer discovery*, *9*(1), 64–81.

[188]: Han, Z., Tian, Z., Lv, G., Zhang, L., Jiang, G., Sun, K., Wang, C., Bu, X., Li, R., Shi, Y., Wu, M., & Wei, L. (2011). Immunosuppressive effect of bone marrow-derived mesenchymal stem cells in inflammatory microenvironment favours the growth of B16 melanoma cells. *Journal of cellular and molecular medicine*, *15*(11), 2343–2352.

[189]: Lv, C., Dai, H., Sun, M., Zhao, H., Wu, K., Zhu, J., Wang, Y., Cao, X., Xia, Z., & Xue, C. (2017). Mesenchymal stem cells induce epithelial mesenchymal transition in melanoma by paracrine secretion of transforming growth factor-β. *Melanoma research*, *27*(2), 74–84.

[190]: Sun, B., Zhang, S., Ni, C., Zhang, D., Liu, Y., Zhang, W., Zhao, X., Zhao, C., & Shi, M. (2005). Correlation between melanoma angiogenesis and the mesenchymal stem cells and endothelial progenitor cells derived from bone marrow. *Stem cells and development*, *14*(3), 292–298.

[191]: Vega Crespo, A., Awe, J. P., Reijo Pera, R., & Byrne, J. A. (2012). Human skin cells that express stage-specific embryonic antigen 3 associate with dermal tissue regeneration. *BioResearch open access*, *1*(1), 25–33.

[192]: Snyder, D., Wang, Y., & Kaetzel, D. M. (2020). A rare subpopulation of melanoma cells with low expression of metastasis suppressor NME1 is highly metastatic in vivo. *Scientific reports*, *10*(1), 1971.

[193]: Lobos-González, L., Aguilar, L., Diaz, J., Diaz, N., Urra, H., Torres, V. A., Silva, V., Fitzpatrick, C., Lladser, A., Hoek, K. S., Leyton, L., & Quest, A. F. (2013). E-cadherin determines Caveolin-1 tumor suppression or metastasis enhancing function in melanoma cells. *Pigment cell & melanoma research*, *26*(4), 555–570.

[194]: Ma, J., Han, H., Liu, D., Li, W., Feng, H., Xue, X., Wu, X., Niu, G., Zhang, G., Zhao, Y., Liu, C., Tao, H., & Gao, B. (2013). HER2 as a promising target for cytotoxicity T cells in human melanoma therapy. *PloS one*, *8*(8), e73261.

[195]: Yang, L., Wang, Y., Li, Y. J., & Zeng, C. C. (2018). Chemo-resistance of A172 glioblastoma cells is controlled by miR-1271-regulated Bcl-2. *Biomedicine & pharmacotherapy = Biomedecine & pharmacotherapie*, *108*, 734–740.

[196]: Hiron, M., Daveau, M., Arnaud, P., Bauer, J., & Lebreton, J. P. (1992). The human hepatoma Hep3B cell line as an experimental model in the study of the long-term regulation of acute-phase proteins by cytokines. *The Biochemical journal*, *287 (Pt 1)*(Pt 1), 255–259.

[197]: Schwartz, C. M., Spivak, C. E., Baker, S. C., McDaniel, T. K., Loring, J. F., Nguyen, C., Chrest, F. J., Wersto, R., Arenas, E., Zeng, X., Freed, W. J., & Rao, M. S. (2005). NTera2: a model system to study dopaminergic differentiation of human embryonic stem cells. *Stem cells and development*, *14*(5), 517–534.

[198]: González-Burguera I, Ricobaraza A, Aretxabala X, Barrondo S, García del Caño G, López de Jesús M, Sallés J. Highly efficient generation of glutamatergic/cholinergic NT2-derived postmitotic human neurons by short-term treatment with the nucleoside analogue cytosine β-D-arabinofuranoside. Stem Cell Res. 2016 Mar;16(2):541-51.

[199]: Schwartz, C. M., Spivak, C. E., Baker, S. C., McDaniel, T. K., Loring, J. F., Nguyen, C., Chrest, F. J., Wersto, R., Arenas, E., Zeng, X., Freed, W. J., & Rao, M. S. (2005). NTera2: a model system to study dopaminergic differentiation of human embryonic stem cells. *Stem cells and development*, *14*(5), 517–534.

[200]: Coyle, D. E., Li, J., & Baccei, M. (2011). Regional differentiation of retinoic acid-induced human pluripotent embryonic carcinoma stem cell neurons. *PloS one*, *6*(1), e16174.

[201]: Song, Y., Lee, S., & Jho, E. H. (2018). Enhancement of neuronal differentiation by using small molecules modulating Nodal/Smad, Wnt/β-catenin, and FGF signaling. *Biochemical and biophysical research communications*, *503*(1), 352–358.

[202]: Zhang, Y., Pak, C., Han, Y., Ahlenius, H., Zhang, Z., Chanda, S., Marro, S., Patzke, C., Acuna, C., Covy, J., Xu, W., Yang, N., Danko, T., Chen, L., Wernig, M., & Südhof, T. C. (2013). Rapid single-step induction of functional neurons from human pluripotent stem cells. *Neuron*, *78*(5), 785–798.

[203]: Marchal-Victorion, S., Deleyrolle, L., De Weille, J., Saunier, M., Dromard, C., Sandillon, F., Privat, A., & Hugnot, J. P. (2003). The human NTERA2 neural cell line generates neurons on growth under neural stem cell conditions and exhibits characteristics of radial glial cells. *Molecular and cellular neurosciences*, *24*(1), 198–213.

[204]: Pal, R., & Ravindran, G. (2006). Assessment of pluripotency and multilineage differentiation potential of NTERA-2 cells as a model for studying human embryonic stem cells. *Cell proliferation*, *39*(6), 585–598.

[205]: Érsek, B., Silló, P., Cakir, U., Molnár, V., Bencsik, A., Mayer, B., Mezey, E., Kárpáti, S., Pós, Z., & Németh, K. (2021). Melanoma-associated fibroblasts impair CD8+ T cell function

and modify expression of immune checkpoint regulators via increased arginase activity. *Cellular and molecular life sciences: CMLS*, *78*(2), 661–673.

[206]: Lysy, P. A., Smets, F., Sibille, C., Najimi, M., & Sokal, E. M. (2007). Human skin fibroblasts: From mesodermal to hepatocyte-like differentiation. *Hepatology (Baltimore, Md.)*, *46*(5), 1574–1585.

[207]: Moon, H., Donahue, L. R., Choi, E., Scumpia, P. O., Lowry, W. E., Grenier, J. K., Zhu, J., & White, A. C. (2017). Melanocyte Stem Cell Activation and Translocation Initiate Cutaneous Melanoma in Response to UV Exposure. *Cell stem cell*, *21*(5), 665–678.

[208]: Li L, Fukunaga-Kalabis M, Yu H, Xu X, Kong J, Lee JT, Herlyn M. Human dermal stem cells differentiate into functional epidermal melanocytes. J Cell Sci. 2010 Mar 15;123(Pt 6):853-60.

[209]: Beug H. (2009). Breast cancer stem cells: eradication by differentiation therapy? *Cell*, *138*(4), 623–625.

[210]: Sułkowski, M., Kot, M., Badyra, B., Paluszkiewicz, A., Płonka, P. M., Sarna, M., Michalczyk-Wetula, D., Zucca, F. A., Zecca, L., & Majka, M. (2021). Highly Effective Protocol for Differentiation of Induced Pluripotent Stem Cells (iPS) into Melanin-Producing Cells. *International journal of molecular sciences*, *22*(23), 12787.

[211]: Hosaka, C., Kunisada, M., Koyanagi-Aoi, M., Masaki, T., Takemori, C., Taniguchi-Ikeda, M., Aoi, T., & Nishigori, C. (2019). Induced pluripotent stem cell-derived melanocyte precursor cells undergoing differentiation into melanocytes. *Pigment cell & melanoma research*, *32*(5), 623–633.

[212]: Horioka, K., Ohuchida, K., Sada, M., Zheng, B., Moriyama, T., Fujita, H., Manabe, T., Ohtsuka, T., Shimamoto, M., Miyazaki, T., Mizumoto, K., Oda, Y., & Nakamura, M. (2016). Suppression of CD51 in pancreatic stellate cells inhibits tumor growth by reducing stroma and altering tumor-stromal interaction in pancreatic cancer. *International journal of oncology*, *48*(4), 1499–1508.

[213]: Kinugasa, Y., Matsui, T., & Takakura, N. (2014). CD44 expressed on cancer-associated fibroblasts is a functional molecule supporting the stemness and drug resistance of malignant cancer cells in the tumor microenvironment. *Stem cells (Dayton, Ohio)*, *32*(1), 145–156.

[214]: Miki, Y., Yashiro, M., Okuno, T., Kitayama, K., Masuda, G., Hirakawa, K., & Ohira, M. (2018). CD9-positive exosomes from cancer-associated fibroblasts stimulate the migration ability of scirrhous-type gastric cancer cells. *British journal of cancer*, *118*(6), 867–877.

[215]: Hutchins, D., & Steel, C. M. (1994). Regulation of ICAM-1 (CD54) expression in human breast cancer cell lines by interleukin 6 and fibroblast-derived factors. *International journal of cancer*, *58*(1), 80–84.

[216]: Peng, L., Wang, D., Han, Y., Huang, T., He, X., Wang, J., & Ou, C. (2022). Emerging Role of Cancer-Associated Fibroblasts-Derived Exosomes in Tumorigenesis. *Frontiers in immunology*, *12*, 795372.

[217]: Wang, S., Coleman, E. J., Pop, L. M., Brooks, K. J., Vitetta, E. S., & Niederkorn, J. Y. (2006). Effect of an anti-CD54 (ICAM-1) monoclonal antibody (UV3) on the growth of human uveal melanoma cells transplanted heterotopically and orthotopically in SCID mice. *International journal of cancer*, *118*(4), 932–941.

[218]: Leñero, C., Kaplan, L. D., Best, T. M., & Kouroupis, D. (2022). CD146+ Endometrial-Derived Mesenchymal Stem/Stromal Cell Subpopulation Possesses Exosomal Secretomes with Strong Immunomodulatory miRNA Attributes. *Cells*, *11*(24), 4002.

[219]: Smith, R. J. P., Faroni, A., Barrow, J. R., Soul, J., & Reid, A. J. (2021). The angiogenic potential of CD271+ human adipose tissue-derived mesenchymal stem cells. *Stem cell research & therapy*, *12*(1), 160.

[220]: Bar, S., & Benvenisty, N. (2019). Epigenetic aberrations in human pluripotent stem cells. *The EMBO journal*, *38*(12), e101033.

[221]: Coyle, D. E., Li, J., & Baccei, M. (2011). Regional differentiation of retinoic acid-induced human pluripotent embryonic carcinoma stem cell neurons. *PloS one*, *6*(1), e16174.

[222]: Galiakberova, A. A., & Dashinimaev, E. B. (2020). Neural Stem Cells and Methods for Their Generation From Induced Pluripotent Stem Cells *in vitro*. *Frontiers in cell and developmental biology*, *8*, 815.

[223]: Donato, M. T., Lahoz, A., Montero, S., Bonora, A., Pareja, E., Mir, J., Castell, J. V., & Gómez-Lechón, M. J. (2008). Functional assessment of the quality of human hepatocyte preparations for cell transplantation. *Cell transplantation*, *17*(10-11), 1211–1219.

[224]: Kang, S. J., Park, Y. I., Hwang, S. R., Yi, H., Tham, N., Ku, H. O., Song, J. Y., & Kang, H. G. (2017). Hepatic population derived from human pluripotent stem cells is effectively increased by selective removal of undifferentiated stem cells using YM155. *Stem cell research & therapy*, *8*(1), 78.

[225]: Du, C., Feng, Y., Qiu, D., Xu, Y., Pang, M., Cai, N., Xiang, A. P., & Zhang, Q. (2018). Highly efficient and expedited hepatic differentiation from human pluripotent stem cells by pure small-molecule cocktails. *Stem cell research & therapy*, *9*(1), 58.

[226]: Bandi, S., Tchaikovskaya, T., & Gupta, S. (2019). Hepatic differentiation of human pluripotent stem cells by developmental stage-related metabolomics products. *Differentiation; research in biological diversity*, *105*, 54–70.

[227]: Vega Crespo, A., Awe, J. P., Reijo Pera, R., & Byrne, J. A. (2012). Human skin cells that express stage-specific embryonic antigen 3 associate with dermal tissue regeneration. *BioResearch open access*, *1*(1), 25–33.

[228]: Pan, S., Chen, W., Liu, X., Xiao, J., Wang, Y., Liu, J., Du, Y., Wang, Y., & Zhang, Y. (2015). Application of a novel population of multipotent stem cells derived from skin fibroblasts as donor cells in bovine SCNT. *PloS one*, *10*(1), e0114423.

[229]: Zhou, Q., Jin, X., Zhao, Y., Wang, Y., Tao, M., Cao, Y., & Yin, X. (2024). Melanoma-associated fibroblasts in tumor-promotion flammation and antitumor immunity: novel mechanisms and potential immunotherapeutic strategies. *Human molecular genetics*, *33*(13), 1186–1193.

10. Bibliography

List of Publications underlying the thesis:

First-authorship:

[I]: Szeky, B., Mayer, B., Gyongy, M., Hajdara, A., Barsi, S., Karpati, S., & Nemeth, K. (2021). Tri-Lineage Differentiation of NTERA2 Clone D1 Cells towards Neural, Hepatic and Osteogenic Lineages in Vitro. *FOLIA BIOLOGICA*, *67*(5–6), 174–182.

Co-first authorship:

[II]: Çakır, U., Hajdara, A., Széky, B., Mayer, B., Kárpáti, S., Mezey, É., … Németh, K. (2021). Mesenchymal-Stromal Cell-like Melanoma-Associated Fibroblasts Increase IL-10 Production by Macrophages in a Cyclooxygenase/Indoleamine 2,3-Dioxygenase-Dependent Manner. *CANCERS*, *13*(24).

List of publications related to the subject of the theses:

[III]: Hajdara, A., Çakır, U., Érsek, B., Silló, P., Széky, B., Barna, G., … Mayer, B. (2023). Targeting Melanoma-Associated Fibroblasts (MAFs) with Activated γδ (Vδ2) T Cells: An In Vitro Cytotoxicity Model. *INTERNATIONAL JOURNAL OF MOLECULAR SCIENCES*, *24*(16), 12893.

Other publications

[IV]: Széky, B. (2018). The Role of Extracellular Matrix Remodeling Enzymes in Dermal Stem Cell Function. *PHD PROCEEDINGS ANNUAL ISSUES OF THE DOCTORAL SCHOOL FACULTY OF INFORMATION TECHNOLOGY AND BIONICS*, *13*, 71.

[V]: Széky, B. (2017). Investigating Molecular Markers and Regulators ofDermal Stem Cell Function. *PHD PROCEEDINGS ANNUAL ISSUES OF THE DOCTORAL SCHOOL FACULTY OF INFORMATION TECHNOLOGY AND BIONICS*, *12*, 34–34.

[VI]: Balázs, S. (2016). Examination of dermal stem cells in healthy and diseased skin. *PHD PROCEEDINGS ANNUAL ISSUES OF THE DOCTORAL SCHOOL FACULTY OF INFORMATION TECHNOLOGY AND BIONICS*, *11*, 97–100.

[VII]: Szeky, B., Sillo, P., Fabian, M., Mayer, B., Karpati, S., & Nemeth, K. (2016). Tumorőssejtek szerepe a melanoma progressziójában és heterogenitásában. *ORVOSI HETILAP*, *157*(34), 1339–1348.